LLNL-TR-553311

# Polar Drive Ignition Campaign Conceptual Design

April 2012

Laboratory for Laser Energetics
University of Rochester

UR LLE

Lawrence Livermore National Laboratory

**Auspices**

Lawrence Livermore National Laboratory is operated by Lawrence Livermore National Security, LLC, for the U.S. Department of Energy, National Nuclear Security Administration under Contract DE-AC52-07NA27344.

The Laboratory for Laser Energetics at the University of Rochester is supported by the U.S. Department of Energy Office of Inertial Confinement Fusion under Cooperative Agreement No. DE-FC52-08NA28302, the University of Rochester, and the New York State Energy Research and Development Authority.

# Table of Contents

# 1 INTRODUCTION

The Laboratory for Laser Energetics (LLE) at the University of Rochester is proposing a collaborative effort with Lawrence Livermore National Laboratory (LLNL), Los Alamos National Laboratories (LANL), the Naval Research Laboratory (NRL), and General Atomics (GA) with the goal of developing a cryogenic polar drive (PD) ignition platform on the National Ignition Facility (NIF). The scope of this proposed project requires close discourse among theorists, experimentalists, and laser and system engineers. This document describes how this proposed project can be broken into a series of parallel independent activities that, if implemented, could deliver this goal in the 2017 timeframe.

This Conceptual Design document is arranged into two sections: mission need and design requirements. Design requirements are divided into four subsystems:

- A point design that details the necessary target specifications and laser pulse requirements;
- The beam smoothing subsystem that describes the MultiFM 1D smoothing by spectral dispersion (SSD);
- New optical elements that include continuous phase plates (CPP's) and distributed polarization rotators (DPR's); and
- The cryogenic target handling and insertion subsystem, which includes the design, fabrication, testing, and deployment of a dedicated PD ignition target insertion cryostat (PD-ITIC).

This document includes appendices covering: the primary criteria and functional requirements, the system design requirements, the work breakdown structure, the target point design, the experimental implementation plan, the theoretical unknowns and technical implementation risks, the estimated cost and schedule, the development plan for the DPR's, the development plan for MultiFM 1D SSD, and a list of acronym definitions.

While work on the facility modifications required for PD ignition has been in progress for some time, some of the technical details required to define the specific modifications for a Conceptual Design Review (CDR) remain to be defined. In all cases, the facility modifications represent functional changes to existing systems or capabilities. The bulk of the scope yet to be identified is associated with the DPR's and MultiFM beam smoothing. Detailed development plans for these two subsystems are provided in Appendices H and I; additional discussion of subsystem requirements based on the physics of PD ignition is given in Section 3. Accordingly, LLE will work closely with LLNL to develop detailed conceptual designs for the PD-specific facility modifications, including assessments of the operational impact of implementation (e.g., changing optics for direct rather than indirect-drive illumination and swapping from a hohlraum-based ITIC to one that supports PD). Furthermore, the experimental implementation plan represents the current best understanding of the experimental campaigns required to achieve PD ignition. This plan will evolve based on the lessons learned from the National Ignition Campaign (NIC) and ongoing indirect-drive ignition experiments. The plan does not take the operational realities of the PD configuration into account; configuration planning for the proposed PD experiments is beyond the scope of this document.

## 2 MISSION NEED

The National Nuclear Security Administration (NNSA) mission need for a robust inertial confinement fusion (ICF) ignition platform flows from top-level national strategic goals articulated in the Nuclear Posture Review and NNSA Strategic Plan. Supporting program plans and objectives are outlined in NNSA Defense Programs documents, including the *Stockpile Stewardship and Management Plan* (SSMP), the Predictive Capability Framework (PCF), the Component Manufacturing Framework (CMF), the Capability and Infrastructure Framework (CIF), and specific program/campaign plans such as the FY2013–FY2018 ICF and High-Yield Program Plan. Figure 1 illustrates how experiments at NIF and other ICF facilities are integrated into the SSP.

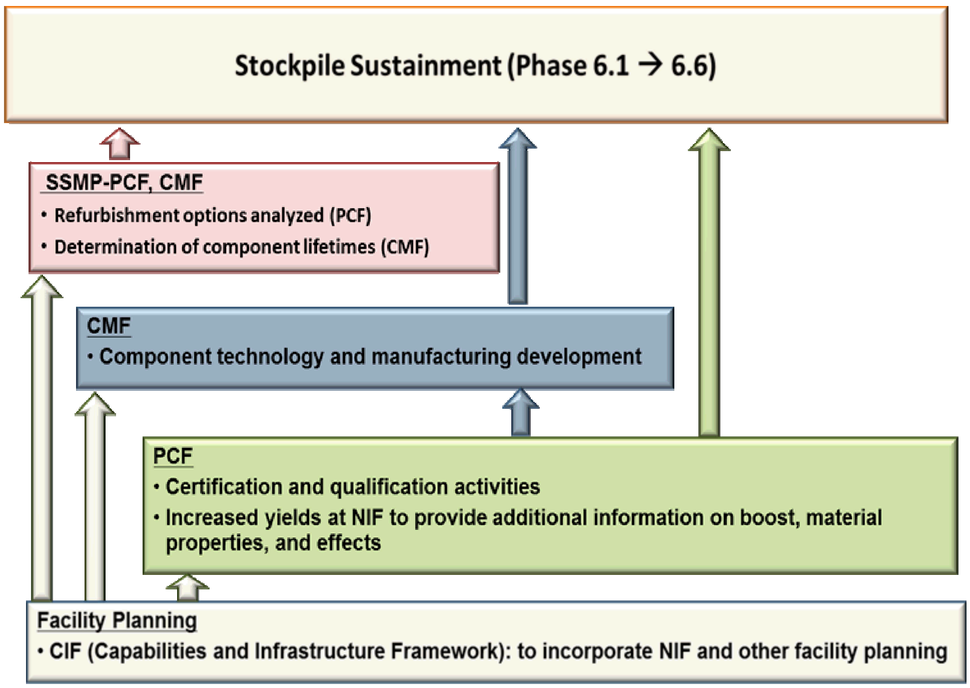


**Figure 1: NIF and its role in the PCF and overall SSP.**

The development of a robust ICF ignition platform for NIF is a major goal within the PCF and the broader Stockpile Stewardship Program (SSP).[1] This platform should have a repeatable fusion gain[2] of 5–20 to support the goals described within the PCF.[1,3] Major PCF "pegposts"[4] within the Nuclear Explosive PCF in the next decade include (text taken from D. Cook's memo from March 24, 2011):

- *2014—Preparation for the 2018 Burn Boost Pegpost*
  - *Specific deliverable: Develop an Ignition platform for the National Ignition Facility (NIF) by 2014 that meets the needs of weapons physics applications of ignition (Inertial Confinement Fusion [ICF], Science) as stated in the 2018 Burn Boost Pegpost.*

- *2015—Pegpost—Boost Initial Conditions (late phase)*
    - *Specific deliverable: Complete the second phase of the Boost Initiative involving late phase conditions and issues and utilize the information obtained to assess the risk in some aspects of stockpile assessment.*
- *2018—Pegpost—Burn–Boost*
    - *Complete the burn phase of the Boost Initiative and utilize the information obtained to assess the risk in some aspects of stockpile assessment.*
- *2019—Pegpost—Secondary Performance*
    - *Specific deliverable: Complete all of the milestones that constitute the Secondary Performance Pegpost and utilize the information to enhance predictive modeling.*

The recently completed Applications of Ignition 90-day study[1] (by LANL, LLNL, SNL, LLE, and NRL) includes a description of campaigns that will use ignition in support of the SSP. Some of this report is reproduced below (italics, with minor changes for clarification):

*The campaigns, which include both non-ignition and ignition experiments, will generate data needed to help maintain the national nuclear deterrent without underground nuclear tests. These campaigns have two major components:*

- *Validation of physics-based models and numerical simulation codes, and*
- *Development of robust and high-yield ignition platforms.*

*<u>Validation of physics-based models</u>*
*The major parts of this component are:*

- *Assessments of weapon performance issues,*
- *Output, environment, and effects,*
- *Other national security issues.*

***Table 1** summarizes the ignition application experiments that could be done with igniting targets with varying performance (as defined). They are described in more detail in a classified appendix to the Applications of Ignition report.*

*<u>Developing robust and advanced ignition platforms</u>*

*Assuming the successful delivery of the "Day-1" ignition platform, the Stockpile Stewardship Program will develop plans to deliver more advanced ignition capabilities including robust ignition platforms that are reproducible and deliver higher-gain (gain 5–20) and eventually a high-yield platform with capsule yield exceeding 100 MJ.*

*Concepts being studied include advanced indirect-drive as well as other approaches such as polar direct drive and shock ignition that rely on direct laser illumination of ICF capsules.*

***Table 1. Ignition application experiments.***

| *Application* | *Day 1* | *Expanded Capabilities* | *Robust* | *High Yield* |
|---|---|---|---|---|
| *Assessment and certifications* | *Code V&V* | *Code V&V* | *Code V&V* | *Code V&V* |
| | *Nuclear Cross section* | *Nuclear Cross section* | *Material properties* | |
| | | *NBI* | *NBI* | *NBI* |
| | | *Initial Condition, NEP performance* | *NEP performance* | *NEP performance* |
| *Output, environment, effects* | | | *Output V&V* | *Effects* |
| *Other national security* | | *Forensics* | *V&H* | *V&H* |
| | | | *FNWA* | *FNWA* |

*Day 1: Assume a 1-MJ indirectly driven ignited capsule with currently available diagnostics and facility capabilities*
*Expanded Capabilities: Day 1 plus additional facility/diagnostics capabilities, such as Advanced Radiography Capability (ARC) and determining performance margins*
*Robust: Reproducible and higher-gain capsule (gain of 5–20)*
*High-yield: Different regime with yield >100 MJ*

*Acronyms:*
*V&V = Validation and Verification*
*NBI = National Boost Initiative*
*NEP = Nuclear Explosive Package*
*V&H = Vulnerability and Hardness*
*FNWA = Foreign Nuclear Weapons Assessment*

A high-yield fusion source, (e.g., from an ignited ICF capsule with yields in excess of 100 MJ) is an important goal for NNSA. Such sources could provide a qualitative increase in our ability to assess nuclear performance issues and potentially allow unprecedented outputs and environments experiments enabled by the neutron, x-ray, and gamma-ray emission of a high-yield source.

As stated above in the 90-day study report, alternatives to the current baseline indirect-drive ignition platform[5] will be developed to meet the SSP needs for robust ignition and provide the potential to demonstrate high yield. The baseline indirect-drive platform is the centerpiece of NIC.[6] The goal of the NIC is to demonstrate indirect-drive ignition (gain = 1) by the end of FY2012. There is a subsequent goal to demonstrate a 5-MJ yield in Q1 FY2013 (gain of a few). Additionally, it is important for the ICF Program to examine alternatives to indirect drive that meet the PCF goals in support of SSP (e.g., the 2018 and 2019 pegposts) or provide a path to high yield. The current NNSA ICF and High-Yield Program Plan includes several milestones leading to a "downselect" of advanced concept ignition schemes in FY2014 and demonstration of ignition in FY2017. The PD Plan outlined in this document is consistent with this schedule.

Direct-drive ICF[7] couples more energy to the target than indirect drive for a given laser energy, and thus may increase the ignition margin and potentially provide higher target gain. This may provide a path towards higher yield and enhanced SSP impacts, particularly in areas such as outputs and effects. Significant progress in demonstrating the physics basis of direct-drive ICF has been made over the past decade,[8] including the measurement of areal densities of ~300 mg/cm$^2$ in cryogenic target implosions on OMEGA.[9,10] These measurements are in agreement with 1- and 2D hydrodynamic simulations showing that the fuel adiabat and the drive symmetry can be controlled throughout the implosion. The highest neutron yields are more than 20% of those predicted by 1D simulations for these high-compression implosions.[11] Direct-drive platforms are being developed for some non-ignition high-energy-density (HED) physics experiments on the NIF, e.g. the Defect-Induced Mix Experiment (DIME) by LANL.

The NIF was designed "not to preclude" symmetric direct-drive illumination of ICF capsules.[12] Significant resources, however, would be required for reconfiguration (both cost and NIF system downtime). While it may eventually be in the nation's interest to perform this reconfiguration, it is unlikely to occur within the next decade. As described below, the current NIF indirect-drive beam illumination geometry could be used to study direct-drive ICF physics that would lead to a direct-drive ignition demonstration as early as the end of FY 2017. Such an accomplishment could well motivate a decision to reconfigure the NIF for symmetric direct drive ignition in the future.

The PD concept[13] was developed by LLE to allow direct-drive ignition experiments to be carried out while the NIF is asymmetrically configured for indirect-drive ignition. It has been part of the research program since the inception of the NIC in 2005. PD involves repointing the NIF beams towards the target equator with specially designed phase plates to provide a spherically symmetric implosion. Recent 2D hydrodynamic simulations including all anticipated nonuniformity sources, predict that a gain of 32 could be achieved on the NIF, if the appropriate beam-smoothing modifications are made.[14] The beam smoothing modifications include the implementation of MultiFM SSD[15] and PD-specific phase plates and polarization rotators. A new NIF PD-ITIC will be required to field layered deuterium–tritium (DT) PD cryogenic targets. LLE is currently validating the performance of MultiFM SSD on an OMEGA EP beam line.[16] The OMEGA EP beam lines are very similar to those of the NIF, so the successful demonstration of MultiFM SSD on OMEGA EP will be a significant step towards deployment on the NIF. The validation includes optical measurements of the focal spot[17] and of the imprint levels in planar target experiments.[18] Phase plates, polarization rotators, and the polar-drive PD-ITIC are being designed.

Initial polar-drive experiments have been carried out on the NIF.[19] These experiments were designed to produce specified DT and $D_2$ neutron yields for nuclear diagnostic qualification and calibration. In these experiments, the NIF beams were repointed and the indirect-drive phase plates were defocused to drive the implosion. While the uniformity achieved is not sufficient for ignition experiments, these experiments provided a first look at PD on the NIF. Through the end of February 2012, 22 polar-drive implosions have been performed, with the highest DT neutron yield of $\sim 7 \times 10^{14}$.

In summary, direct-drive ICF potentially offers to provide a higher gain and more robust platform for applications of ignition. The draft PD experimental plan includes a direct-drive ignition experiment by the end of FY2017, with potential benefit to the goals of the PCF. The acquisition of PD optics and beam smoothing would also benefit the non-ignition high energy density PD experiments proposed by LANL and LLNL. The NIF PD plan will be developed and executed consistent with HQ plans for assessing advanced fusion concepts at the NIF. The current ICF Program Plan includes milestones to define options for (Q2FY2013) and downselect (Q1FY2014) of advanced ignition platforms. The activities outlined in this document support this assessment process.

# 3 DESIGN REQUIREMENTS

The system primary criteria and functional requirements and system design requirements are contained in **Appendices A and B.** The subsystems from which these requirements are derived are discussed in the following sections:

## 3.1 Overview

LLE has developed a symmetric hot-spot ignition point design[14,20] that has been placed under configuration management control; see **Appendix D.** This design has evolved from an initial "all-DT" design[22,22,23] which was extensively explored numerically by McKenty.[24] Significant modifications to the design were applied by Goncharov addressing adiabat control,[25] shock timing,[26] and hot-electron pre-heat.[27] The point design comprises a cryogenic DT fuel layer held at just below the triple-point temperature surrounded by a thick CH ablator. Two-dimensional numerical simulations of the symmetric design predict a target gain of 45 when all sources of non-uniformities are considered.[14,27]

The PD hot-spot ignition design,[14] shown schematically in Figure 2, is modeled after the symmetric design above and achieves a gain of 32 when all sources of non-uniformities are considered.[14] The high gain is maintained in the PD geometry by using appropriately designed phase plates and judicious re-pointing of the NIF beams. The 192 NIF beams are grouped into 4 rings of beam in each hemisphere having angular offsets of 23.5°, 30°, 44.5°, and 50° from the pole. For PD, the 30°, 50°, and some of the 44.5° beams are re-pointed to positions on the target as shown in Figure 3. This results in five effective PD beam groups or rings, with the target being irradiated at 23.5°, 44.5°, and 83.0°.

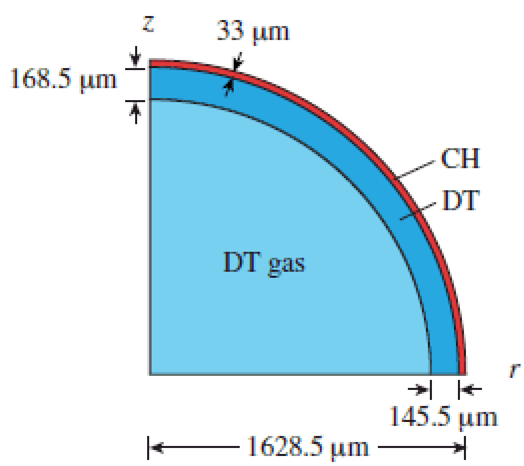


**Figure 2: The PD hot-spot ignition design consists of a thin (33 mm) CD ablator with a 168-mm-thick DT ice layer. As discussed later, the ice layer may be shimmed to be thinner at the equator than at the pole to optimize the use of the beam energy available on the NIF.**

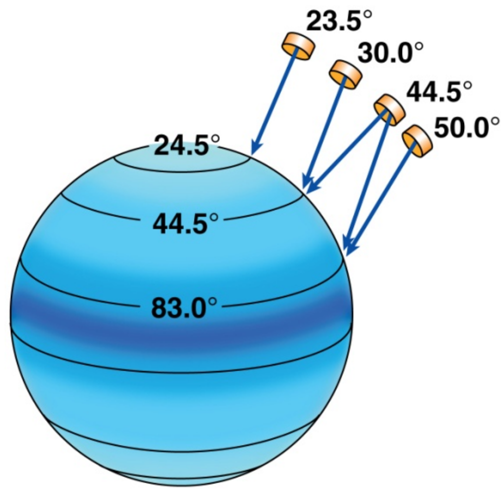


**Figure 3: PD pointing configuration showing the four rings of NIF beams and five PD beam groups or rings, yielding irradiation at three different latitudes on the target.**

Ignition experiments with PD require that each of the five PD beam rings have a unique pulse shape, and continuous phase plate. The combination of these components, coupled with single-beam smoothing provided by the MultiFM 1D SSD on the pickets and polarization smoothing, provide the required drive uniformity to achieve ignition conditions. Figure 4 illustrates the pulse power vs. time (a) and the resultant beam intensity profiles (b) (obtained from the requisite phase plate) for each ring of NIF beams. The use of the triple-picket pulse (Figure 4a) represents a quantitative change from the strategy employed in previous PD ignition designs.[7] OMEGA experiments have shown that picket pulses can be experimentally tuned for optimal shock timing.[26] Furthermore, adiabat shaping and increased shell stability can be realized by adjusting the strength of the shocks launched by the pickets. A step pulse at the start of the main drive launches a fourth shock giving further control over the adiabat. Shock tuning of this four-shock design will be conceptually identical to the tuning performed for indirect-drive targets. A cone-in-sphere target design either filled with liquid $D_2$ or using a thick ablator design (to appropriately spread the shock arrival times at the inner shell wall) will be used. Due to the inherent asymmetry of PD, these shock timing experiments will rely on the dual-axis target design employed by the NIC campaign and currently under development for PD experiments on OMEGA.

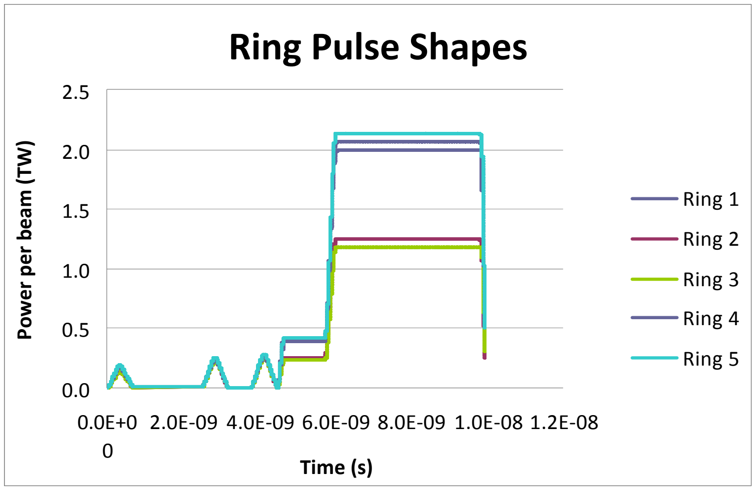


(a)

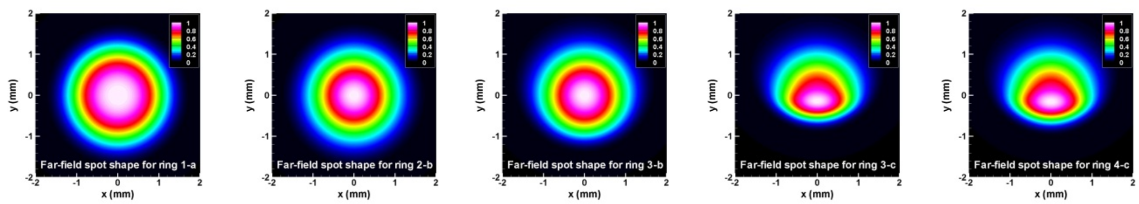


(b)

Ring 1 Ring 2 Ring 3 Ring 4 Ring 5

**Figure 4a: The pulses in each of the five NIF PD beam rings are amplified to a different degree as illustrated by the pulse shapes shown. Figure 4b: The resultant beam focal spot shapes are shown after being modified by their respective phase plates.**

Phase plate design is an iterative process between target designers and laser scientists to determine if the amplitude modulations produced by the phase plates are safe to propagate through the laser system. A study is underway to evaluate the spot shape required near the target equator. The equatorial phase plate design provides the most difficult challenge in attempting to symmetrically drive the implosion. The designed spot shape for PD beam Ring 5 is shown at the far right of Figure 4b. It shows the redistribution of the beam intensities from a circular shape into a highly elliptical one having a strong shear near the bottom edge of the beam. The resulting asymmetric spot requires one of the most challenging phase plate designs ever attempted. Such a shape efficiently uses all of the energy in the equatorial beams, relaxing the maximum laser energy required. Initial designs have been reviewed by LLNL and been found to meet the NIF phase-to-amplitude modulation conversion requirements.

The PD hot-spot design requires shimming the target fuel layer at the equator to assist in balancing the poloidal distribution of laser energy on target (the ice is deliberately thinned at the equator to reduce the total mass being driven by the higher incidence beams). A 10-µm, Legendre mode $\ell = 2$ shim is induced in the ice layer oriented along the north-south axis of the target. By shimming the fuel layer, the laser energy between the equator and the pole can be rebalanced by 10%, relaxing the higher energy required near the equator.

## 3.2 Beam Smoothing

PD ignition requires MultiFM 1D SSD single-beam smoothing to achieve the required on target irradiation uniformity when used in combination with CPP's and DPR's. The system point design requires laser pulse shapes with multiple picket pre-pulses to improve adiabat shaping and shell stability; this strategy requires improved beam-smoothing to limit imprint of laser-pulse-induced non-uniformities that disrupt the implosion.

One-dimensional SSD with multiple phase-modulation frequencies requires pre-conditioning the laser pulse with three high-frequency modulators to increase the bandwidth and is followed by a dispersion grating to increase the temporal skew, as shown in Figure 5. MultiFM 1D SSD[28] has been optimized to provide the required beam smoothing to enable PD ignition. Modifications required to implement this technology on the NIF are limited to the fiber-based systems located in the Master Oscillator Room (MOR), a new diffraction grating in the preamplifier module (PAM) and new final optics, including CPP's and DPR's specifically designed for polar-drive illumination of directly-driven targets. LLE has implemented a NIF PAM into beam four of the OMEGA EP laser, including the new diffraction grating, and will fully validate the operation and smoothing effectiveness of 1D MultiFM SSD (imprint efficiency experiments and equivalent target plane [ETP] images) before the end of FY12. LLE and LLNL are currently examining the modifications required for the NIF MOR to determine the optimal means to provide both current and PD capability.

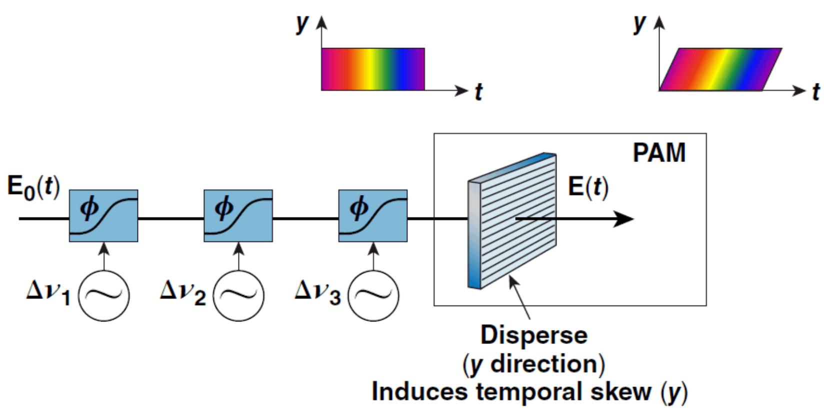


**Figure 5: MultiFM 1D SSD uses three high-frequency modulators to create a total ultraviolet (UV) bandwidth of 500 GHz and ±100 μ-rad divergence. The uncompensated dispersion grating in the NIF PAM introduces a spatio-temporal shear across the near-field beam, increasing the number of color cycles and reducing the beam imprint on the target.**

Figure 6 shows the UV effective divergence and the non-uniformity reached after the first picket pulse. This optimized MultiFM 1D SSD system smoothes the target irradiation with a maximum applied UV bandwidth of 500 GHz and laser divergence of ±100 μ–rad (at full beam size), limited by the NIF PAM and Transport Spatial Filter (TSF) pinholes. Phase-modulation at 21.2, 22.8, and 31.9 GHz produce independent UV bandwidths of 57.3, 142.8, and 397 GHz, respectively.

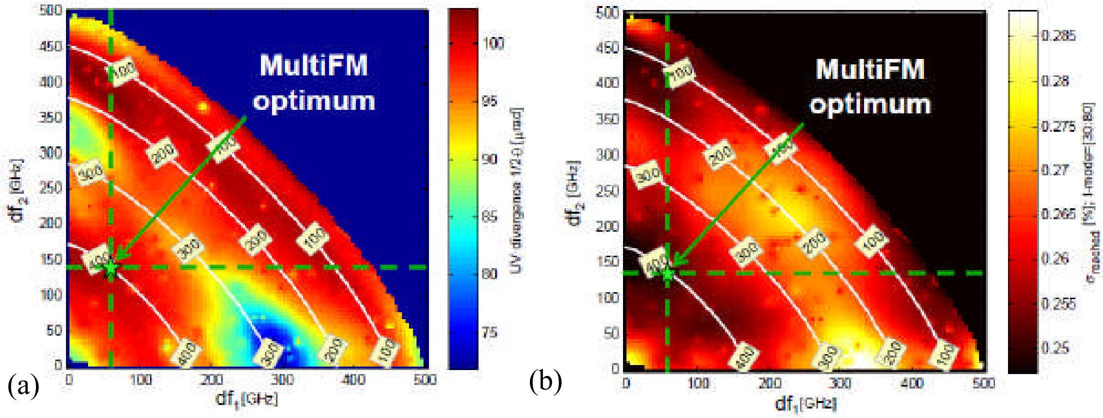


**Figure 6: The UV effective divergence (a) and non-uniformity reached (ℓ = 30 to 80) after the first picket pulse has an optimum (b) in the six-dimensional MultiFM parameter space ($f_1$, $f_2$, $f_3$; $\Delta f_1$, $\Delta f_2$, $\Delta f_3$), as shown. Contours of constant $\Delta f_3$ are shown that correspond to the first two individual-modulator bandwidths that sum to a total UV bandwidth of 500 GHz for the optimal modulation frequencies.**

Figure 7 shows the pulse shape for the PD point design.[14] Three "picket" pulses precede the main drive pulse with peak power less than the NIF laser system limit. The large bandwidth and divergence required for MultiFM 1D SSD would cause this limit to be exceeded if it were also applied to the main drive pulse due to phase-to-amplitude modulation conversion, limiting its application to the picket pulses only. This technique, termed dynamic bandwidth reduction (DBWR), minimizes stress on the laser system with only small reductions of target gain calculated in 2D hydrodynamic simulations (the blue diamonds in Figure 7).

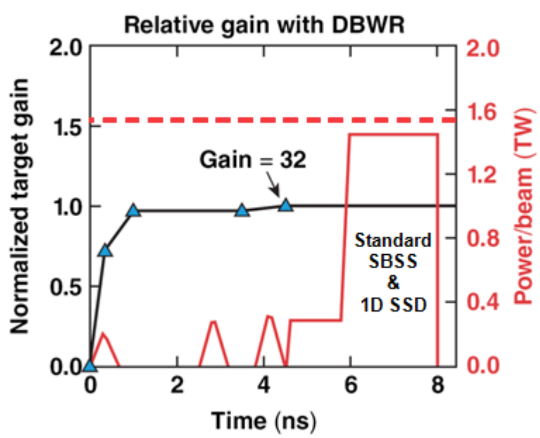


**Figure 7: The schematic on-target, UV pulse shape is shown, illustrating how the ignition gain does not increase if the increased bandwidth from the MultiFM 1D SSD is applied to the second, third picket, or the step foot pulse. The model assumes that the standard SBSS and 1D SSD (single FM) modulations are applied to the main drive pulse. Plotted in red are the pulse power per beam and power limit for the NIF.**

A fail-safe scheme to ensure that sufficient phase modulation is applied during every part of the PD pulse is required. Technical limitations in rapidly switching the microwave power on and off in less than approximately one nanosecond preclude using a common set of phase modulators for both the pickets and main drive pulses. Separately creating and then optically combining picket pulses having the MultiFM bandwidth with a main drive pulse with Stimulated Brillouin Scattering (SBS) bandwidth added, as shown schematically in Figure 7, meet this need and is the baseline approach. The main drive pulse can be produced from the existing NIF MOR, and a new fiber-optic-based seed source and an arbitrary waveform generator (AWG) that produces multiple picket pulses with phase modulation applied at optimal modulation frequencies (see Figure 5) is being developed. The development plan for implementation of MultiFM 1D SSD on the NIF is given in **Appendix I**.

SBS in NIF final optics must be suppressed by applying phase modulation to the pulse to stay below the SBS threshold for this nonlinear optical process. The required level of SBSS bandwidth is currently achieved with the standard NIF SBSS system, which uses 3- and 17-GHz modulators that produce at least 33- and 40-GHz (1ω) of bandwidth, respectively.

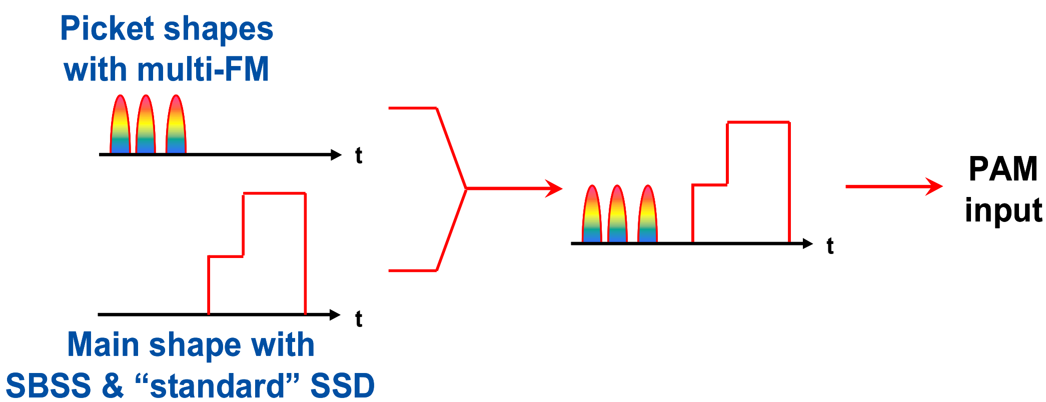


**Figure 8: The PD ignition pulse shape will be produced by optically combining the two separate seed sources that produce the triple-picket pulse shape and a main drive pulse.**

A new diffraction grating is required in each of the NIF PAM’s to provide the increased angular dispersion. The PAM currently includes a diffraction grating for indirect drive 1D SSD at an image relay plane located after two passes in the multi-pass Nd-glass rod amplifier (MPA). This grating or a retro-reflection mirror may be selected using a translation stage, depending on the selected mode of operation. The translation stage will be redesigned to accommodate the additional optic required for MultiFM 1D SSD and tested on the PAM currently in operation on beam four of the OMEGA EP laser system. LLE will work closely with LLNL staff to develop a plan for modifying the NIF PAM’s.

### 3.3 User Optics

Optics that further improve the beam-smoothing are critical to the success of PD ignition. Uniquely designed phase plates and distributed phase rotators are needed to meet the stringent irradiation uniformity requirements for high-gain target performance. The top and bottom sets of 96 beams are sub-divided into five rings based on their current cone angles (see Figure 3). Phase plates are being designed to produce focal spots (see Figure 4b) having the sizes and shapes necessary to create uniform illumination of the target in an optimized PD configuration. Three phase plate designs (Rings 1, 2 and 3; the required on target focal spots are shown in the three images on the left side of Figure 4b) produce circularly-symmetric focal spots; while the other two phase plates (Rings 4 and 5; the two right-hand images of Figure 4b) produce skewed, elliptical focal spots. The design is compatible with the current NIF configuration that places all phase plates between the frequency conversion crystals located in the final optics assembly (FOA). The design and manufacture of all phase plates must meet the NIF specifications for acceptable near-field modulation to control the probability of laser damage in other optical elements within the FOAs. Advanced phase plate design techniques are being developed to simultaneously achieve steep irradiance slopes in the focal plane while limiting the near-field modulation when operating the NIF beams at the energies and peak powers required for PD ignition. LLE will lead the design of these phase plates while LLNL will procure (subject to funding) the optics and fold the installation and use into the facility operational planning.

Polarization smoothing[29] provides additional beam smoothing by producing two orthogonally polarized focal spot patterns on target. The additional smoothing of the focal spots, provided by DPR's, is critical for PD target performance. Two polarization concepts are being developed for use in the UV portion of the NIF FOA's. The current NIF polarization rotation scheme does not provide adequate smoothing for the most important PD imprinting modes. The baseline design includes a 2 x 2 checkerboard array of KD*P half-wave plates. Two diagonal quadrants of the array will be populated with the KD*P plates. **Appendix H** provides a detailed development plan for the DPR's. LLE will develop and test a suitable concept and work with LLNL to develop a fabrication and qualification plan. LLNL will procure the optics and fold the installation and use into the facility operational plan.

Performance of the DPR's will be characterized prior to their implementation at NIF. The best means to perform this work is under discussion by LLE and LLNL, but it will likely involve reconstruction and reactivation of the NIF Precision Diagnostic Station (PDS). The PDS has the same final optics configuration as the NIF FOA and contains an extensive suite of diagnostics that can be used for detailed performance characterization of the selected NIF beam. The PDS will be used for a number of measurements, including the irradiance modulation from the edges of the DPR's and the level of Stimulated Raman Scattering (SRS) generated by a segmented DPR.

Approximately 400 optical elements will be fabricated for use in the NIF FOA's (192 CPP's and 192 DPR's plus spares). Additional manufacturing capability is being developed to meet the project schedule. Close cooperation between LLE and LLNL scientists and engineers will ensure successful design, fabrication, and deployment of PD phase plates and DPR's.

## 3.4 Cryogenic Target Handling and Insertion

The approach taken in the design of the PD-ITIC is to minimize the impact to the NIF facility. The project has emphasized maintaining the existing NIF space envelope as much as possible, while employing several existing NIF systems including the Target Alignment System (TAS) illustrated in Figure 9, the Load, Layer, and Characterization Station (LLCS), and the cryogenic target positioner (cryoTARPOS) interface.

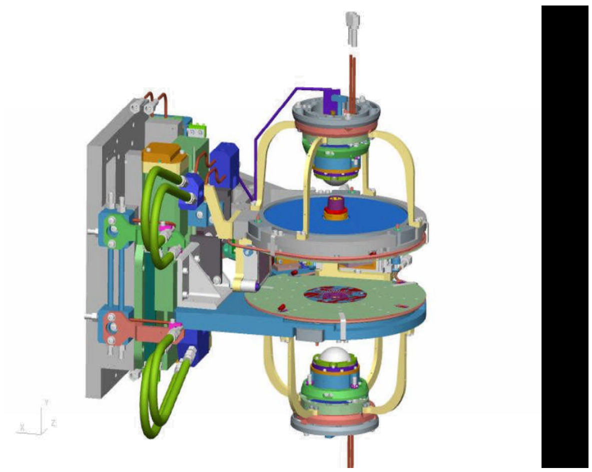

**Figure 9: The NIF TAS is used to simultaneously view the target and the location of all 192 beam focal spots. The maximum allowable axial height between the two target alignment plates is 37.6 mm setting the design constraint for the PD-ITIC.**

Three key requirements that will have a substantial impact on the PD-ITIC project are:

- Target exposure—the target ice layer must survive exposure to the TC environment for up to 5 seconds without compromising the layer quality;
- Use of the current Cryogenic NIF ITIC space envelope; and
- Single-sided shroud retraction.

These requirements impose severe limitations on the handling of the cryogenic target and the sequencing of pre-shot operations (e.g., sub-cooling, alignment, layering). LLE is deploying a DT-capable target development test stand to optimize layered target survival once it is exposed to the ambient radiation of the NIF (and OMEGA) target chamber. Should design requirements not be met under the constraints of the TAS and single-sided shroud retraction, redesign of the TAS will be required. The deployment of an opposed port shroud retractor as originally base-lined is currently not being considered as an alternative. Furthermore, LLE will develop the techniques required to layer, shim, and characterize an ignition target that has been filled with fuel through a fill tube. LLE will develop and test schemes for single-sided shroud retraction. Efforts to develop the required capability and techniques began in FY11 and will continue until a working PD-ITIC concept is ready for a CDR in the FY14–FY15 timeframe. LLE will work directly with LLNL cryogenic engineers to develop a PD-ITIC that uses as much of the existing cryoTARPOS as possible. The goal is to develop a replaceable ITIC that can be swapped with the indirect drive ITIC with minimal impact on facility operations. LLE will fabricate a prototype PD-ITIC and work with LLNL staff to install and test at the NIF.

# 4 NOTES AND REFERENCES


1. Applications of Ignition 90-day study, submitted to NNSA on Feb. 29, 2012.
2. Gain is defined as the fusion yield divided by the laser energy used to drive the target.
3. Memo from D. Cook to C. Deeney, March 24, 2011.
4. A "pegpost" is similar to a milestone.
5. S.W. Haan et al. "Point Design Targets, Specifications, and Requirements for the 2010 Ignition Campaign on the National Ignition Facility." *Phys. Plasmas* **18** (5), 051001 (2011).
6. UCRL-AR-213718, Rev 4.0.
7. R.L. McCrory et al. "OMEGA ICF Experiments and Preparation for Direct-Drive Ignition on NIF," *Nuclear Fusion* **41** (10), 1413–1422 (2001).
8. R.L. McCrory et al. "Progress in Direct-Drive Inertial Confinement Fusion Research." *Phys. Plasmas* **15** (5), 055503 (2008).
9. V.N. Goncharov et al. "Demonstration of the Highest Deuterium-Tritium Areal Density Using Multiple-Picket Cryogenic Designs on OMEGA." *Phys. Rev. Lett.* **104** (16), 165001 (2010).
10. T.C. Sangster et al. "Shock-Tuned Cryogenic-Deuterium-Tritium Implosion Performance on Omega." *Phys. Plasmas* **17** (5), 056312 (2010).
11. T.C. Sangster et al., presented at the 2011 APS/DPP meeting.
12. D. Eimerl et al. *Configuring NIF for Direct Drive Experiments*. First Annual International Conference on Solid State Lasers for Application to Inertial Confinement Fusion, Bellingham, WA, SPIE (1995).
13. S. Skupsky et al. "Polar Direct Drive on the National Ignition Facility." *Phys. Plasmas* **11** (5), 2763–2770 (2004).
14. T.J.B. Collins et al., "Preparing for Polar Drive at the National Ignition Facility," accepted for publication in *Phys. Plasmas* (May 2012).
15. J.A. Marozas et al. "Smoothing by Spectral Dispersion (SSD) for Multiple-Picket Pulses on OMEGA and the NIF." *Bull. Am. Phys. Soc.* **55** (15), 294 (2010).
16. J.H. Kelly et al. "OMEGA EP: High-Energy Petawatt Capability for the OMEGA Laser Facility." *J. Phys. IV France* **133,** 75–80 (2006).
17. S.P. Regan et al. "Performance of 1-THz-Bandwidth, Two-Dimensional Smoothing by Spectral Dispersion and Polarization Smoothing of High-Power, Solid-State Laser Beams." *J. Opt. Soc. Am. B*. **22** (5), 998–1002 (2005).
18. T.R. Boehly, et al. "Reduction of Laser Imprinting Using Polarization Smoothing on a Solid-State Fusion Laser." *J. Appl. Phys.* **85** (7), 3444–3447 (1999).
19. P.W. McKenty, et al. "Design of High-Neutron-Yield, Polar-Drive Targets for Diagnostic Activation Experiments on the NIF." *J. Phys.: Conf. Ser.* **244,** 032054 (2010).
20. OMEGA Point Design for High Yield, Spherical, Cryogenic ICF Experiments; LLE, S-AA-G-078.
21. See National Technical Information Service Document No. DOE/SF/19460-317 [Laboratory for Laser Energetics LLE Review **79,** 121 (1999)]. Copies may be obtained from the National Technical Information Service, Springfield, VA 22161.

22. S.E. Bodner, et al., *Phys. Plasmas* **5**, 1901 (1998).
23. C.P. Verdon, *Bull Am. Phys. Soc.* **38**, 2010 (1993).
24. P.W. McKenty et al., *Phys. Plasmas* **8**, 2315 (2001).
25. V.N. Goncharov et al., *Phys. Plasmas* **10**, 1906 (2003).
26. T.R. Boehly et al., *Phys. Rev. Lett.* **106**, 195005 (2011).
27. V.N. Goncharov et al., *Phys. Plasmas* **15**, 056310 (2008).
28. J.A. Marozas, J.D. Zuegel, and T.J.B. Collins, *Bull. Am. Phys. Soc.* **55** 294 (2010).
29. J.E. Rothenberg, *J. Appl. Phys*., **87** 3654 (2000).

# Appendix A: Primary Criteria and Functional Requirements

## A1 INTRODUCTION

### A1.1 Objectives

This document establishes the scientific and engineering requirements that must be achieved at the NIF to fulfill the campaign requirements to achieve PD Ignition. Program goals have been translated into laser power, laser beam characteristics, target and other performance specifications. The basis for these requirements is specified in the LLE Point Design document, *Triple Picket Point Design for Polar Drive Ignition on the NIF*[2]. LLE and LLNL may revise the Primary Criteria and Functional Requirements as plans for the NIF PD campaign are further developed.

The Functional Requirements and Primary Criteria described herein serve as a technical baseline for the project.

Top-level safety, environmental protection, safeguards and security, building systems, and quality assurance requirements are in accordance with the *NIF Functional Requirements and Primary Criteria* (NIF-0001006-OE, September 2006). The sections below are hereby adopted and incorporated into this document by reference.

- Section 3: Safety Requirements
- Section 4: Environmental Protection
- Section 5: Safeguards and Security
- Section 6: Building Systems
- Section 7: Operational Availability
- Section 8: Decontamination and Decommissioning
- Section 9: Quality Assurance
- Section 10: Orders, Codes, and Standards

### A1.2 Terms

The terms “should” and “shall” have important implications beyond what might be implied by common usage. “Shall” denotes a requirement that is mandatory and must be met. “Should” denotes a non-mandatory recommendation or goal.

### A1.3 Site-Specific Requirements

These requirements are applicable to the LLNL site, selected by the DOE in the Record of Decision for the Programmatic Environmental Impact Statement for Stockpile Stewardship and Management.

# A2 CAMPAIGN-RELATED REQUIREMENTS

The laser system shall be designed to meet the following requirements simultaneously, although all performance requirements need not be demonstrated simultaneously on a single event.

## A2.1 Laser

### A2.1.1 Laser Pulse Energy and Peak Power

The laser shall be capable of routinely producing a temporally-shaped pulse of energy at least 1.8 MJ incident on a PD capsule. Table A1 lists the details of the PD beam pointing, energy per beam, full NIF equivalent 192-beam energy, total energy per beam group/ring, and peak power per beam.

**Table A1. Details of the laser configuration and energy required to drive a PD ignition capsule.**

| Beam group | Polar angle | Quads- (Northern Hemi.) | Quads- (Southern Hemi.) | # beams | Energy/ beam (kJ) | 192- beam FNE energy (MJ) | Total energy (MJ) | Peak Power (TW) |
|---|---|---|---|---|---|---|---|---|
| 1a | 23.5 | 33T, 24T, 15T, 42T | 33B, 24B, 15B, 42B | 32 | 9.068 | 1.741 | 0.2902 | 2.06 |
| 2b | 30 | 36T, 26T, 13T, 41T | 16B, 21B, 31B, 44B | 32 | 5.293 | 1.016 | 0.1694 | 1.18 |
| 3b | 44.5 | 12T, 22T, 32T, 45T | 14B, 25B, 35B, 43B | 32 | 5.777 | 1.171 | 0.1785 | 1.25 |
| 3c | 44.5 | 14T, 25T, 35T, 43T | 12B, 22B, 32B, 45B | 32 | 8.773 | 1.684 | 0.2807 | 1.99 |
| 4c | 50 | 11T, 16T, 21T, 23T, 31T, 34T, 44T, 46T | 11B, 13B, 23B, 26B, 34B, 36B, 41B, 46B | 64 | 9.402 | 1.805 | 0.6017 | 2.13 |
| | | | | 192 | | | 1.520 | |

### A2.1.2 Laser Pulse Wavelength

The wavelength of the laser pulse delivered to the target shall be 0.35 μm. A wave length separation of up to 2 Angstroms will be required.

### A2.1.3 Beamlet Power Balance

The rms deviation in the power delivered by the laser beams from the specified power shall be ≤ 8% root-mean-square (rms) (quad-to-quad) of the specified power. For the picket pulse portion of the pulse, this shall be averaged across all pickets; for the main drive pulse it shall be averaged over any 2-ns time interval.

### A2.1.4 Beamlet Positioning Accuracy

The rms deviation in the position of the centroids of all beams from their specified aiming points shall not exceed 50 μm at the target plane or its equivalent.

### A2.1.5 Laser Pulse Shaping

The laser shall be capable of producing a pulse with overall duration of up to 20 ns. The PD pulse shall include at least three picket pulses independent from each other and temporally separate from a main drive pulse.

### A2.1.6 Laser Pulse Dynamic Range

The laser shall be capable of delivering UV pulses to the PD target with a dynamic range of at least 50:1, wherein the dynamic range is defined as the ratio of intensity at the peak of the pulse to the intensity in the initial "foot" portion of the pulse.

### A2.1.7 Capsule Irradiation Symmetry

The NIF target chamber has four rings of laser ports in each hemisphere. Each port is fitted with a quad of (four) laser beams. For PD ignition, the rings at 44.5$^o$ and 135.5$^o$ are each conceptually divided into two rings having beam pointing latitudes of 44$^o$ and 83$^o$ in the northern hemisphere and 97$^o$ and 146$^o$ in the southern hemisphere, resulting in five independent PD beam rings per hemisphere, with each ring having its own energy on target. These five rings concentrate energy on the polar (24.5$^o$ and 155.5$^o$), mid-latitude (44$^o$ and 146$^o$) and equatorial regions (83$^o$ and 97$^o$) of the target. Quad polar angles and beam pointing are described in Table A2. Variations in the UV energy deposited on the PD fusion target are determined from a sum-in-quadrature summation of all sources of illumination perturbations.

**Table A2. NIF PD laser-beam and quad pointing latitudes.**

| Quad Polar Angle** | Beam Pointing Latitude** | Quad |
|---|---|---|
| 23.5$^o$ | 24.5$^o$ | 15T, 24T, 33T, 42T |
| 30.6$^o$ | 44$^o$ | 13T*, 26T, 36T*, 41T |
| 44.5$^o$ | 44$^o$ | 12T, 22T, 32T, 45T |
| 44.5$^o$ | 83$^o$ | 14T, 25T, 35T, 43T |
| 50$^o$ | 83$^o$ | 11T, 16T, 21T, 23T, 31T, 34T, 44T, 46T |
| 130$^o$ | 97$^o$ | 11B, 13B, 23B, 26B, 34B, 36B, 41B, 46B |
| 135.5$^o$ | 97$^o$ | 12B, 22B, 32B, 45B |
| 135.5$^o$ | 146$^o$ | 14B, 25B, 35B, 43B |
| 150$^o$ | 146$^o$ | 16B, 21B*, 31B, 44B* |
| 156.5$^o$ | 155.5$^o$ | 15B, 24B, 33B, 42B |

** 0$^o$ is Target Chamber vertical axis

*These quads have polar angles 0.58$^o$ closer to the equator than the nominal angle listed.

### A2.1.8 Pre-Pulse Power

The laser intensity delivered to the target during the 20-ns interval prior to arrival of the main laser pulse shall not exceed $10^8$ W/cm$^2$.

#### A2.1.9 Laser Pulse Spot Profile

Each beam shall deliver its design energy and power encircled in a spot at the target plane defined by the *Triple Picket Point Design for Polar Drive Ignition on the NIF.*[2] Polar ($24.5^o/155.5^o$) and mid-latitude ($44^o/146^o$) ring beams shall have circular spots and the equatorial beams ($83^o/97^o$) shall have spot profiles defined to maximize beam uniformity and laser energy coupling to the target.

#### A2.1.10 Beam Smoothness

The NIF shall have spatial and temporal beam conditioning to control intensity fluctuations in the target plane.

##### *A2.1.10.1 MultiFM 1D SSD Beam Smoothing*

The NIF shall provide MultiFM 1D SSD applied to the picket pulses that provide additional beam smoothing in the target plane.

##### *A2.1.10.2 Dynamic Bandwidth Reduction*

The NIF shall apply MultiFM 1D SSD beam smoothing to only the picket portion of the main drive pulse in order to minimize laser imprint non-uniformity and minimize stress on the laser system during propagation of the main drive pulse. Fail-safe mechanisms shall be deployed to assure that, for every system shot, MultiFM is applied during the picket portion of the pulse and not during the main drive pulse, and that at least 30 GHz of modulation at 3 GHz modulation frequency is applied during the main pulse. Reliability of these fail-safe mechanisms shall be at least $1/10^6$.

##### *A2.1.10.3 Phase Plates*

The NIF shall be equipped with CPP specifically designed for the requirements specified in Sect. 2.1.10 to provide the required irradiance balance and beam smoothing of each beam.

##### *A2.1.10.4 Polarization Smoothing*

The NIF shall provide polarization beam smoothing for each beam that will smooth the focal plane speckle by the square root of two, averaged over the spatial frequencies of primary concern for the target point design.

#### A2.1.11 Beamlet Mistiming

The NIF shall have the capability to co-time the delivery of the laser pulse to target to $\leq 30$ ps-rms.

### A2.2 Experimental Area

Sections 2.2 and 2.2.1–2.2.8 and 2.2.10–2.2.12 of the NIF Primary Criteria and Functional Requirements document (NIF-0001006-OE, September 2006) are hereby incorporated into this document. Section 2.2.9 is modified as follows:

### A2.2.9 Diagnostic Instrument Capabilities for Ignition and Applications Experiments

The target chamber and area shall be capable of accommodating diagnostic instruments for the following measurements necessary for polar direct drive fusion ignition and applications experiments (specific diagnostic intended):

- Symmetry of x-ray emission from imploded cores with 5- to 10-micrometer spatial resolution (X-ray Framing Camera).
- Time-dependent laser light backscattered into the focusing lens (FABS).
- Strength of radiation-driven shocks with 5- to 10-micron resolution and time resolution of 10 ps (VISAR).
- Fusion yield over a range from $10^{14}$ to $10^{19}$ neutrons (NAD, nTOF).
- Primary and scattered images of neutron emission from imploded cores with 15-micron spatial resolution (NIS).
- Temperature of the compressed fusion fuel with 200 eV or 3% accuracy (whichever is greater) for ion temperatures of 2 keV or greater (nTOF).
- Time dependent measure of $T_{hot}$ and $F_{hot}$ using the number and energy distribution of fast electrons from 5 keV to 300 keV (HXRD).
- Absolute bang-time to +/- 30 ps (SPBT).
- Reaction history with 30 ps-rms timing accuracy (GRH).
- Average cold fuel areal density, ρR with +/- 7% accuracy (MRS).
- Imaging of the ablator shell to 30-μm resolution (backlighting).

# Appendix B: System Design Requirements for Polar Drive Ignition Campaign

## B1 SCOPE

This System Design Requirement (SDR) document establishes the performance, design, and development requirements for the NIF PIC. The modifications to the existing NIF includes changes to the MOR and PAM to implement MultiFM 1D smoothing by spectral dispersion, PD continuous phase plate and polarization rotator beam smoothing optics, and implementation of a PD target insertion cryostat to layer the fuel and position PD targets in the target chamber. LLE and LLNL may revise the System Design Requirements as plans for the NIF PD campaign are further developed.

The Campaign consists of the following work breakdown structure (WBS) elements:

- 1.1 Management and Administration
- 1.2 Systems Engineering
- 1.3 Target Physics
- 1.4 Integrated Target Systems
- 1.5 Target Diagnostics and Experimental Systems
- 1.6 User Optics
- 1.7 Laser System
- 1.8 Operational Capabilities

Descriptions of each of the WBS elements are contained in **Appendix C.**

## B2 APPLICABLE DOCUMENTS

### B2.1 Applicable Documents

The following Project Documents apply to the Laser System as specifically referenced in later sections.

#### B2.1.1 Applicable NIF/NIC/PIC Project Documents

The following NIF/NIC Project Documents apply to the Laser System as specifically referenced in later sections.

- Functional Requirements and Primary Criteria, NIF-0001006-OE, September, 1996.
- National Ignition Campaign Execution Plan, UCRL-AR-213718/NIF-0111975.
- National Ignition Facility System Design Requirements, Laser System, NIF-0000192-2, UCRL-ID-126998.
- Conceptual Design; Polar Drive Ignition Campaign.
- Work Breakdown Structure, Polar Drive Ignition Campaign, **Appendix C**.

### B2.2 Applicable LLE Documents

The following LLE Project Documents apply to the Laser System as specifically referenced in later sections.

- Triple Picket Point Design for Polar Drive Ignition of the NIF, **Appendix C**.
- Requirements for the NIF Polar Drive Ignition Target Cryostat, LLE, Q-NP-R-001.
- Laser Sources, MultiFM 1D SSD on OMEGA EP, LLE, T-BW-R-005.

### B2.3 Applicable US Government Orders and Standards

This applicable government orders and standards cited in the NIF Primary Criteria and Functional Requirements document (NIF-0001006-OE) apply and are incorporated into this plan.

## B3 SYSTEM DEFINITION

The NIF Laser System was designed to support ICF experiments with the goal of fusion ignition. Weapons physics experiments, radiation effects simulation, and other experiments including HED science and inertial fusion energy will also be conducted as permitted by the system design. The Laser System is defined as the equipment that generates and delivers high-power optical pulses to the target chamber, from optical pulse generation (OPG) through the final optics assemblies. It includes supporting structures, optical components, and the laser control system and auxiliary systems. In addition, it includes the relevant target chamber support systems that facilitate production and integration of cryogenic PD targets that contain the DT fuel layer.

### B3.1 System Description

The NIF Laser system is configured in a four-pass architecture with laser pulse injection into the output spatial filter. The beams are arranged in groups of contiguous beams packed in an array that is four beams high. A total of 192 beams are deployed. The master oscillator in the pulse generation system creates the initial optical signal, which is temporally shaped and distributed to individual beam line amplifiers.

Recent advances in the theoretical modeling of ICF implosions[1,2] where a cryogenic shell of DT fuel is driven inward by means of direct or indirect laser illumination have achieved high compression resulting in fusion of nuclei. This is accomplished using complex pulse shape designs such as combining three picket pulses with the main drive pulse as illustrated in Figure B1.

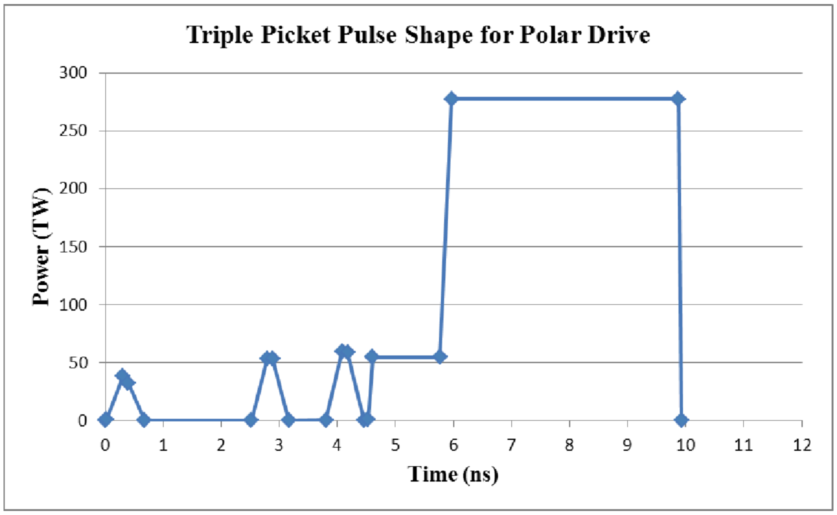


**Figure B1: Illustration of triple picket pulse shape design used in the PIC point design.**

Polar-drive implosions on the NIF require smoothing of the laser-imposed non-uniformities.[3] Beam SSD smoothes the far-field speckle pattern in a time-integrated sense by continuously changing the near-field phase front of the laser pulse. The current configuration of the NIF uses a single modulation frequency (17 GHz) and bandwidth (90 GHz maximum) in one dimension (i.e., 1D SSD), that are insufficient for polar-drive targets. The main drive pulse is also phase modulated at 3 GHz to suppress SBS.

MultiFM 1D SSD[4] employs multiple frequencies (21, 23, and 32 GHz) to improve the smoothing rate of low-spatial-frequency beam non-uniformities without producing resonances at higher spatial frequencies because multiple modulators interact to average the resonant spectral features using a carefully selected choice of modulator frequencies.

The PIC will provide a second seed source in the MOR that generates a triple-picket pulse shape with MultiFM 1D SSD modulation and a main pulse with standard phase modulation for SBS Suppression (SBSS) and 1D SSD. The two seed pulse components will be optically combined to provide a fail-safe method of realizing DBWR that is required to provide sufficient beam smoothing during the initial imprint phase without exceeding laser limits during the main pulse. The combined pulses will be injected into the PAM.

The PAM is a compact stand-alone system with a nominal gain of ~$10^{10}$ that includes a Nd-doped phosphate glass regenerative amplifier (regen), beam shaping, and a MPA. A new diffraction grating in the PAM is required to increase the dispersion of the pulse generated by the MultiFM 1D SSD system.

After amplification, the beam is transported to and injected into the far-field of the transport spatial filter, which directs the beam through the booster and cavity amplifiers in a multi-pass scheme. The nominal hard aperture size is ~40 cm. Amplifier flash lamps uniformly pump the amplifier glass slabs. The power conditioning system providing this power utilizes banks of dielectric capacitors. Switch-out of the pulse from the amplifier cavity is accomplished with the Plasma Electrode Pockels Cell switch.

After passing through the booster amplifier and TSF each of the l92 beams is directed to the target chamber using a number of high-reflectivity mirrors. At the chamber the beams are directed to one of four rings of ports in each hemisphere. Clustered into groups of four beams, they are directed through the final optics assembly. Within each final optic system, the frequency of each beam is tripled using a KDP doubler crystal and a KD*P tripler crystal. CPP's produce a focal spot with a defined spatial envelope and speckle pattern and DPR's provide additional beam smoothing before the beam is focused onto the target with the focusing lens.

During the transport of each laser beam from the preamplifier to the target, precision systems provide for the beam alignment, and the measurement of beam spatial and temporal characteristics. In the target chamber, the spherical target is maintained at cryogenic temperature (~18$^{o}$K) and precisely positioned by the PD-ITIC.

The PIC modifications to the existing NIF laser system are comprised of five Level-2 WBS elements that are covered by this SDR document and are listed below. The complete Work Breakdown structure is given in **Appendix C.**

- 1.4 Integrated Target Systems
- 1.5 Target Diagnostics and Experimental Systems
- 1.6 User Optics
- 1.7 Laser Systems
- 1.8 Operational Capabilities

Elements of the existing NIF architecture that are not covered by this SDR document but are already defined in the NIF Laser System Design Requirements[5] document include, and are incorporated by reference:

- Amplifier System
- Pockels Cell System
- Amplifier Power Conditioning System
- Laser Auxiliary Systems
- Beam Transport Enclosures
- Interstage Subsystems
- Support Structures
- Opto-mechanical Systems (except for User Optics Subsystems defined in 3.2.1.3)
- Amplifier Slabs
- Lenses
- Mirrors
- Polarizers
- KDP and KD*P Crystals
- Debris Shields and Optics
- Alignment Systems
- Beam Diagnostics
- Wavefront Control Systems
- Final Optic Assemblies (except for User Optics Subsystems defined in 3.2.1.3)

### B3.2 System Functions

The overall functions of the Laser System are listed below. Primary Criteria and Functional Requirements of the PIC Laser System are described in **Appendix A.** Specific requirements are listed in Sections B3.2.1.1–B3.2.1.4.

Functions drawn from the existing NIF System Functions as outlined in the NIF SDR (Sec. 3.1.2) include:

- Provide capability to routinely produce a high-quality, 1.8 MJ, temporally-shaped optical pulse at 3ω frequency, incident on the target.
- Provide capability of producing a pulse with peak power of at least 500 TW.
- Produce laser wavelength of 0.35 μm with separation between rings of up to 2 Angstroms.
- Provide for a rms deviation in power delivered by the beams from the power specified, averaged over any 2-ns time interval, of less than 8%.
- Provide for beam-to-beam timing accuracy of ≤ 30 ps-rms.
- Provide a beam pointing accuracy with rms. deviation ≤ 50 μm in the target plane.
- Capable of producing the combined pickets and main drive pulse shapes as a single pulse.
- Capable of applying MultiFM 1D SSD beam smoothing to the picket pulses.
- Produce a pulse with overall duration of up to 20 ns in an individual beam line.
- Deliver pulses to the fusion target with a dynamic range of at least 50:1, where dynamic range is defined as the ratio of intensity at the peak of the pulse to the intensity in the initial "foot" portion of the pulse.
- Provide beam smoothing on the target using CCP's and DPR's.
- Provide for focusing of the beam onto the target.
- Provide for layering of the DT fuel in the PD target having an inner surface roughness of ≤ 1 μm-rms.
- Provide for placing a cryogenic PD target at target chamber center within ± 10 μm.
- Provide for removal of the target's thermal shrouds while preserving the fuel layer uniformity prior to the shot.

Modified or additional System Functions prescribed by this PD plan include:

- Provide capability to routinely produce a high-quality, 1.8 MJ, temporally-shaped optical pulse at 3ω frequency, incident on the target.
- Produce laser-wavelength of 0.35 μm with separation between rings of up to 2 Angstroms.
- Provide for beam-to-beam timing accuracy of ≤ 30 ps-rms.
- Capable of producing the combined pickets and main drive pulse shapes as a single pulse.
- Capable of applying MultiFM 1D SSD beam smoothing to the picket pulses.
- Provide beam smoothing on the target using continuous phase plates and DPR's.
- Provide for layering of the DT fuel in the PD target having an inner surface roughness of ≤ 1 μm-rms.
- Provide for placing a cryogenic PD target at target chamber center within ± 10 μm.

- Provide for removal of the target's thermal shrouds while preserving the fuel layer uniformity prior to the shot.

The functions of the major subsystem modifications required of the laser are described in Section B3.2.1 of this document.

### B3.2.1 Major Subsystem Modifications

The required system modifications are composed of four major elements and new Operational Capabilities: Integrated Target Systems, Target Diagnostics and Experimental Systems, User Optics, Laser Systems (Optical Pulse Generation), and Operational Capabilities.

#### *B3.2.1.1 Integrated Target Systems*

##### B3.2.1.1.1 Target Capsule Requirements

The baseline design[6] of the spherical target capsule is (complete specifications are provided in **Appendix D**):

- The capsule shall be 3.257 mm in diameter with a wall thickness of 0.033 mm.
- The capsule shall be manufactured from CH (47 at%/53 at%).
- The capsule shall be filled with DT (nominally 50 at%/50 at%)
- An ice layer shall be formed within the capsule wall to a thickness of 157 μm.
- The ice layer shall be shimmed by 11.5 μm (Mode-index=2 cosine shim amplitude).
- The inner ice surface roughness shall be < 1 μm-rms (0.25 μm for modes > 10).
- The void region of the capsule shall have a gas density of 0.225 mg/cc.
- The capsule shall be attached to the fuel reservoir via a glass tube that is 2-mm long, with a 30-um outside diameter and 10-um wall thickness where it attaches to the capsule.
- A more rigid support shall be used beyond this 2-mm length of glass tube.

##### B3.2.1.1.2 Polar Drive Ignition Target Insertion Cryostat

This section defines the requirements for the PD-ITIC.[7]

The PD-ITIC is a cryogenic system to create a fuel ice layer in a spherical target and to hold the target at target chamber center (TCC) for a laser shot. There are two sub-assemblies: the Ignition Target Assembly (ITA) and ITIC. ITA supports the target during the fueling and layering operations. ITA attaches to the body of the ITIC. The ITIC assembly provides the cryostat and support infrastructure to layer the fuel within the target, control the temperature of the target and a mechanism to expose the target prior to the shot. The ITIC is attached to the NIF cryoTARPOS.

The ITIC is attached to the cryoTARPOS after being inserted into the LLCS. At this point, connections to the Integrated Computer Control System (ICCS) and the Industrial Control System (ICS) are also made. The ITA is then attached to the body of the ITIC. The LLCS is then closed re-establishing vacuum and radiological boundaries. After establishing a vacuum environment within the LLCS, the fuel is delivered to the target and the fuel ice layer is formed. The cryoTARPOS inserts, positions, and retracts the PD-ITIC in/out of the target chamber (TC). After fuel layering, the PD-ITIC assembly is inserted into the TC and positioned at TCC by the cryoTARPOS control system in conjunction with the TAS. Once positioned, the laser shot sequence is begun and the target shroud is removed 3 to 5 seconds prior to T-0.

Primary Criteria:

- The system shall be capable of fielding PD ignition targets at up to 1.8 MJ of laser energy and maintain the target positional stability and accuracy requirements within the NIF target chamber.
- The system shall be able to form and maintain a uniform cryogenic DT layer on the inside of a spherical PD target with the specified gas density to the instant of the implosion.

Functional requirements of the combined target systems assemblies are to:

- Provide a stable mounting point for the target capsule.
- Provide for fueling the target with the required DT mixture.
- Provide for layering the fuel at cryogenic temperatures (≤ 19.73° K).
- Maintain target temperature and temperature stability as required by the design between 15°K and 25°K.
- Maintain target vibration amplitude within the LLCS to < 1 µm rms.
- Accommodate target alignment within the target chamber using the existing TAS.
- Provide a mechanism to expose the target no more than 5 seconds prior to T-0.
- Maintain target vibration amplitude within the TC at T-0 to < 10 µm rms.
- Operate within the on-shot radiological environment.

#### *B3.2.1.2 Target Diagnostics and Experimental Systems*

3.2.1.2.1 Sections 2.2 and 2.2.1–2.2.7 and 2.2.10–2.2.12 of the NIF Primary Criteria and Functional Requirements (PCFR) document are incorporated into this section.

##### B3.2.1.2.2 Diagnostic Instrument Capabilities to Verify Laser Performance

The facility shall have the following measurement capabilities that are required to verify the Primary Criteria and Functional Requirements, see **Appendix A**:

- Laser pulse energy and power.
- Laser pulse duration and dynamic range.
- Laser beam power balance.
- Simultaneity of arrival of pulses from individual beam lines at target chamber center with 10 ps rms accuracy.
- Laser beam pointing accuracy with 10–20 µm spatial resolution.
- Laser pre-pulse intensity.
- Laser pulse spot size.
- Laser pulse smoothness.
- Laser beam thermal recovery time.

##### B3.2.1.2.3 Diagnostic Instrument Capabilities for Ignition and Applications Experiments

The target chamber and area shall be capable of accommodating diagnostic instruments for the following measurements necessary for PD fusion ignition and applications experiments (specific diagnostic intended):

- Symmetry of x-ray emission from imploded cores with 5- to 10-micrometer spatial resolution (X-ray Framing Camera).

- Time dependent laser light backscattered into the focusing lens (FABS).
- Strength of radiation driven shocks with 5- to 10-micron resolution and time resolution of 10 ps (VISAR).
- Fusion yield over a range from $10^{14}$ to $10^{19}$ neutrons (NAD, nTOF).
- Primary and scattered light images of neutron emission from imploded cores with 15-micron spatial resolution (NIS).
- Temperature of the compressed fusion fuel with 200 eV or 3% accuracy (whichever is greater) for ion temperatures of 2 keV or greater (nTOF).
- Time dependent measure of $T_{hot}$ and $F_{hot}$ using the number and energy distribution of fast electrons from 5 keV to 300 keV (HXRD).
- Absolute bang-time measurement to +/- 30 ps (SPBT, nTOF4.5BT).
- Reaction history with 30 ps-rms timing accuracy (GRH).
- Average cold fuel areal density, ρR to +/- 7% accuracy (MRS).
- Area backlighter capable of imaging the ablator shell to 30 μm resolution.

#### *B3.2.1.3 User Optics*

##### B3.2.1.3.1 Continuous Phase Plate

- A phase plate is required in each of the 192 beam lines.
- Up to five different phase plate designs for the different beam rings are required to produce focal spots having the sizes and shapes as determined by an optimized PD configuration.
- Each phase plate will be located between the doubler and tripler within the FOA.
- The design and manufacture of the phase plates shall meet the NIF specifications for acceptable probability of laser damage when operating the NIF beams at the energy and peak power required for PD ignition.
- Each phase plate must be tilted to prevent back-reflected light, with high irradiance modulation, from damaging upstream optics.

##### B3.2.1.3.2 Distributed Polarization Rotator

- A DPR is required in each of the 192 beam lines;
- The baseline design includes a 2 x 2 checkerboard array of KD*P half-wave plates; two diagonal quadrants will be populated by the KD*P plates.
- Each DPR will be located just prior to the debris shield, in the UV portion of the FOA.
- Diffraction-induced irradiance modulation will be mitigated to prevent excessive damage to the debris shields.
- Material degradation from SRS in KD*P will be mitigated.

#### *B3.2.1.4 Laser Systems (Optical Pulse Generation)*

The NIF OPG system produces the 1ω, temporal and spatially smoothed, formatted pulses with the correct energetics and optical characteristics required for injection into the main amplifier TSF on an individual beam line basis. The initial pulse is generated by the master oscillator, phase modulated, temporally shaped in the amplitude modulator and transferred to each PAM via fiber optic cable. The PAM is a two-stage amplifier consisting of a regenerative amplifier stage followed by a beam shaper and an MPA. Spectral dispersion for beam smoothing is provided by a diffraction grating in the MPA. The pulse is optically matched to the main amplifier and spatially filtered by the preamplifier beam transport subsystem.

Functions of the required upgrade to the NIF OPG System:

- Generate and deliver to the main laser cavity injection point, on an individual beam line basis, optical pulses with MultiFM 1D SSD characteristics specified in the Technical Requirements Document,[8] which include:
  - Polar-drive ignition pulse shapes that include triple pickets and a continuous main drive pulse.
  - Three separate phase modulation frequencies of 21, 22, and 32 GHz producing a total MultiFM bandwidth of up to 500 GHz after frequency conversion in the ultraviolet.
  - MultiFM bandwidth applied to triple pickets only and the standard 3- and 17-GHz phase modulation applied to the main drive pulse for SBS suppression.
  - A new MultiFM 1D SSD grating in the PAM MPA to produce a divergence up to +/-100 μrad (at NIF full-beam size).

# B4 LASER SYSTEM REQUIREMENTS

The laser system shall be designed to meet the following requirements simultaneously, although all performance requirements need not be demonstrated simultaneously on a single event.

## B4.1 Laser Beam Characteristics

### B4.1.1 Laser Pulse Energy

The laser shall be capable of routinely producing a temporally-shaped pulse of energy of up to 1.8 MJ incident on a PD capsule.

### B4.1.2 Laser Pulse Peak Power

The laser shall be capable of producing a pulse with peak power of at least 500 TW.

### B4.1.3 Laser Pulse Wavelength

The wavelength of the laser pulse delivered to the target shall be 0.35 μm.

### B4.1.4 Beam Power Balance

The rms. deviation in the power delivered by the laser beams from the specified power shall be ≤ 8% rms. (quad-to-quad) of the specified power. For the picket pulse portion of the pulse, this shall be averaged across all pickets; for the main drive pulse, it shall be averaged over any 2-ns time interval.

### B4.1.5 Beam Positioning Accuracy

The rms deviation in the position of the centroids of all beams from their specified aiming points shall not exceed 50 micrometers (μm) at the target plane or its equivalent.

**B4.1.6 Laser Pulse Shaping**

The laser shall be capable of producing a pulse with overall duration of up to 20 ns. The PD pulse shall include at least three picket pulses independent from one another and temporally separate from a main drive pulse.

**B4.1.7 Laser Pulse Dynamic Range**

The laser shall be capable of delivering UV pulses to the PD target with a dynamic range of at least 50:1, wherein the dynamic range is defined as the ratio of intensity at the peak of the pulse to the intensity in the initial "foot" portion of the pulse.

**B4.1.8 Capsule Irradiation Symmetry**

The NIF target chamber has four rings of laser ports in each hemisphere. Each port is fitted with a quad of laser beams. For PD ignition, the rings at 44.5$^o$ and 135.5$^o$ are each conceptually divided into two rings having beam pointing latitudes of 44$^o$ and 83$^o$ in the northern hemisphere and 97$^o$ and 146$^o$ in the southern hemisphere, resulting in five independent rings of beams per hemisphere, with each ring having its own energy on target. These five rings concentrate energy on the polar (24.5$^o$ and 155.5$^o$), mid-latitude (44$^o$ and 146$^o$), and equatorial regions (83$^o$ and 97$^o$) of the target. Quad polar angles and beam pointing are described in Table B1. Variations in the UV energy deposited on the PD fusion target are determined from a sum-in-quadrature summation of all sources of illumination perturbations.

**Table B1. NIF Polar Drive beam and quad pointing latitudes.**

| Beam Group | CPP | Northern hemisphere | | | Southern hemisphere | | |
|---|---|---|---|---|---|---|---|
| | | Quad Polar Angle (deg) | Beam Pointing Latitude (deg) | *Quads* | Quad Polar Angle (deg) | Beam Pointing Latitude (deg) | Quads |
| 1-a | 1 | 23.5 | 24.5 | 33T, 24T, 15T, 42T | 156.5 | 155.5 | 33B, 24B, 15B, 42B |
| 2-b | 2 | 30 | 44 | 36T*, 26T, 13T*, 41T | 150 | 146 | 16B, 21B*, 31B, 44B* |
| 3-b | 3 | 44.5 | 44 | 12T, 22T, 32T, 45T | 135.5 | 146 | 14B, 25B, 35B, 43B |
| 3-c | 4 | 44.5 | 83 | 14T, 25T, 35T, 43T | 135.5 | 97 | 12B, 22B, 32B, 45B |
| 4-c | 5 | 50 | 83 | 11T, 16T, 21T, 23T, 31T, 34T, 44T, 46T | 130 | 97 | 11B, 13B, 23B, 26B, 34B, 36B, 41B, 46B |

*These quads have polar angles 0.58$^o$ closer to the equator than the nominal angle listed.

**B4.1.9 Pre-Pulse Power**

The laser intensity delivered to the target during the 20-ns interval prior to arrival of the main laser pulse shall not exceed $10^8$ W/cm$^2$.

**B4.1.10 Laser Pulse Spot Profile**

Each beam shall deliver its design energy and power encircled in a spot at the target plane defined by the Triple Picket Point Design for PD Ignition on the NIF (see **Appendix D**). Polar ($24.5^o/155.5^o$) and mid-latitude ($44^o/146^o$) ring beams shall have circular spots and the equatorial beams ($83^o/97^o$) will have spot profiles defined to maximize beam uniformity and laser energy coupling to the target.

**B4.1.11 Beam Smoothness**

The NIF shall have spatial and temporal beam conditioning to control intensity fluctuations in the target plane.

***B4.1.11.1 MultiFM 1D SSD Beam Smoothing***

The NIF shall provide MultiFM 1D SSD that is applied to the picket pulses to provide beam smoothing in the target plane.

***B4.1.11.2 Dynamic Bandwidth Reduction***

The NIF shall apply MultiFM 1D SSD beam smoothing to only the picket portion of the drive pulse in order to minimize laser imprint non-uniformity and minimize stress on the laser system during propagation of the main drive pulse.

***B4.1.11.3 Phase Plates***

The NIF shall provide CPP's specifically designed for the requirements specified in Sect. 3.2.1.3.1 for additional beam smoothing of each beam.

***B4.1.11.4 Polarization Smoothing***

The NIF shall provide polarization beam smoothing specifically designed for the requirements specified in Sect. 3.2.1.3.2 for additional beam smoothing of each beam.

***B4.1.11.5 Beam Focusing and Pointing***

The NIF should have flexibility in beam focusing and pointing to address the needs of radiation effects testing and other users.

***B4.1.11.6 Beam Mistiming***

The NIF shall have the capability to co-time the delivery of the laser pulse to target to $\leq$ 30 ps-rms.

## B5 DESIGN AND CONSTRUCTION

Sections 3.3, 3.4, and 4.0 of the NIF SDR document (NIF 0000192-2) will apply in this area.

## B6 REFERENCES

1. V. N. Goncharov et al., "Improved performance of direct-drive inertial confinement fusion target designs with adiabat shaping using an intensity picket," *Phys. Plasmas* **10**, 1906–1918 (2003), and *LLE Review* **93**, 18–32 (2002).

2. V. N. Goncharov et al., "Demonstration of the Highest Deuterium–Tritium Areal Density Using Triple-Picket Cryogenic Designs on OMEGA." *LLE Review* **121**, 1–5 (2009).
3. S. Skupsky et al., *Phys. Plasmas* **11**, 2763 (2004).
4. J.A. Marozas, T.J. Collins, and J.D. Zuegel, "Multiple-FM Smoothing by Spectral Dispersion—An Augmented Laser Speckle Smoothing Scheme," *LLE Review* **114**, 73–80 (2008).
5. National Ignition Facility System Design Requirements, Laser System, NIF-0000192-2, UCRL-ID-126998.
6. Triple Picket Point Design for Polar Drive Ignition on NIF; LLE, S-AA-G-082.
7. Requirements for the NIF Polar Drive Ignition Target Cryostat; LLE, Q-NP-R-001.
8. MultiFM 1D SSD on OMEGA EP; LLE, T-BW-R-005.

# Appendix C: Work Breakdown Structure

| WBS Code | WBS Description | | | | | |
|---|---|---|---|---|---|---|
| | Lvl 2 | Lvl 3 | Lvl 4 | Lvl 5 | Lvl 6 | Lvl 7 |
| **1** | **Polar Drive Ignition** | | | | | |
| **1.1** | **Management** | | | | | |
| 1.1.1 | | Reserved | | | | |
| 1.1.2 | | Reserved | | | | |
| 1.1.3 | | Reserved | | | | |
| 1.1.4 | | Reserved | | | | |
| 1.1.5 | | Reserved | | | | |
| 1.1.6 | | Reserved | | | | |
| 1.1.7 | | Reserved | | | | |
| 1.1.8 | | Reserved | | | | |
| 1.1.9 | | Reserved | | | | |
| **1.2** | **System Engineering** | | | | | |
| 1.2.1 | | System Performance | | | | |
| 1.2.1.1 | | | Mission and Risk Analysis | | | |
| 1.2.1.2 | | | System Modeling | | | |
| 1.2.2 | | Configuration Management | | | | |
| 1.2.3 | | Safety Engineering | | | | |
| 1.2.4 | | Cleanliness and Expert Groups | | | | |
| 1.2.5 | | System Alignment | | | | |
| 1.2.6 | | System Integration | | | | |
| 1.2.6.1 | | | Requirements Maintenance | | | |
| 1.2.6.2 | | | Interface Control Maintenance | | | |
| 1.2.6.3 | | | Design Integration | | | |
| 1.2.6.4 | | | SI Integration | | | |
| 1.2.7 | | Commissioning Management and Planning | | | | |
| 1.2.8 | | Material Flow | | | | |
| 1.2.9 | | System Engineering Integration | | | | |
| 1.2.9.1 | | | Target Experiments Integration | | | |
| **1.3** | **Target Physics** | | | | | |
| 1.3.1 | | Coupling | | | | |
| 1.3.1.1 | | | Ablator optimization | | | |
| 1.3.1.1.1 | | | | Baseline CH | | |
| 1.3.1.1.2 | | | | Dopants | | |
| 1.3.1.1.3 | | | | Higher Z ablators | | |
| 1.3.1.2 | | | 2D transport (polar vs. equatorial) | | | |
| 1.3.1.3 | | | Long scale length physics | | | |

| | | | | |
|---|---|---|---|---|
| 1.3.1.3.1 | | | SRS | |
| 1.3.1.3.2 | | | TPD | |
| 1.3.1.3.3 | | | SBS/CBET | |
| 1.3.1.4 | | High intensity (SI) | | |
| 1.3.2 | Symmetry | | | |
| 1.3.2.1 | | Power balance | | |
| 1.3.2.2 | | Beam pointing | | |
| 1.3.2.3 | | Beam timing | | |
| 1.3.2.4 | | Imprint | | |
| 1.3.2.4.1 | | | Multi-FM validation | |
| 1.3.2.5 | | Continuous Phase Plate design | | |
| 1.3.2.6 | | DPR design | | |
| 1.3.2.7 | | SBS/CBET | | |
| 1.3.3 | Compression/adiabat control | | | |
| 1.3.3.1 | | Moderate convergence demonstration Day 1 | | |
| 1.3.3.2 | | High convergence demonstration using PD CPPs | | |
| 1.3.3.2.1 | | | Shock timing (polar vs. equatorial) | |
| 1.3.3.2.1.1 | | | | Cone-in-shell platform |
| 1.3.3.3 | | High convergence cryogenic DT | | |
| 1.3.3.4 | | Diagnostics | | |
| 1.3.3.4.1 | | | Ambient backlighter development | |
| 1.3.3.4.2 | | | Cryogenic backlighter development | |
| 1.3.3.5 | | Preheat mitigation | | |
| 1.3.3.6 | | SBS/CBET mitigation | | |
| 1.3.3.7 | | Mix | | |
| 1.3.4.6 | | Backlighter design | | |
| 1.3.5 | Baseline target design | | | |
| 1.3.5.1 | | Hydra/Draco | | |
| 1.3.5.1.1 | | | PD design requirements | |
| 1.3.5.1.2 | | | SI design requirements | |
| 1.3.5.2 | | Design validation experiments on OMEGA | | |
| 1.3.5.2.1 | | | DT cryogenic implosions | |
| 1.3.5.2.1.1 | | | | Symmetric |
| 1.3.5.2.1.2 | | | | PD |
| 1.3.5.2.1.3 | | | | SI |
| 1.3.5.2.2 | | | Shock timing | |
| 1.3.5.3 | | Target fabrication | | |
| 1.3.5.3.1 | | | Capsule surface quality to specifications | |
| 1.3.5.3.2 | | | Backlighter design | |
| **1.4** | **Integrated Target Systems** | | | |
| 1.4.1 | Target Development and Manufacturing | | | |
| 1.4.1.1 | | Target Manufacturing | | |
| 1.4.1.1.1 | | | Direct Drive Capsule Manufacture | |
| 1.4.1.1.1.1 | | | | DT Capsule |

| | |
|---|---|
| 1.4.1.1.1.2 | DT foam capsule (if required) |
| 1.4.1.1.2 | Fill-tube manufacture and attachment to the capsule |
| 1.4.1.1.3 | Target Reservoir |
| 1.4.1.1.3.1 | 1st concept |
| 1.4.1.1.3.2 | 2nd concept |
| 1.4.1.1.4 | Target Metrology |
| 1.4.1.1.4.1 | Measure surface features |
| 1.4.1.1.4.2 | Measure vibration at RT |
| 1.4.1.1.4.3 | Measure vibration at 20K |
| 1.4.1.1.5 | Target Assembly into the NIF PD Cryostat |
| 1.4.1.1.5.1 | Assembly station |
| 1.4.1.1.5.2 | ITIC |
| 1.4.1.1.6 | Target Proofing |
| 1.4.1.1.7 | Target Layering |
| 1.4.1.1.7.1 | DT layering |
| 1.4.1.1.7.2 | DT measurement (ratio) |
| 1.4.1.1.7.3 | DT vapor pressure |
| 1.4.1.1.7.4 | DT ice rms. |
| 1.4.1.1.7.5 | Exposed target life in TC |
| 1.4.1.1.7.6 | Layer shimming |
| 1.4.1.1.7.7 | Void elimination in foam targets (if required) |
| 1.4.1.1.8 | Layer Characterization |
| 1.4.1.2 | Target Test Station (ITPS equivalent) |
| 1.4.2 | Cryogenic Target Insertion System |
| 1.4.2.1 | PD-ITIC |
| 1.4.2.1.1 | Structure |
| 1.4.2.1.1.1 | Structural frame |
| 1.4.2.1.1.2 | Thermal system |
| 1.4.2.1.1.3 | Neutron and x-ray shielding |
| 1.4.2.1.2 | Inner heat path |
| 1.4.2.1.2.1 | Cold rod modifications |
| 1.4.2.1.2.2 | ITA gripper |
| 1.4.2.1.2.3 | Inner shroud |
| 1.4.2.1.2.4 | Layering sphere |
| 1.4.2.1.2.5 | Blast shield |
| 1.4.2.1.3 | Outer heat path |
| 1.4.2.1.3.1 | Outer shrouds |
| 1.4.2.1.4 | Retraction system |
| 1.4.2.1.4.1 | Retraction mechanics |
| 1.4.2.1.4.2 | Retraction motor |
| 1.4.2.1.5 | ITA |
| 1.4.2.1.5.1 | Fuel reservoir |
| 1.4.2.1.5.2 | Target support assembly |
| 1.4.3.2.6 | Control System |
| 1.4.2.3.6.1 | ICCS software |

| | | | | |
|---|---|---|---|---|
| 1.4.2.3.6.2 | | | | ICS software |
| 1.4.4.2 | | LLE Cryo Test Stand | | |
| 1.4.4.2.1 | | | Vacuum chamber | |
| 1.4.4.2.2 | | | Vacuum system | |
| 1.4.2.2.3 | | | Vibration test equipment | |
| 1.4.2.2.4 | | | Controls | |
| 1.4.2.2.5 | | | Data acquisition | |
| 1.4.2.3 | | LLNL Cryo Test Stand | | |
| 1.4.2.3.1 | | | Hardware | |
| 1.4.2.3.2 | | | Controls | |
| 1.4.2.3.3 | | | Data acquisition | |
| 1.4.2.4 | | TAS modifications (If required) | | |
| 1.4.2.5 | | LLCS modifications (If required) | | |
| 1.4.2.6 | | OPSR modifications (If required) | | |
| **1.5** | **Target Diagnostics and Experimental Systems** | | | |
| 1.5.1 | New Diagnostics/Diagnostics Impacted | | | |
| 1.5.1.1 | | Scattered light Calorimetry | | |
| 1.5.1.1.1 | | | 351-nm spectroscopy and streaked light | |
| 1.5.1.1.2 | | | 234-nm spectroscopy and streaked light | |
| 1.5.1.1.3 | | | 400–700nm spectroscopy and streaked light | |
| 1.5.1.1.4 | | | 351-nm calorimetry | |
| 1.5.1.2 | | Hard X-Ray Detector | | |
| 1.5.2 | Diagnostic Alignment | | | |
| 1.5.3 | ICCS Modifications | | | |
| **1.6** | **User Optics** | | | |
| 1.6.1 | Continuous Phase Plates | | | |
| 1.6.1.1 | | Prototype phase plates | | |
| 1.6.1.1.1 | | | CPP1 and/or 5 | |
| 1.6.1.1.2 | | | Mount | |
| 1.6.1.1.3 | | | Coating | |
| 1.6.1.2 | | Final phase plates | | |
| 1.6.1.2.1 | | | CPP1 | |
| 1.6.1.2.2 | | | CPP2 | |
| 1.6.1.2.3 | | | CPP3 | |
| 1.6.1.2.4 | | | CPP4 | |
| 1.6.1.2.5 | | | CPP5 | |
| 1.6.1.2.6 | | | Mount | |
| 1.6.1.2.7 | | | Coating | |
| 1.6.2 | DPR's | | | |
| 1.6.2.1 | | Prototype DPR | | |
| 1.6.2.1.1 | | | DPR | |
| 1.6.2.1.2 | | | Mount | |
| 1.6.2.1.3 | | | Coating | |
| 1.6.2.2 | | Final DPR | | |

| | |
|---|---|
| 1.6.2.1.1 | DPR |
| 1.6.2.1.2 | Mount |
| 1.6.2.1.3 | Coating |
| **1.7** | **Laser Systems** |
| 1.7.1 | PD Beam Smoothing Demo on OMEGA EP |
| 1.7.1.1 | Activate NIF PAM in EP BL4 |
| 1.7.1.2 | Develop MultiFM 1D SSD Seed Source for Omega EP |
| 1.7.1.3 | Activate MultiFM 1D SSD in Laser Sources |
| 1.7.1.4 | Activate MultiFM 1D SSD in Omega EP |
| 1.7.1.5 | Demonstrate PD smoothing with ETP Measurements |
| 1.7.1.6 | Demonstrate MultiFM 1D SSD target imprint |
| 1.7.2 | PD Beam Smoothing for NIF |
| 1.7.2.1 | MOR modifications |
| 1.7.2.1.1 | MOR PD electro-optical systems |
| 1.7.2.1.1.1 | MOR PD Seed pulse source |
| 1.7.2.1.1.2 | MultiFM phase-modulation chassis |
| 1.7.2.1.1.3 | MultiFM fail-safe chassis |
| 1.7.2.1.1.4 | MultiFM fail-safe optical gate |
| 1.7.2.1.1.5 | FM phase-modulation chassis |
| 1.7.2.1.1.6 | FM fail-safe chassis |
| 1.7.2.1.1.7 | FM fail-safe optical gate |
| 1.7.2.1.1.8 | Time-multiplexed Amplitude Modulator Chassis |
| 1.7.2.1.1.9 | Pulse De-multiplexing Chassis |
| 1.7.2.1.1.10 | Optical Splicer and Compensator Chassis |
| 1.7.2.1.2 | MOR PD optical pulse distribution system |
| 1.7.2.1.2.1 | Dual PM fiber amplifier chassis |
| 1.7.2.1.2.2 | MultiFM Failsafe Delay |
| 1.7.2.1.2.3 | FM Failsafe Delay |
| 1.7.2.1.3 | MOR PD controls |
| 1.7.2.1.3.1 | MOR PD front end processor |
| 1.7.2.1.3.1.1 | MOR PD FEP hardware |
| 1.7.2.1.3.1.2 | MOR PD FEP software |
| 1.7.2.1.3.2 | MOR PD timing |
| 1.7.2.1.3.3 | MOR PD Supervisory Control |
| 1.7.2.1.4 | MOR PD safety systems |
| 1.7.2.1.4.1 | Overlap Fail-Safe System |
| 1.7.2.1.5 | MOR PD integration |
| 1.7.2.2 | PAM system modifications |
| 1.7.2.2.1 | MultiFM SSD grating mount assembly |
| **1.8** | **Operational Capabilities** |
| 1.8.1 | Facility Modifications |
| 1.8.2 | Re-qualify Precision Diagnostic Station |
| 1.8.3 | Shot Cycle ICCS Modifications |
| 1.8.4 | T-1 Shroud Opening (Machine Safety Issue) |

# Appendix D: Triple Picket Point Design

## D1 Overview

This appendix provides the target and laser system requirements for the triple-picket PD hot-spot ignition design for NIF. This information is under configuration control and represents the design as of August 2011. More recent design information is discussed in this document; the differences are not consequential.

## D2 SUMMARY

The triple-picket PD hot-spot ignition design for the National Ignition Facility is based on the triple-picket design[1] used on OMEGA that achieved an areal density[2] of nearly 300 mg/cm$^2$. The theoretical design was optimized using a simplex method in 1D, and manually in 2D, for both higher energy (~1.5 MJ) and PD beam configuration.

The use of a triple-picket pulse represents a qualitative change from the strategy employed by the previous PD hot-spot ignition design[3]. Experiments on OMEGA have demonstrated that picket pulses are better suited to experimental shock tuning[4]. In addition, relaxation pickets, for which the laser power is small or zero between the pickets, allow for greater adiabat shaping and shell stability[5]. Furthermore, use of a high-contrast drive pulse reduces uncertainties in shock timing caused by low-adiabat lower contrast drive pulses. A “step” pulse prior to the start of the drive pulse reduces the required drive-pulse power. The final pulse specifications lie within the NIF single-beam energy and power thresholds.

This design differs from previous PD hot-spot designs in four ways: First, a thicker CH ablator is used to minimize the risk of hot-electron preheat. Second, a newly optimized beam smoothing technique using MultiFM is employed,[6,7] improving upon the MultiFM beam smoothing used in previous designs.[3] Third, a shim is used on the inner surface of the DT ice to reduce the mass being driven at the equator. This helps offset the reduced drive power caused by greater angles of incidence for the equatorial beams. Fourth, a phase plate design for NIF beam rings 4 and 5 produces an asymmetric focal spot on the target reducing the energy lost over the target horizon and concentration more energy in the equatorial region.

Key requirements for this design are adequate power imbalance, beam mispointing, target placement, and ice roughness. This design assumes the use of both polarization smoothing wedges and distributed phase plates, as described. When NIF-standard specifications are used, this design achieves a 2D gain of 32 with zero target offset.

The triple picket point design for PD ignition on the NIF is given below in several tables. Table D1 lists the specifications and requirements for the PD target; Table D2 lists the specifications and requirements on the laser system (configuration); Table D3 lists the specifications and requirements on the laser drive pulse shape; Table D4 lists the specifications and requirements on the laser beam pointing on the targets; and Table D5 lists the specifications and requirements on the laser beam spot shapes.

# D3 REFERENCES


1. V.N. Goncharov et al., *Phys. Rev. Lett.* **104**, 165001 (2010).
2. T.C. Sangster et al., *Phys. Plasmas* **17**, 056312 (2010).
3. LLE Point Design for Polar Drive Ignition on the NIF, S-AA-G-079.
4. T.R. Boehly et al., *Phys. Plasmas* **16**, 056302 (2009); T. R. Boehly et al., *Phys. Rev. Lett.* **106**, 195005 (2011).
5. K. Anderson and R. Betti, *Phys. Plasmas* **11**, 5 (2004)
6. J.A. Marozas, MultiFM Specification Document, to be published.
7. J.A. Marozas et al., "Multiple-FM Smoothing by Spectral Dispersion—an Augmented Laser Speckle Smoothing Scheme." *LLE Review* **114** (2008).


**Table D1. Specifications and requirements for the PD target.**

| Item | Parameter | | Specification | Note |
|---|---|---|---|---|
| 1 | **Target Characterisitics** | | | |
| 1.1 | | Layer constituents | CH (47 atom%/53 atom%) | Formulated by target contractor |
| 1.2 | | Outer Diameter | 3257 µm | |
| 1.3 | | Shell thickness | 33 µm | |
| 1.4 | | Thickness variation | < 0.1 µm | |
| 1.5 | | Density | 1.04 g/cc | |
| 1.6 | | Density variation | Measured to ± 1% | |
| 1.7 | | Outer surface variations | NIF standard power spectrum | 115 nm for modes 2-200 |
| 1.8 | | Inner surface roughness | NIF standard power spectrum | Phys. Plasmas 8 #5 2001, 2318 |
| 1.9 | | Layer makeup | composition >95% CH | Current IDI specification |
| 1.10 | | Layer contaminants | < 100%/Z2 (eg. <0.5% for Si) | Current IDI specification |
| | | | | |
| 2 | **Wetted Foam Layer** | | None | |
| | | | | |
| 3 | **Ice Layer** | | | |
| 3.1 | | Layer constituents | DT (50%-50%) | |
| 3.2 | | Outer Diameter | 3191 µm | |
| 3.3 | | Thickness (mean) | 157 µm | |
| 3.3.1 | | Shim | 11.5 µm | Mode-index=2 cosine shim amplitude |
| 3.3.2 | ` | Thickness (N and S pole) | 168.5 µm | |
| 3.3.3 | | Thickness (Equator) | 145.5 µm | |
| 3.4 | | Inner surface roughness | 1 µm-rms | 0.25 µm for modes > 10 |
| 3.5 | | Thickness variation | < 1 µm | |
| 3.6 | | Density | 0.264 g/cc +/- 0.066 | Standard DT at 18°K |
| 3.7 | | Density variation | < 1% | |
| 3.8 | | Outer Surface roughness | Compliance with shell | |
| 3.9 | | Layer temperature | 18.0°K +/- 0.5 | Bull. Am. Phys. Soc., 45 No. 7 301 (2000). |
| 3.10 | | Layer temperature variation | < 1° K | Bull. Am. Phys. Soc., 45 No. 7 301 (2000). |
| 3.11 | | Layer constituents | DT, DD, TT | |
| 3.12 | | Layer fractionation | < 10% | J. Appl. Phys. 100, 073302 (2006) |
| 3.13 | | Layer contaminants | < 1% Entrained He3 | |
| | | | | |
| 4 | **Void Region** | | | |
| 4.1 | | Layer constituents | DT (50%-50%) | |
| 4.2 | | Outer Diameter | 2877 µm | |
| 4.3 | | Density | 0.225 mg/cc | Bull. Am. Phys. Soc., 45 No. 7 301 (2000). |
| | | | | |
| 5 | **Target Support/Mount** | | No requirements specified | |

**Table D2. Specifications and requirements for the PD laser configuration.**

| Parameter | Specification | Note or reference |
|---|---|---|
| **Beam Characteristics** | | |
| Principal harmonic | 351 nm | On-target |
| Energy on target (total) | $1.54 \times 10^6$ J | All beams combined |
| | | |
| **Power Balance and Timing (48 clusters)** | | |
| Static energy variance | 8% | Current NIF specification |
| Beam mis-timing | ≤ 30 ps-rms | Current NIF specification |
| | | |
| **Pointing (48 clusters)** | | |
| Beam mis-pointing | < 50 µm-rms | Configuring the NIF for Direct Drive UCRL-ID-120758 LLNL (1995) |
| Total Divergence (FWHM) | < 100 µ-rad half-angle at full beam size (39.7 cm) | |
| | | |
| **Target Positioning** | | |
| Target centering | 0 µm from TCC | +/- 10 µm radius |
| | | |
| **On-target Energy (kJ) per Beam** | | |
| Beam Group 1a | 9.33 | |
| Beam Group 2b | 5.55 | |
| Beam Group 3b | 5.75 | |
| Beam Group 3c | 8.74 | |
| Beam Group 4c | 9.34 | |
| | | |
| **Frequency Modulation** | | |
| **Picket 1** | | |
| No. of 1D frequency modulators | 3 | Specified in T-AD-R-005 |
| Modulator frequencies | 1) 21.165 GHz<br>2) 22.837 GHz<br>3) 31.881 GHz | Specified in T-AD-R-005 |
| UV Bandwidth (GHz) | 1) 57.32 GHz<br>2) 142.81 GHz<br>3) 397.04 GHz | Note: T-AD-R-005 specifies IR bandwidth |
| **Picket 2** | | |
| No. of 1D frequency modulators | 3 | Specified in T-AD-R-005 |
| Modulator frequencies | 1) 21.165 GHz<br>2) 22.837 GHz<br>3) 31.881 GHz | Specified in T-AD-R-005 |
| UV Bandwidth (GHz) | 1) 57.32 GHz<br>2) 142.81 GHz<br>3) 397.04 GHz | Note: T-AD-R-005 specifies IR bandwidth |

| Parameter | Specification | Note or reference |
|---|---|---|
| **Continuous Phase Plates** | 1ω + 2ω | |
| **Beam Group 1a** | | |
| Spot Diameter | 3257 μm | 5% Energy point |
| Order (Super-gaussian) | 3 | |
| **Beam Group 2b** | | |
| Spot Diameter | 3257 μm | 5% Energy point |
| Order (Super-gaussian) | 2.2 | |
| **Beam Group 3b** | | |
| Spot Diameter | 3257 μm | 5% Energy point |
| Order (Super-gaussian) | 2.2 | |
| **Beam Group 3c** | | |
| Spot Diameter | 3257 μm | 5% Energy point |
| Order (Super-gaussian) | 2.2 | |
| Secondary ellipse energy fraction | 30% | |
| Secondary ellipse offset | - 244 μm (V), 0 μm (H) | Relative to center (Vertical, Horizontal) |
| Secondary ellipse ellipticity | 3 | Relative ratio of ellipse height to width |
| **Beam Group 4c** | | |
| Spot Diameter | 3257 μm | 5% Energy point |
| Order (Super-gaussian) | 2.2 | |
| Secondary ellipse energy fraction | 30% | Energy in ellipse relative to total energy in spot |
| Secondary ellipse offset | - 244 μm (V), 0 μm (H) | Relative to center (0, 0 um Vertical, Horizontal) |
| Secondary ellipse ellipticity | 3 | Ratio of ellipse width to height |
| | | |
| **Polarization Rotator** | | |
| Angular tilt | X/100 μ-rad<br>Y/50 μ-rad | Wedges not checkerboarded |
| Material | KDP | |
| **Picket 3** | | |
| No. of 1D frequency modulators | 3 | Specified in T-AD-R-005 |
| Modulator frequencies | 1) 21.165 GHz<br>2) 22.837 GHz<br>3) 31.881 GHz | Specified in T-AD-R-005 |
| UV Bandwidth (GHz) | 1) 57.32 GHz<br>2) 142.81 GHz<br>3) 397.04 GHz | Note: T-AD-R-005 specifies IR bandwidth |
| **Step Pulse** | | |
| No. of 1D modulators | 1 | |
| Modulator frequency | 17 GHz | |
| UV Bandwidth | 186.56 GHz | |
| **Main Drive Pulse** | | |
| No. of 1D modulators | 1 | |
| Modulator frequency | 17 GHz | |
| UV Bandwidth | 186.56 GHz | |
| | | |

**Table D3. Specifications and requirements for the PD laser pulse shape.**

| Item | Parameter and Specification | | | | | |
|---|---|---|---|---|---|---|
| 15 | **Pulse Timing and Beam Group (BG) UV Power (TW) per Beam** | | | | | |
| | Time (ns) | BG1a | BG2b | BG3b | BG3c | BG4c |
| | 0.00 | 0.000 | 0.000 | 0.000 | 0.000 | 0.000 |
| | 0.03 | 0.004 | 0.003 | 0.004 | 0.005 | 0.005 |
| | 0.31 | 0.155 | 0.142 | 0.150 | 0.192 | 0.200 |
| | 0.40 | 0.129 | 0.118 | 0.125 | 0.160 | 0.167 |
| | 0.68 | 0.000 | 0.000 | 0.000 | 0.000 | 0.000 |
| | 2.52 | 0.000 | 0.000 | 0.000 | 0.000 | 0.000 |
| | 2.79 | 0.233 | 0.222 | 0.234 | 0.243 | 0.253 |
| | 2.89 | 0.235 | 0.224 | 0.236 | 0.245 | 0.256 |
| | 3.17 | 0.000 | 0.000 | 0.000 | 0.001 | 0.001 |
| | 3.81 | 0.001 | 0.001 | 0.001 | 0.001 | 0.001 |
| | 4.08 | 0.262 | 0.249 | 0.262 | 0.273 | 0.284 |
| | 4.18 | 0.257 | 0.245 | 0.258 | 0.268 | 0.280 |
| | 4.46 | 0.001 | 0.001 | 0.001 | 0.001 | 0.001 |
| | 4.53 | 0.008 | 0.005 | 0.005 | 0.008 | 0.009 |
| | 4.61 | 0.398 | 0.232 | 0.244 | 0.399 | 0.416 |
| | 5.77 | 0.398 | 0.232 | 0.244 | 0.399 | 0.416 |
| | 5.97 | 2.015 | 1.173 | 1.235 | 2.018 | 2.106 |
| | 9.88 | 2.015 | 1.173 | 1.235 | 2.018 | 2.106 |
| | 9.93 | 0.000 | 0.000 | 0.000 | 0.000 | 0.000 |
| | | | | | | |
| 16 | **Base UV Pulse Shape and Energy** | | | | | |
| 16.1 | **First Picket** | | | | | |
| 16.1.1 | Pulse shape | | Trapezoidal | | See item 15 | |
| 16.1.2 | Peak power | | 0.20 TW | | | |
| 16.1.3 | Peak power variations | | < 2% rms on target | | Bull. Am. Phys. Soc., 50, No. 8, 114 (2005) | |
| 16.2 | **Second Picket** | | | | | |
| 16.2.1 | Pulse shape | | Trapezoidal | | See item 15 | |
| 16.2.2 | Peak power | | .256 TW | | | |
| 16.2.3 | Peak power variations | | < 2% rms on target | | Bull. Am. Phys. Soc., 50, No. 8, 114 (2005) | |
| 16.3 | **Third Picket** | | | | | |
| 16.3.1 | Pulse shape | | Trapezoidal | | See item 15 | |
| 16.3.2 | Peak power | | .284 TW | | | |
| 16.3.3 | Peak power variations | | < 2% rms on target | | Bull. Am. Phys. Soc., 50, No. 8, 114 (2005) | |
| 16.4 | **Step Pulse** | | | | | |
| 16.4.1 | Pulse shape | | Rectangular | | See item 15 | |
| 16.4.2 | Peak Power | | 0.416 TW | | | |
| 16.5 | **Drive Pulse** | | | | | |
| 16.5.1 | Pulse shape | | Rectangular | | See item 15 | |
| 16.5.2 | Peak Power | | 2.106 TW | | | |
| 16.5.3 | Peak power variations | | < 2% rms on target | | | |
| 16.5.4 | Rise time variations | | < 100 ps | | | |

**Table D4. Specifications and requirements for the PD laser beam pointing on target.**

| | | Northern hemisphere | | | Southern hemisphere | | |
|---|---|---|---|---|---|---|---|
| **Beam Group** | **CPP** | **Quad Polar Angle (deg)** | **Beam Pointing Latitude (deg)** | **Quads** | **Quad Polar Angle (deg)** | **Beam Pointing Latitude (deg)** | **Quads** |
| 1-a | 1 | 23.5 | 24.5 | 33T, 24T, 15T, 42T | 156.5 | 155.5 | 33B, 24B, 15B, 42B |
| 2-b | 2 | 30 | 44 | 36T*, 26T, 13T*, 41T | 150 | 146 | 16B, 21B*, 31B, 44B* |
| 3-b | 3 | 44.5 | 44 | 12T, 22T, 32T, 45T | 135.5 | 146 | 14B, 25B, 35B, 43B |
| 3-c | 4 | 44.5 | 83 | 14T, 25T, 35T, 43T | 135.5 | 97 | 12B, 22B, 32B, 45B |
| 4-c | 5 | 50 | 83 | 11T, 16T, 21T, 23T, 31T, 34T, 44T, 46T | 130 | 97 | 11B, 13B, 23B, 26B, 34B, 36B, 41B, 46B |

*These quads have polar angles 0.58 deg closer to the equator than the nominal angle listed (30 deg/150 deg).

CPP = continuous phase plate
T = top (upper hemisphere)
B = bottom (lower hemisphere)

**Table D5. Beam pointing specifications with associated far-field spot shape.**

| Beam Group | Quad Polar Angle | Pointing Latitude | Far-field spot shape |
|---|---|---|---|
| 1-a | 23.5°/156.5° | 24.5°/155.5° | 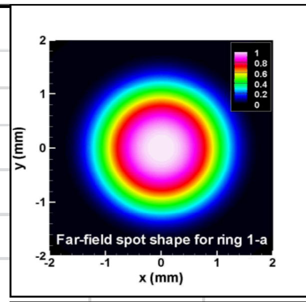  |
| 2-b | 30.6°/150° | 44°/146° | 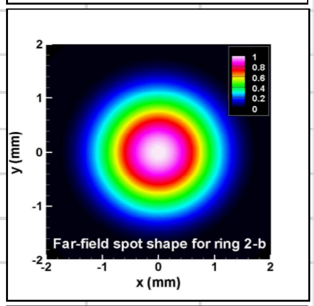  |
| 3-b | 44.5°/135.5° | 44°/146° | 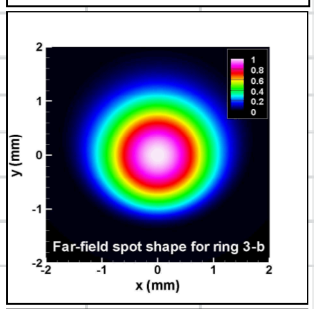  |
| 3-c | 44.5°/135.5° | 83°/97° | 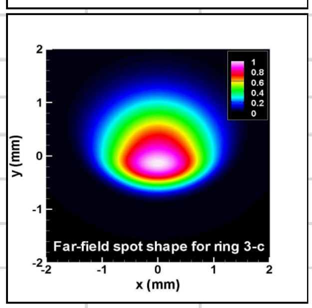  |
| 4-c | 50°/130° | 83°/97° | 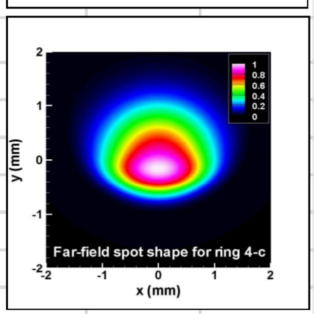  |

# Appendix E: Experimental Implementation Plan

## E1 INTRODUCTION

This appendix describes an integrated experimental plan of OMEGA and NIF activities culminating in a demonstration of PD ignition on the NIF. The proposed research plan is focused on conventional hot-spot ignition (adiabatic compression leading to self-ignition via alpha heating) but may be easily recast as a shock ignition[1] program by adjusting the laser and target specifications.

This plan assumes fundamental physics issues key to PD—including laser plasma absorption, capsule hydrodynamics, and other topics—are largely resolved using OMEGA and OMEGA EP experiments, and this knowledge base is successfully transferred to NIF. The proposed NIF experiments are largely focused on optimization of laser and target parameters rather than detailed fundamental physics investigations. The plan makes no attempt to describe the operational impact of PD experiments (e.g., reconfiguration of the FOAs with PD-specific optics or of the cryoTARPOS with the PD-ITIC). These impacts will be addressed, as needed, by the Experimental Facility Committee. As presented here, the plan is a snapshot of the experimental requirements for PD ignition and is based on over 250 cryogenic implosions on OMEGA; it does not yet incorporate detailed input from other elements of the US ICF program. LLE and LLNL will work together with NNSA ICF program management to define the appropriate experimental schedule and scope based on mission need, program priorities, and funding.

## E2 BACKGROUND ON POLAR DRIVE AND RELATED OMEGA/EP CAMPAIGNS

The PD concept[2] was developed in 2004 in recognition that the NIF would remain configured for x-ray (hohlraum) drive into the foreseeable future. Preliminary assessment of PD hot-spot target designs showed that direct-drive ignition might be achieved with as little as 1 $MJ_{UV}$.[3] The current PD point design (see Section 3a and Appendix D) is predicted to give a gain of 32 at 1.5-$MJ_{UV}$. While shock ignition requires adiabatic compression of the fuel to assemble areal densities adequate to sustain a thermonuclear burn wave, the burn wave is initiated using a strong converging shock as the fuel reaches peak density (the shock is launched at the end of the drive pulse using a spike with laser intensities approaching $10^{16}$ W/cm$^2$). This significantly relaxes the requirements on the in-flight aspect ratio (IFAR) and implosion velocity relative to those for hot-spot ignition. This means that shock ignition is potentially a much more robust design for ignition if adequate pressure can be achieved when the strong shock converges in the core. This is the main scientific challenge for the validation of the shock ignition concept. Experiments are being designed now to begin the study of strong shock coupling through long-scale-length plasmas. The final validation will require at-scale experiments on the NIF.

The FY08–FY12 OMEGA experimental plan was based primarily on the validation of ignition-scaled symmetric drive hot-spot target designs. This work led to the development of new physics models that better predict laser coupling[4] and thermal transport,[5] hot-electron generation,[6] and adiabat control[7] in the multi-dimensional radiation hydrodynamics simulations used to design targets for direct drive ignition. This work led to the development of new diagnostic capabilities that will be needed for non-symmetric drive experiments (e.g., Spherical Crystal Imaging, Thomson Scattering Spectroscopy, and TIM-based Calorimeters). Since LLE expects to achieve the penultimate spherical drive performance sometime in FY13, the proposed experimental plan for FY13–FY17 will focus primarily on PD performance validation. The proposed research plan combines long-scale-length plasma physics on the OMEGA EP laser with 40-beam PD implosion experiments on OMEGA using a new set of dedicated phase plates. A proposed parallel NIF experimental plan will validate the predicative capabilities of the design codes at scale. The NIF experiments will be based on the indirect-drive facility configuration (phase plates and smoothing) until the required facility modifications to support PD ignition experiments are complete. The proposed plans follow a simple rule based on anticipated access to the NIF during the period of performance—discovery and development on OMEGA followed by validation on the NIF.

The LLE experimental program has been based primarily on the OMEGA laser since the completion of the 60-beam upgrade in 1995. The first $D_2$ cryogenic target implosions[8] were performed in 2000 and cryogenic DT implosions[9] began in late 2006. The cryogenic campaign has resulted in over 250 layered fuel implosions over the past decade and has historically accounted for nearly 40% of the LLE-led experiments on OMEGA. Other key experimental campaigns include PD, various campaigns associated with laser–plasma interactions, coupling and cross-beam energy transfer, hot-electron and radiation preheat, ablator equation of state, and diagnostics development (see Table E1).

Several new campaigns were introduced once the OMEGA EP laser was completed in 2008. These included long-scale plasmas, two-plasmon decay, cryogenic backlighting, and isochoric heating (high-intensity coupling). Many of the other OMEGA EP campaigns are natural extensions of existing OMEGA campaigns that take advantage of the long UV drive pulses to generate long-scale-length plasmas and independent IR backlighting (short pulse).

Many of the campaigns on both laser systems depend on specialized diagnostic capabilities. The development of these capabilities is an important part of the LLE mission and often dictates the scheduling of specific campaigns. For example, LLE delayed scheduling significant numbers of cryogenic DT implosions until the Magnetic Recoil Spectrometer (MRS) was qualified in December 2008 (the MRS was the first OMEGA diagnostic sensitive to the compressed fuel areal density; the first cryogenic DT implosions were performed in early 2007). LLE has historically devoted about 10% of its shot time for the development, validation, and calibration of new instrumentation for the ICF program and external users. This level of effort is expected to continue into the foreseeable future.

The OMEGA and EP experimental campaigns have been developed in parallel with the dedicated PIC on the NIF (these campaigns are described in detail below). The PIC experimental plan on the NIF will be based on approximately 50–100 shots during the FY13–17 time frame and culminate in a series of PD ignition attempts. The bulk of the PD Ignition Campaign experiments will be performed on OMEGA and EP to prepare for the limited number of shots on the NIF.

# E3 OMEGA EXPERIMENTAL PLAN

## E3.1 Hot-Spot Ignition

Table E1 lists the anticipated campaigns on OMEGA and OMEGA EP during the FY13–17 time frame along with the number of shots days required per year. A number of assumptions have gone into the development of this table. The first is that the OMEGA laser facility is funded at full capacity and the fractions of the facility time allocated for ignition and HED science will remain 40% and 25%, respectively. Based on the historic allocations for ignition and renewed funding from MTE 10.2, the number of shot days per year for the various LLE missions will be around 68 across the two facilities (roughly 40–45 on OMEGA and 20–25 on EP including joint shot days). The second is that LLE will devote 55 of these shot days per year to ignition and the remaining 11 shot days per year to HED science. This split will be determined annually by the LLE Director with guidance from the NNSA ICF office. The third is that LLE will procure and qualify a new set of PD phase plates for OMEGA by the end of FY13. The majority of the planned campaigns support the ongoing development of the science basis for direct/PD hot-spot and shock ignition.

Spherically symmetric direct-drive cryogenic $D_2$ and DT implosions have dominated the LLE ignition effort for a decade and will continue at least through FY13. Recent cryogenic DT performance has improved significantly over the past year as improved modeling and design, laser uniformity, shock tuning, target alignment, and target surface quality have combined to produced yields-over-clean (YOCs) well in excess of 20% with areal densities matching the 1D predictions. Further improvements in the ion temperature and yield are expected based on the experiments planned for the remainder of FY12 and FY13. Continuing improvements in target alignment (small offsets from target chamber center at shot time) based on new Moving Cryostats should push YOCs close to 30% (based on the current implosion quality and trends with offset). Absolute yields should increase as the implosion velocity is raised by thinning the DT ice and optimizing the thickness of the CD ablator (primary DT yields are expected into the low $10^{13}$ range). The final ice thickness will depend on the shell stability as the in-flight aspect ratio is increased. Experiments in FY11 and early FY12 showed a significant reduction in imprint efficiency by doping the CD ablator with several % of silicon or germanium. Cryogenic DT experiments with a doped ablator will begin in April 2012 (the delay has been due to the development effort to make adequate quality doped shells)

The ultimate spherical cryogenic DT implosion performance should be achieved in FY13. This performance is expected to scale to ignition on the NIF at laser energies of 1.5 MJ or less with implosion velocities of around $3.5\times10^7$ cm/s. Figure E1 shows three hydro-scaling curves[10] plotted as a function of the inferred burn-averaged ion temperature without alpha heating (there is no alpha heating in OMEGA experiments) and the measured total fuel areal density. In 2009, cryogenic DT implosion experiments concurrently produced implosions with areal densities close to 300 mg/cm$^2$ and ion temperatures of ~2.0 keV. While this performance scales to ignition, the laser energy required far exceeds the capability of the NIF. Based on the energy available to drive the shell, it is unlikely that future experiments will produce areal densities in excess of 300 mg/cm$^2$. A number of options are being pursued to increase the implosion velocity and ion temperature. These include doped ablators (reduced imprint efficiency/mix and improved laser absorption) and higher in-flight aspect ratios (IFAR; a higher IFAR is most easily achieved by simply thinning the DT ice). LLE expects to have achieved ion temperatures between 2.5 and

3 keV by the end of FY13 with areal densities matching the 1D predictions and yields-over-1D clean around 30%. As shown in the figure, this performance regime would scale to ignition with the present capabilities (up to 1.5 $MJ_{UV}$) of the NIF.

After demonstrating hydro-equivalent ignition performance using symmetric implosions on OMEGA, the focus of the hot-spot ignition effort will shift to demonstrating comparable hydrodynamic scaling with polar-driven implosions. The primary challenge will be to demonstrate drive symmetry with 40-beam OMEGA implosions comparable to that achieved with the symmetric 60-beam implosions. PD experiments with the symmetric drive phase plates (SG4) have led to shell asymmetries that are well reproduced by 2D simulations[11]. Pointing optimization experiments are complete. The final SG4-based PD campaigns on OMEGA (in FY13) will use beam energy variations (with a fixed pulse shape) and target mass shimming to improve the PD shell symmetry near stagnation.

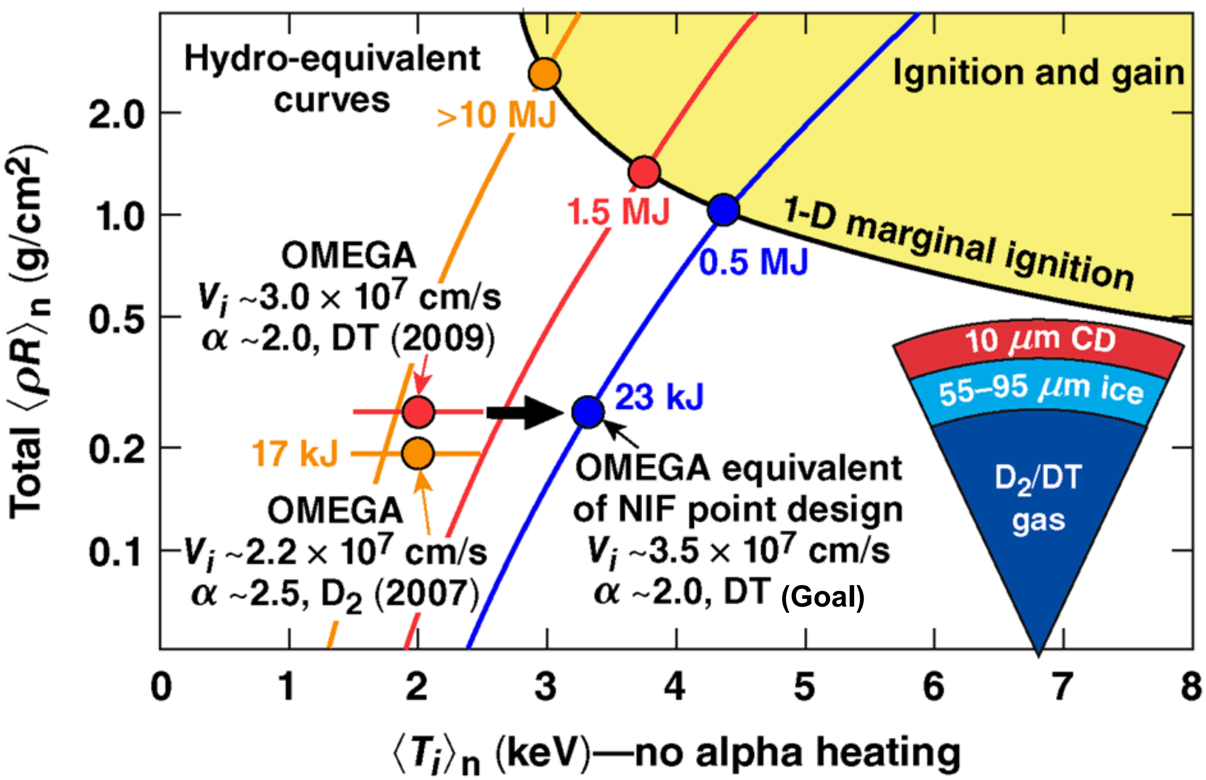


**Figure E1: Recent OMEGA target performance is plotted with hydro-equivalent scaling curves in <Ti>n–<pR>n space. Symmetric drive implosions on OMEGA will scale to ignition once the ion temperature is increased from 2 keV to around 3 keV.**

Target mass shimming reduces the shell thickness at the equator so that the lower coupling efficiency for the oblique beams is better matched to the mass of the shell being accelerated. General Atomics is developing non-cryogenic versions of these targets (in FY12) with a specific thickness variation from pole to equator. Once suitable targets are available, PD shimming experiments could begin as early as Q3FY12 (based on the current FY12 schedule). These shells will be gas-filled and imploded with the standard suite of PD diagnostics. While the PD point design relies on being able to adjust the pulse shape on each of the 48 quads on the NIF, it is not possible to do this on OMEGA. A "poor man's" concept for pulse shape variation is energy variation. Predictions suggest that some improvement in the overall shell symmetry can be expected if the appropriate beam energy distributions can be achieved. The energy balance on OMEGA is quite good but it will likely take many shots to get the energies optimized and the cores round. Once demonstrated with ambient targets, these techniques will be applied to a limited set of cryogenic DT targets in FY13.

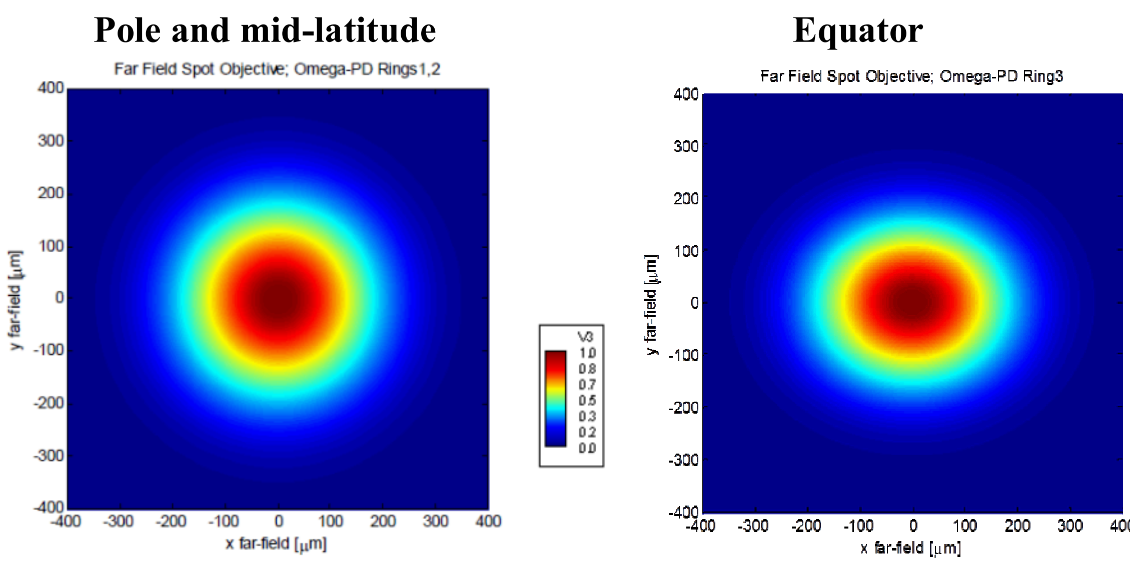


**Figure E2. The 2D profiles for a dedicated set of 40 PD phase plates for experiments on OMEGA in FY14 and beyond. The round spot in the left hand panel will be used for the twenty pole and mid-latitude beams; the spot shape in the right hand panel is a superposition of a super-Gaussian profile with an elliptical spot and will be used for the twenty equatorial beams.**

Beginning in FY14, a new set of dedicated phase plates will be available for PD implosions on OMEGA. These phase plates have been designed using DRACO (with 3D ray tracing, no cross-beam energy transfer, and a flux-limited heat diffusion model). The design goal is to improve both the 40-beam PD symmetry and maintain the 60-beam drive intensity and implosion velocity. The PD target design has been optimized for two on-target beam profiles. Figure E2 shows the two-dimensional profiles for the beam spots on the pole and mid-latitudes (left-hand panel) and for the equator (right-hand panel). Twenty of the 40 phase plates are circular with a super-Gaussian profile on the order of 2.2 modulated with a super-Gaussian envelope (these are for the pole and mid-latitude beams). The role of the envelope function is to redistribute the energy in the super-Gaussian tails closer to the center of the beam. The beam spot diameter is nominally 300 μm to match the anticipated target radius. The radius is smaller (the SG4 phase plates were designed for a target diameter of 860 μm) so that the 40-beam intensity is the same as the 60-beam symmetric intensity when the laser is operating at the same power setting. This will ensure that the PD implosion velocity is comparable to the symmetric implosion velocity. The convergence ratio of the smaller diameter targets may be reduced to keep the hot spot diameter similar to that achieved in the symmetric implosions (e.g., to keep the yield high enough so that the MRS can be used to infer the areal density). The other twenty phase plates (for the more oblique equatorial beams) are circular with a super-Gaussian profile on the order of 2.2 superimposed with an elliptical spot (of ellipticity three). The ellipse is offset from the center of the spot by 38 μm and has an intensity that is 30% of the peak intensity of the main spot. Fabrication of the phase plates will begin in mid-FY12.

Qualification of the full set of 40 phase plates is expected before the end of FY13. In FY1, LLE will shift its emphasis to 40-beam polar-driven implosions. This is shown in Table E3 as the number of expected shot days for symmetric cryogenic DT implosions drops while the number for PD increases sharply. The requirement for any further spherically symmetric cryogenic implosions (for hot-spot ignition) may vanish entirely depending on hydro-scaling progress through FY13. The number of ambient (warm gas-filled plastic shells) PD implosions is expected to increase in FY14 and the number of ambient spherical implosions could drop below the historical average of 2–3 shot days a year. The number of days devoted to cryogenic cone-in-shell shock tuning experiments is expected to increase in FY14 and beyond to support the tuning of the 40-beam PD platform.

The goals of these 40-beam polar-driven implosions will be to optimize core symmetry at bang time and correlate with neutron yield and shell areal density performance. Improved symmetry with the dedicated PD phase plates on OMEGA will validate the phase plate designs for the NIF where higher convergence amplifies any residual drive non-uniformity. The drive and core symmetry will be measured using a combination of self-emission and backlighting. The shell radius vs. time will be measured up to a convergence ratio of a few using x-ray framing cameras set up to see the self-emission near the ablation surface. The areal density will be inferred using charged particle techniques, neutron scattering off the fuel (there is a yield performance threshold of around $1\times10^{12}$ for this to work effectively[12]), or from the x-ray opacity of the fuel/shell when backlighting. Yield, ion temperature, and burn history are standard diagnostic measurements made on all PD (and symmetric) implosions. Time-dependent and time-integrated scattered light measurements will be made using existing instrumentation to infer the absorption fraction and energy losses due to cross-beam energy transfer[4] (CBET).

Symmetry tuning will be done by adjusting the individual beam energies (the pulse shapes are fixed) and repointing beams (a new optimum pointing will be determined with the new PD phase plates). Once optimal drive symmetry is established with the new phase plates, shock tuning will be used to ensure the best possible compression. Dopants may be used to suppress imprint and the two-plasmon-decay (TPD) instability. The final metric will be yield performance, an integrated measure of core symmetry, mix, and coupling efficiency (implosion velocity). The usual metric of comparing PD with symmetric performance for constant drive energy will not be possible as LLE does not plan to acquire 60 symmetric phase plates that match the 300 mm radius of the new PD plates. The combination of total fuel areal density and yield (and/or ion temperature) will be used to establish hydro-equivalent scaling (as in Figure E1).

The bulk of the remaining ignition campaign experiments on OMEGA will focus on laser coupling and preheat. The physics goals for these experiments and the technical details are discussed in the LLE Cooperative Agreement for FY13–FY17 and are beyond the scope of this document. The combined number of shot days per year on OMEGA and EP for these campaigns is expected to be around 8–10 (basically, two shot days a quarter). The experimental details for FY13 are under review. The goals of these experiments include validating absorption models for high intensity direct-drive implosions, using the new Thomson Scattering systems to measure $n_e$ and $T_e$ profiles in spherical geometry and to measure the amplitude of ion-acoustic waves driven by the TPD instability to benchmark simulations, TPD mitigation experiments, using the 4ω probe beam on OMEGA EP to measure radial hydrodynamic profiles ($n_e$, $T_e$, and blow-off velocity), and using the EP FABS to measure backscatter at ignition-relevant plasma scale-lengths.

**Table E1. Proposed campaign plan for OMEGA and EP during the FY13–FY17 period of performance.**

| OMEGA Campaigns | FY13 | FY14 | FY15 | FY16 | FY17 |
|---|---|---|---|---|---|
| Spherical (Cryogenic DT) | 10 | 5 | 2 | 1 | |
| Spherical (Ambient) | 2 | 2 | 2 | 2 | 2 |
| Polar Drive (Cryogenic DT) | 1 | 5 | 7 | 7 | 6 |
| Polar Drive (Ambient) | 2 | 2 | 4 | 3 | 2 |
| Shock Ignition (Cryogenic DT) | 1 | 1 | 2 | 3 | 4 |
| Shock Ignition (Ambient) | 2 | 1 | 2 | 4 | 4 |
| Diagnostics & Technique development | 4 | 3 | 3 | 4 | 5 |
| Shock Timing (Cryogenic & Ambient) | 2 | 3 | 3 | 1 | 1 |
| Coupling (LPI-CBET) | 3 | 3 | | | |
| Preheat (LPI-TPD) | 2 | 3 | 2 | | |
| Fast Ignition | 2 | 2 | 2 | 2 | 2 |
| Magnetized Targets | 2 | 2 | 2 | 3 | 3 |
| Dyn BW reduction | | | | 1 | 2 |
| Hydro (Imprint, RT, Transport,…) | 3 | 3 | 3 | 2 | 2 |
| | 36 | 35 | 34 | 33 | 33 |
| **EP Campaigns** | | | | | |
| Coupling (LPI-Long Scale Length) | 4 | 4 | 4 | 4 | 3 |
| Coupling (LPI-Strong Shocks) | | 1 | 2 | 2 | 2 |
| Diagnostics & Technique development | 3 | 3 | 3 | 3 | 4 |
| Smoothing (MFM) | 2 | 1 | | | |
| Preheat (LPI-TPD) | 3 | 3 | 3 | 3 | 3 |
| Hydro (B, RT, Transport,…) | 1 | 2 | 2 | 2 | 2 |
| Fast Ignition (channeling, transport, etc) | 2 | 2 | 3 | 3 | 3 |
| | 15 | 16 | 17 | 17 | 17 |
| **Joint Campaigns** | | | | | |
| Backlighting (Cryogenic and ambient) | 4 | 4 | 4 | 4 | 4 |
| Fast Ignition (Cryogenic and ambient) | 2 | 2 | 2 | 3 | 3 |
| | 6 | 6 | 6 | 7 | 7 |
| **HED Campaigns (OMEGA & EP)** | | | | | |
| Materials properties (EOS, release, etc) | 5 | 5 | 5 | 5 | 5 |
| Properties of warm dense matter | 3 | 3 | 3 | 3 | 3 |
| Polar Drive HED platform development | 3 | 3 | 3 | 3 | 3 |
| | 11 | 11 | 11 | 11 | 11 |
| **Total facility shot days per year** | 68 | 68 | 68 | 68 | 68 |

### E3.2 Shock Ignition

Shock ignition and shock-ignition-relevant experiments have been performed on OMEGA since 2007. A number of key results have been published.[13,14] These results are based on OMEGA implosion experiments using the shock-ignition concept with both ambient gas-filled plastic shells and cryogenic DT-filled targets.[13] Warm target performance improved significantly using shock-ignition-specific pulse shapes with neutron yields increasing (relative to a baseline performance without the shock spike at the end of the pulse) by nearly a factor of four and peak ρR exceeding ~0.3 g/cm$^2$.[13,14] Shock ignition will represent a significant fraction of the overall LLE ignition effort during FY13–17. The experiments outlined in Table E1 will include shock ignition hydrodynamics and laser–plasma instabilities, and hot electron generation under shock ignition relevant conditions.

The goals for shock ignition hydrodynamics experiments are to demonstrate relevant core pressures and high areal density (ρR) fuel assembly. Shock ignition relevant pressures can be demonstrated in planar and spherical (implosion) target experiments. Recent planar foil experiments demonstrated shock pressures of up to 100 Mbar[15] at a shock pulse intensity of $1.5\times10^{15}$ W/cm$^2$. Similar experiments are being planned for FY13 with intensities up to $3\times10^{15}$ W/cm$^2$ where the predicted shock pressure is approximately 150 Mbar. Higher pressures are difficult to diagnose with the current platforms because hard x-ray radiation and hot electrons at the higher intensities blank the optical diagnostics (VISAR and SOP); the optics become opaque to the signal.[16] Accessing higher pressures at higher intensities will require the development of a platform to directly image strong shocks propagating in flat, solid-density targets via high-resolution, side-on x-ray radiography. Proof-of-concept experiments have been done with encouraging results (the platform requirements for signal levels, alignment, timing, etc. are feasible). This platform will be used to diagnose shock propagation through a plastic ablator in the presence of a long scale-length pre-plasma and to time shock coalescence of multiple shocks propagating through the target. Such experiments can be performed both on OMEGA and EP. Spherical experiments with thick shells (~100 µm) and argon-doped fuel ($D_2$) will be used to infer the shock pressure from the x-ray bang time. Such experiments are predicted to generate shock pressures of about 200 Mbar.

Spherical implosions will be used to test NIF ignition-scale hydrodynamically-equivalent shock-ignition fuel assembly on OMEGA. This requires thick shell implosions with an IFAR of about 10–15 and implosion velocities of 2.0 to $2.5\times10^7$ cm/s. Such experiments can be carried out using cryogenic surrogate gas-filled warm plastic shell implosions as well as layered DT capsules with a 10-µm-thick CD ablator and 80 to 90 µm thick ice layers. 1D target designs for OMEGA show that shock ignition fuel assembly pulses should be able to produce areal densities exceeding 300 mg/cm$^2$. At such areal densities, the required neutron yield for obtaining a ρR measurement with the MRS and nTOF diagnostics can be as low as ~ $10^{12}$. As shown in Table E1, the number of days devoted to integrated shock ignition implosions is expected to increase throughout the renewal period.

A pair of experimental campaigns is being developed to infer the hot electron fraction ($F_{hot}$) and temperature ($T_{hot}$) at shock-ignition relevant intensities and plasma scale-lengths. Flat foil target experiments have been used to infer the characteristics of the hot electron populations ($F_{hot}$ and $T_{hot}$) at intensities up $1.5\times10^{15}$ W/cm$^2$. These experiments use $K_\alpha$ emission from a buried Mo signature layer to infer $F_{hot}$, and the data from the hard x-ray detector (HXRD) to determine the $T_{hot}$. The first campaign is being designed to extend these earlier results to intensities of up to $8\times10^{15}$ W/cm$^2$. Hot electron production and laser backscatter will be characterized for scale-lengths close to NIF shock ignition designs. The effect of phase plates and SSD smoothing on the backscattered light from SRS and SBS will be explored.

A second campaign will implode gas-filled, 300-μm radius shells using the standard indirect drive phase plates (EIDI-300). These phase plates focus to a much smaller spot and should achieve an on-target intensity of $2 \times 10^{15}$ W/cm$^2$ in a spherical implosion. The HXRD will be used to infer $F_{hot}$ and $T_{hot}$ while the FABS and NBI will be used to infer the absorbed laser energy by measuring the direct backscattered light. A combination of the two campaigns will be used to explore laser coupling in the NIF-relevant intensity regime (~$1\times10^{16}$ W/cm$^2$). The working design is to coat a molybdenum ball, whose diameter is matched to the best focus of the EIDI phase plates, with a thin plastic ablation layer to create the long-scale-length plasma into which overlapped high intensity beams are focused with full beam smoothing. The hot electron fraction will be inferred from the Mo $K_\alpha$ emission.

## E4 NIF POLAR-DRIVE EXPERIMENTAL PLAN

The goal of the PIC is to add the facility capabilities and validate the science and engineering required to achieve ignition on the NIF using a polar direct drive implosion by the end of FY17. The PIC is based on strategies developed for the demonstration of indirect-drive ignition (IDI) through NIC. These strategies include validation of specific physics models incorporated into multi-dimensional hydrodynamic design codes (e.g., cross-beam energy transfer and nonlocal thermal transport), and empirical tuning of multi-shock drive pulses (minimize shock pre-heating and the fuel adiabat during compression). Similar strategies were applied to the symmetric and PD campaigns on OMEGA and EP and led to the demonstration of ignition-relevant areal densities in ignition-scaled cryogenic DT implosions on OMEGA.[7,17] As described in Section E3.1, experiments are expected to demonstrate symmetric scaled ignition performance on OMEGA by the end of FY13.

The PIC will require facility modifications including dedicated phase plates, polarization rotators, additional single beam smoothing, and a dedicated cryogenic target insertion capability (the requirements for these capabilities are described in Section E3). While these modifications will take a few years to implement and validate, much of the initial PIC point-design validation can be done on the NIF using established configurations and diagnostics (i.e., the current indirect-drive configuration). For example, the NIF Diagnostic Commissioning campaign that began in 2010 is based on a PD platform in which 192 beams are repointed to achieve the symmetry required to drive a series of "exploding pusher" implosions using DT, $D_2$, and $D^3He$ fuels. The early PIC tuning experiments will be based initially on the "exploding pusher" platform and will be used to validate coupling, symmetry, and performance scaling from symmetric and PD experiments on OMEGA. Although this experimental plan outlines the requirements for achieving ignition on the NIF by the end of FY17, the bulk of the experimental campaign will be conducted on OMEGA and EP (e.g., continuing efforts on PD performance optimization, including cryogenic DT implosions and shock tuning, as well as Shock and Fast Ignition, preheat mitigation, absorption modeling validation, etc.). Section E3.1 provides a comprehensive overview of the OMEGA experimental plans during the FY13–17 time frame.

As presently envisioned, the PIC consists of eleven campaigns on the NIF with the first scheduled for late FY12. The number of tuning campaigns and shots required prior to beginning the ignition campaign in FY17 depends on many factors outside the control of LLE. The campaign schedule is shown in Figure E3 along with the anticipated completion dates for the facility modifications required to perform PD ignition experiments. This plan is intended to be consistent with the discovery-based OMEGA experimental plan and convey the logical order of model validation leading to a viable ignition design by the time the required facility modifications are complete. Section E4 gives a brief overview of each campaign as currently envisioned. The initial campaigns will use the existing IDI phase plates and ambient targets delivered to chamber center using the existing TARPOS. The phase plate spot size is somewhat smaller than the cryogenic PD ignition point-design target diameter. The beam spots can be defocused to drive larger targets but this is limited by the degradation of the far-field focal spot distribution. This degradation reduces the drive symmetry and single beam drive uniformity.

Appropriately scaled targets have been designed that require some phase plate defocus with minimal compromise of the spot shape and single beam uniformity (the lack of sufficient SSD bandwidth is the limiting factor in designing the early experiments; imprint will severely impact higher convergence implosions). ETP images of the IDI phase plates will be used to determine the final target diameter. While these images can be acquired using the OMEGA EP ETP platform, the PDS at the NIF would be the preferred platform to ensure the highest accuracy between the simulated and actual beam spots on target. The nominal initial target diameters will be approximately 2 mm (comparable to the diameter of the highest yield diagnostic commissioning targets). The ablator will be either strong CD or strong CD doped with a higher-Z element such as silicon or germanium (other dopants may be considered for x-ray spectroscopic diagnostic purposes). This is the same ablator used in the PD ignition point design. The gas fill will be either DT (nominally 50:50), $D_2$, $H_2$ (for LPI-related shots where yield may impact the primary diagnostics), or $D^3He$ (for diagnostic purposes).

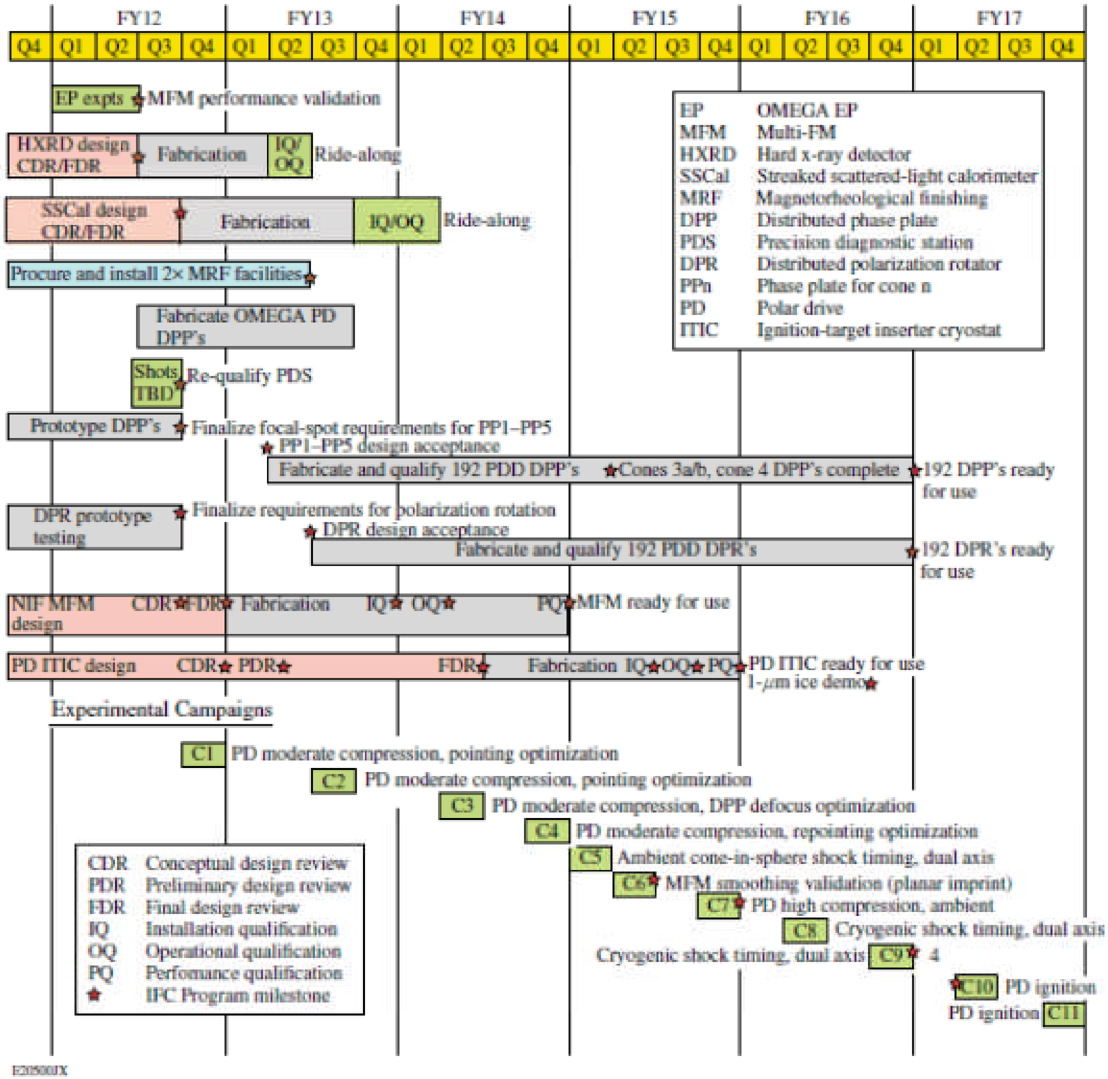


**Figure E3: Proposed schedule for the Polar Ignition Campaign on the NIF. Implementation of dedicated PD optics, single beam smoothing (MultiFM 1D SSD), diagnostics and a PD cryogenic ignition target capability will be staged based on engineering estimates and fabrication schedules. The specific sub-campaign objectives depend on the implementation of these capabilities. Final shock tuning and the first ignition target implosions would begin in FY17.**

The goal of the early sub-campaigns is to validate target performance predictions and to optimize the beam pointing for higher compression PD implosions. New diagnostics are being developed to provide measurements of the time-resolved hard x-ray emission (related to hot-electron fuel preheat) and the time-resolved scattered light. These diagnostics will be based on OMEGA instrumentation that has been used to validate models of CBET[4] and absorption losses/gains due to the excitation of the TPD instability.[6] The measurements are required to validate the final beam spot size and preheat levels for higher compression experiments through FY16 (prior to the scheduled completion of the required optics and single-beam smoothing for full ignition-scale PD target implosions).

A series of experiments will be performed to validate the single-beam imprint efficiency[18] once MultiFM 1D SSD[18] has been implemented at the end of FY14. These experiments will be conceptually similar to those being performed on OMEGA EP in FY12 to validate 1D MFM SSD. The validation metric[20] is the demonstration of smoothing levels comparable to 2D SSD. In these planar foil experiments, broadband imprint as well as the growth of pre-imposed perturbations of known wavelength and amplitude will be inferred using Rayleigh–Taylor (RT) growth to amplify the perturbations to a level that can be measured. Careful measurements of the foil trajectory will be used to infer the initial broadband perturbation amplitudes from the final measured amplitudes while the pre-imposed modulations will be used to verify the RT amplification.

The intermediate shock-timing campaigns will be based on the cryogenic cone-in-shell target platform developed on OMEGA,[21] filled with liquid $D_2$ and delivered to chamber center using the Cryogenic TARPOS (the target positioner used for layered THD/DT targets as well as the hohlraum-based cone-in-shell targets for IDI shock timing). This target concept has been used extensively on OMEGA to tune multi-shock drive pulses[21] and a hohlraum-based version is currently being used for shock tuning of the NIC point-design on the NIF. The shell will be the same ablator material used in the PD ignition point design and the laser beam spots sizes similar to those in the initial campaigns. LLE will work to develop an ambient shock-timing platform for the NIF. This non-cryogenic platform will require thicker ablators but would be based on the cone-in-shell concept. Such a platform may prove easier to implement than a full cryogenic target and provide data quality comparable to that of a cryogenic target. With either target, the main goal is to measure laser coupling and shock timing at the appropriate plasma scale length. These measurements would validate the models developed using conceptually identical experiments on OMEGA.

A final ambient campaign will be conducted to validate the PD platform. The goal will be to achieve high compression using an appropriately scaled version of the point design drive pulse (multiple pickets). This integrated test will prepare for at-scale tuning and ignition campaigns using the new PD optics (phase plates and polarization rotators).

The PD-ITIC will be completed in FY16 so that layering studies can begin well before the final optics are ready for full-scale ignition experiments (these optics will be complete in late FY16). The at-scale ignition campaign begins with the final shock tuning of the drive pulse followed by a series of ignition attempts later in FY17. Details of the final target design will depend on what is learned in the preceding campaigns. The uncertainties of physics scaling from the smaller ambient hydro-equivalent targets to the larger ignition capsules will be minimal. Symmetry, adiabat, and absorption control will be established during these campaigns.

## E5 NIF POLAR-DRIVE CAMPAIGN DETAILS

The goals and configuration of the PIC campaign are described in the following sections. The first three campaigns will use warm, gas-filled targets that are energy scaled from the PD point design described in Section 3. The initial implosions may contain hydrogen and/or helium rather than mixtures of deuterium and tritium. The initial predictions (based on scaling from OMEGA PD performance) is that yields for a DT-filled target would approach $10^{14}$, eliminating the GXD as an imaging diagnostic [the GXD framing camera using charged-coupled devices to record the images rather than film; film is used in the higher-yield complementary device, the hGXI]. The capsule diameter for these experiments is a compromise between drive symmetry and hydro scaling—the targets should be large enough to produce plasma scale-lengths comparable to the point design with peak drive intensities approaching $10^{15}$ W/cm$^2$ but not so large that the defocus of the current IDI phase plate spot sizes induces significant drive non-uniformity. Following a preliminary assessment of the IDI phase plates, the target diameter for the initial implosions campaigns will likely be 2 mm. The primary performance metrics include neutron yield (with the appropriate gas fill), in-flight shell symmetry and areal density (based on framed imaging and backlighting), core symmetry (backlighting) and neutron-averaged shell areal density (neutronics and backlighting), limited time-dependent absorption (scattered light measurements), and possibly corona temperatures and densities (this will depend on diagnostic availability).

Table E2 summarizes the laser configurations for the proposed NIF polar-drive campaigns. Table E3 summarizes the target configurations for the campaigns described in Table E2. Table E4 summarizes the diagnostic requirements for the campaigns described in Table E2.

The requirement for x-ray backlighting is shown in Table E4 for a number of campaigns. Backlighting is needed to assess the in-flight uniformity of the imploded target. While the removal of drive beams to illuminate a backlighter target can upset the drive uniformity, it is anticipated that only a fraction of the shots in each campaign will use backlighting as a diagnostic, and that for those shots, adjustments will be made to adjacent beam energies and pointings to restore the drive symmetry. For shock ignition drive-only experiments, up to half of the quads will be available for backlight. A joint effort with LANL to develop the backlighter platform is underway. This effort will support not only PD implosions but also the LANL DIME.

**Table E2. Summary of the laser configuration for the eleven proposed PD campaigns described in the text.**

| Campaign | Shots | Beams | Energy (kJ) | Pulse Shape | Phase Plates | DPR's |
|---|---|---|---|---|---|---|
| 1 | 5 | 192 | 500 to 700 | Ramp to flattop | Indirect drive (defocused) | n/a |
| 2 | 5 | 192 | 500 to 700 | Ramp to flattop based upon results of previous campaigns | Indirect drive (defocused) | n/a |
| 3 | 5 | 192 | 500 to 700 | Ramp to flattop based upon results of previous campaigns | Indirect drive (defocused) | n/a |
| 4a | 5 | 192 | 500 to 700 | Ramp to flattop, potentially multipicket | Indirect drive (defocused) | n/a |
| 4b | 5 | 192 | 800 to 900 | Multipicket with shock spike | Indirect drive (defocused) | n/a |
| 5 | 5 | ~128 | 500 to 600 | Hydrodynamic scaling of multiple-picket design | Indirect drive (defocused) | n/a |
| 6 | 6 | 16 | 150 | Point design multipicket | Indirect drive (defocused) | n/a |
| 7 | 4 | 192 | 500 to 700 | Multipicket from Campaign 5 | Indirect drive (defocused) | n/a |
| 8 | 5 | ~128 | 800 | Polar-drive point design | Polar drive | Polar drive |
| 9 | 5 | ~128 | 800 | Polar-drive point design | Polar drive | Polar drive |
| 10 | 5 | 192 | 1200 | Polar-drive point design | Polar drive | Polar drive |
| 11 | 5 | 192 | 1200 | Polar-drive point design | Polar drive | Polar drive |

Note that the sequence of experimental campaigns described in Figure E3 necessarily assumes a baseline ignition attempt based on hot-spot ignition. One of the campaigns will be devoted to the validation of strong shock coupling under relevant plasma conditions. Final shock ignition validation will likely require the full PIC optics and an at-scale target and could be done before the final ignition experiments in FY17. Recasting the polar ignition campaign details for shock-ignition would be straight-forward and not require additional facility capabilities. At that point, the primary difference between a hot-spot and a shock-ignition campaign would be the target details (ice and ablator thicknesses).

### E5.1 Campaign 1

The campaign at the end of FY12 will establish the baseline pointing and phase plate defocus strategy for the PIC implosion platform. A number of different beam pointing configurations will be tested to validate predictive capability. Hot electron production will be measured and the final pointing configuration will be repeated to ensure experimental reproducibility.

**Goals:**

1. Moderate compression (convergence ratio, CR ~10)
2. Pointing optimization
3. Drive pulse optimization
4. Establish in-flight shell backlighting
5. Initial assessment of hot-electron production

**Table E3. Summary of the target requirements for the eleven proposed PD campaigns described in the text.**

| Campaign | Target | Fuel | Target 2 |
|---|---|---|---|
| 1 | 2-mm-diam CD plastic shell (wall thickness TBD) | H or He for backing pressure (atm. TBD) | Backlighter |
| 2 | 2-mm-diam CD plastic shell (wall thickness TBD) | $D_2$ or DT (atm. TBD) | Backlighter |
| 3 | 2-mm-diam CD plastic shell (wall thickness TBD) | $D_2$ or DT (atm. TBD) | Backlighter |
| 4a | 2-mm-diam CD plastic shell (wall thickness TBD) | $D_2$ or DT (atm. TBD) | Backlighter |
| 4b | 2-mm-diam CD plastic shell (wall thickness TBD) | $D_2$ or DT (atm. TBD) | Backlighter |
| 5 | Cone-in-shell using the NIC indirect-drive Cryo TARPOS (wall thickness based on earlier campaigns) | Liquid $D_2$ | n/a |
| 6 | CD foils with and without preimposed modulations (wavelength and amplitude TBD) | n/a | Backlighter |
| 7 | 2-mm-diam CD plastic shell (wall thickness TBD) | $D_2$ or DT (atm. TBD) | Backlighter |
| 8 | Cone-in-shell (point-design shell specifications); dual-axis design pending success with indirect drive and OMEGA versions | Liquid $D_2$ | n/a |
| 9 | Cone-in-shell (point-design shell specifications); dual-axis design pending success with indirect drive and OMEGA versions | Liquid $D_2$ | |
| 10 | 3.3-mm-diam CD shell with ~33-$\mu$m wall thickness; DT layer thickness TBD | Layered DT | |
| 11 | 3.3-mm-diam CD shell with ~33-$\mu$m wall thickness; DT layer thickness TBD | Layered DT | |

## E5.2 Campaign 2

The second campaign will continue the drive symmetry optimization based on beam pointing, drive pulse shaping, beam defocus, and beam cone frequency shifts to control cross-beam energy transfer (a preliminary assessment of the cone color suggests improved coupling symmetry due to the minimization of CBET with wavelength differences by beam cone of order 1 Å). Details of the pulse shapes will depend on the results in Campaign 1. Time-dependent hard x-ray measurements will be used to assess preheat levels. The goal is to demonstrate predictive capability for the drive symmetry and target performance achieved.

**Table E4. Summary of the target diagnostic requirements for the eleven proposed PD campaigns described in the text.**

| Campaign | GXD or hGXI | Neutronics | FABS/ NBI | SXI | FFLEX, HXRD | VISAR SOP | Scattered-Light Diagnostics |
|---|---|---|---|---|---|---|---|
| 1 | X | X | X | X | X | | X |
| 2 | X | X | X | X | X | | X |
| 3 | X | X | X | X | X | | X |
| 4a | X | X | X | X | X | | X |
| 4b | X | X | X | X | X | | X |
| 5 | X | | X | X | | X | X |
| 6 | X | | X | X | X | | X |
| 7 | X | X | X | X | X | | X |
| 8 | X | | X | X | | X | X |
| 9 | X | | X | X | | X | X |
| 10 | X | X | X | X | X | | X |
| 11 | X | X | X | X | X | | X |

**Goals:**
1. Moderate compression (CR~10)
2. Continue pointing optimization
3. Continue drive pulse optimization
4. Test phase plate defocus for optimal absorption and target performance
5. Begin testing cone frequency shifts for symmetry optimization
6. Begin to assess preheat levels at ignition relevant scale-lengths and intensities

## E5.3 Campaign 3

The third campaign will be used to optimize the phase plate defocus conditions for maximum absorption and target performance. Details of the pulse shapes will depend on the results in campaigns 1 and 2; expect to begin varying the pulse shape by cone to further improve symmetry.

**Goals:**
1. Moderate compression (CR~10; may push to high compression depending on the results of the first two campaigns)
2. Continue pointing optimization
3. Begin drive pulse optimization by varying pulse shape and energy by beam cone
4. Finalize phase plate defocus for optimal absorption and target performance

5. Continue testing cone frequency shifts for symmetry optimization
6. Continue to assess preheat levels at ignition relevant scale-lengths and intensities

### E5.4 Campaign 4a

The initial part of the fourth campaign will be used to finalize the drive symmetry including pointing, drive pulse and energy balance optimization among the beam cones, phase plate defocus and wavelength shifts. Details of the pulse shapes will depend on the results of the earlier campaigns. The first implosions with multiple picket drive pulses will occur during this campaign.

**Goals:**

1. Moderate compression (CR~10; high using a multiple picket drive pulse)
2. Finalize pointing optimization
3. Finalize energy balance
4. Finalize cone frequency shifts for symmetry optimization
5. Continue to assess preheat levels at ignition relevant scale-lengths and intensities

### E5.5 Campaign 4b

The second part of the fourth campaign will test potentially higher compression using a shock ignition drive pulse. These experiments will be the first to study shock spike absorption at intensities approaching $1\text{x}10^{16}$ W/cm$^2$. The target diameter may be increased up to 2.5 mm (this will depend on the phase plate ETP defocus spot distributions) and the drive energy (including the shock spike) may be as high as 800 to 900 kJ. The goal is to demonstrate predictive capability for the drive symmetry, spike absorption, and target performance achieved.

**Goals:**

1. Higher compression (CR~20); assess uniformity
2. Assess preheat levels at ignition relevant scale-lengths and intensities
3. Assess high intensity absorption of the shock spike

### E5.6 Campaign 5

The fifth campaign will be the first shock tuning for high performance validation of the ambient PD target design. These targets will be dual-axis, cone-in-shell designs with capsule diameters matched to those used in the earlier PD campaigns (approximately 2.0 mm). The drive pulse will be the multiple picket design planned for Campaign 7 (high compression of the ambient target design) and initially tested during Campaign 4b. Shock tuning measurements will be used to optimize the picket energies and timing for high compression. The primary performance metrics include shock velocities and coalescence times, time-dependent absorption, and possibly corona temperatures and densities (this will depend on diagnostic availability). A non-cryogenic target design will be developed as contingency for difficulties fielding a PD cryogenic cone-in-shell target. The ambient design would require much thicker CD plastic shells (100 to 150 μm). This platform may be sufficient given the experimental shock timing database from OMEGA.

**Goals:**

1. Shock tuning of the high compression multiple-picket design for Campaign 7

### E5.7 Campaign 6

This campaign will be devoted to the validation of the operation of MultiFM 1D SSD. The campaign will be conceptually similar to the MFMVal campaigns that will be performed on OMEGA EP in FY12. To validate adequate single beam smoothing, broadband imprint efficiency[22] will be measured in a simple planar foil configuration. By driving the foil following the initial imprint phase, the sub-micron imprint features grow due to the Rayleigh–Taylor (RT) instability to a scale that can be measured using a GXD. The RT amplification step is monitored using pre-imposed modulations where the amplitude and wavelength are known. Through-foil radiography will be used to measure the modulation growth, and side-on foil radiography will be used to determine the acceleration history of the foil. The imprint efficiency derived from the acceleration history and measured modulation growth will be compared with similar measurements from OMEGA EP experiments.

**Goals:**

1. Measure the growth of broadband imprint with MultiFM 1D SSD using the point-design multiple-picket drive pulse

### E5.8 Campaign 7

This is the final tuning campaign based on the ambient target design of the earlier campaigns. The goal is to achieve predicted high compression in the PD configuration based on the empirical tuning and physics model validation of the earlier campaigns. This campaign will follow the validation of the 1D MFM SSD. The ambient targets are energy scaled from the PD point design[20] and are expected to produce a primary DT yield of up to $1\times10^{14}$. The pulse shape will be the final design based on the results of the tuning done in Campaign 5. The on-target intensities will approach $1\times10^{15}$ W/cm$^2$ (the peak intensity of the ignition point design). The goal is to demonstrate predictive capability for the drive symmetry and target performance achieved.

**Goals:**

1. High compression (CR~25)
2. Continue to assess preheat levels and laser coupling
3. Backlight the compressed capsule

### E5.9 Campaigns 8 and 9

These campaigns will be the first to use the PIC phase and polarization plates. Since the number of plates required will be approximately 126 (about two-thirds of the beams are needed to drive the cone-in-shell targets), these experiments could be conducted earlier depending on the DPP production schedule. The pacing items will be the optics and a validated target platform. The targets will be ignition-scale cone-in-shells (the shell diameter will be approximately 3.3 mm). The basic target platform and laser configuration will be identical to that of Campaign 5. The shock tuning of the ignition scale target and drive pulse will require more than one dedicated campaign to account for subtle differences in laser absorption at the full overlap intensity, the complexity of the dual-axis measurement (pole/equator), plasma scale-lengths, CBET, etc. The primary performance metrics include shock velocities and coalescence times and time-dependent absorption. Pending the results of Campaign 5 and continued development of a PD cryogenic cone-in-shell platform, a non-cryogenic target design may be developed as contingency.

**Goals:**

1. Shock tuning of the point-design pulse shape

### E5.10 Campaigns 10 and 11

These are the ignition attempts using the PIC phase and polarization plates, a layered DT target and 1D MFM SSD.

**Goals:**

1. Demonstrate polar-drive ignition

## E6 REFERENCES


1. R. Betti et al., *Phys. Rev. Lett.* **98**, 155001 (2007).
2. S. Skupsky et al., *Phys. Plasmas* **11**, 2763 (2004).
3. S. Skupsky et al., *J. de Physique* IV **133**, 59 (2006).
4. Igumenshchev et al., *Phys. Plasmas* **17**, 122708 (2010); S. Hu et al., *Phys. Rev. Lett.* **104**, 235003 (2010).
5. S. Hu et al., *Phys. Rev. Lett.* **101**, 055002 (2008).
6. B. Yaakobi et al., *Phys. Plasmas* **19**, 012704 (2012).
7. V. Goncharov et al., *Phys. Rev. Lett.* **104**, 165001 (2010); V. Goncharov et al., *Phys. Plasmas* **10**, 1906 (2003).
8. C. Stoeckl et al., *Phys. Plasmas* **9**, 2195 (2002).
9. C. Sangster et al., *Phys. Plasmas* **14**, 058101 (2007).
10. R. Betti et al., *Phys. Plasmas* **17**, 058102 (2010).
11. J. Marozas et al., *Phys. Plasmas* **13**, 056311 (2006).
12. J. Frenje et al., *Phys. Plasmas* **17**, 056311 (2010).
13. W. Theobald et al., *Phys. Plasmas* **15**, 056306 (2008).
14. W. Theobald et al., *Plasma Phys. Contr. Fusion* **41**, 124052 (2009).
15. W. Theobald et al., APS presentation 2011.
16. W. Theobald et al., *Phys. Plasmas* **13**, 122702 (2006).
17. T.C. Sangster et al., *Phys. Plasmas* **17**, 056312 (2010).
18. V.A. Smalyuk et al., *Phys. Plasmas* **14**, 032702 (2007).
19. J.A. Marozas et al., "Multiple-FM Smoothing by Spectral Dispersion—an Augmented Laser Speckle Smoothing Scheme," *LLE Review* **114** (2008).
20. T. Collins et al., "Preparing for Polar Drive at the National Ignition Facility," accepted for publication in *Phys. Plasmas* (May 2012).
21. T.R. Boehly et al., *Phys. Rev. Lett* **106**, 195005 (2011).
22. V.A. Smalyuk et al., *Phys. Rev. Lett.* **95**, 215001 (2005).

# Appendix F: Theoretical Unknowns and Technical Implementation Risks

## F1 INTRODUCTION

The scientific unknowns and technical implementation risks for a PIC on NIF are identified and assessed in this appendix. A summary of the risk events are identified in Risk Event Summary Table below. The details of each risk event including their descriptions, event likelihood, and mitigation measures follows the Summary Table.

This risk management plan is preliminary but has been reviewed by LLNL. LLE and LLNL are working together to ensure proper review (including other elements of the U.S. ICF Program) prior to final submission in Q4FY12.

## F2 RISK LIKELIHOOD LEVELS

The likelihood of occurrence has been estimated in an order-of-magnitude fashion. The most likely (high) includes risk events that may be expected to occur during the life of the program. The least likely level (low) includes risk events that will probably not occur during the life of the program or that are extremely unlikely. The intermediate likelihood level (moderate) includes risk events that could possibly occur during the life of the program.

## F3 RISK MITIGATION IDENTIFICATION

For identified risk events, there are three potential courses of action:

1. Accept the risk with no additional action, or
2. Eliminate the risk to the maximum extent, or
3. Mitigate the risk to an acceptable level.

Once risks events have been identified, a determination of acceptability is made. If the risk is not acceptable, means of eliminating is considered. If elimination is not possible, then measures for mitigating the risk are identified. Risk mitigation measures are implemented until the level of risk becomes acceptable.

Risk mitigation measures can function in two ways. They can:

- Reduce the likelihood of the risk event (preventive).
- Reduce the consequences of the risk event (mitigative).

Preventive measures are proactive measures that assure the risk event does not occur. They work on the causes of why a certain risk event might occur and focus on making it less likely for a specific cause to actually take place. The second type of risk mitigation measure attempts to alleviate the consequences of a risk event, if it occurs. This type focuses on ways of mitigating the consequence or providing an alternate pathway to follow if the risk event does occur. Measures already implemented qualify as risk mitigation measures, if they have had an impact on reducing the likelihood of the risk event. Ongoing activities may also be included as risk mitigation measures.

A risk mitigation measure is developed and implemented; otherwise the risk is accepted with no further action required based on the assessed relative risk priority level. Each identified risk event is assigned to a risk owner.

## F4 RISK EVENT SUMMARY TABLE

| Risk Event ID | Risk Event Description | Relative Risk Likelihood | Risk Event Owner |
|---|---|---|---|
| 1 | The dedicated PD phase plates do not meet the point-design irradiance profile on target requirement. | High | T. Kessler |
| 2 | Polarization smoothing of the individual NIF laser beams does not meet the requirements of the point design. | High | T. Kessler |
| 3 | The PDS is unavailable to test dedicated PD DPR's and DPP's. | High | T. Kessler |
| 4 | The required angular divergence and bandwidth of MultiFM 1D SSD cannot be cleanly propagated through the NIF. | Moderate | J. Zuegel |
| 5 | The PDS is unavailable to test and validate MultiFM 1D SSD on the NIF. | Moderate | J. Zuegel |
| 6 | The picket pulse widths cannot be generated or measured on the NIF. | High | J. Zuegel |
| 7 | The NIF 3-TW power limit is exceeded due to limitations in the UV temporal diagnostics. | Moderate | J. Zuegel |
| 8 | The required implosion velocity and/or drive symmetry do not meet specifications due to drive losses caused by CBET. | Moderate | D. Froula |
| 9 | Failure to properly model laser absorption and loss mechanisms. | Low | D. Froula |
| 10 | The required implosion velocity and/or drive symmetry do not meet specifications due to drive losses caused by laser backscatter. | Moderate | D. Froula |
| 11 | Hot-electron preheat (increased adiabat) reduces in-fuel compression, peak areal density, and hot-spot temperature below the point design requirements. | High | V. Goncharov |
| 12 | Inaccurate shock timing increases the in-flight adiabat above the point design requirements. | Moderate | V. Goncharov |
| 13 | The NIF fails to meet the laser specifications for energy, power balance, pulse shaping, beam-to-beam timing, and beam pointing. | Low | P. McKenty |
| 14 | The PD point design fails to achieve ignition due to inadequate computational design or unanticipated physics phenomenology. | Moderate | P. McKenty |
| 15 | The NNSA target vendor cannot manufacture the PD target (capsule and fill tube) to the required specifications. | Low | D. Harding |
| 16 | The DT ice layer does not meet the required smoothness at the desired internal gas density. | Moderate | D. Harding |
| 17 | DT ice layer cannot be "shimmed" with adequate precision. | Moderate | D. Harding |
| 18 | The PTIC does not meet the requirements for mechanical (vibration) and thermal stability (exchange gas pressure). | Moderate | M. Shoup |
| 19 | The PTIC will not fit within the existing space envelope of NIF ITIC support equipment (TAS and LLCS). | Moderate | M. Shoup |

| Risk Event ID | Risk Event Description | Relative Risk Likelihood | Risk Event Owner |
|---|---|---|---|
| 20 | The number of PD shots scheduled on the NIF is adequate to achieve ignition. | Moderate | Sangster |

## F5 RISK EVENT IDENTIFICATION, ASSESSMENT, AND MITIGATION STATUS

| **Risk Event ID:** 1 | **Risk Event Owner:** T. Kessler | **Risk Event Status:** |
|---|---|---|
| **Risk Event Description:**<br><br>**The dedicated PD phase plates do not meet the point-design irradiance profile on target requirement.** Phase plates will be designed to meet the focal spot and near-field beam modulation requirements as specified in Section 3a. Although vendor capability to manufacture PD phase plates has been demonstrated, the cumulative wave-front error of a NIF beam may distort the focal spot beyond an acceptable tolerance, particularly in the case of the equatorial beams for which the tailor-shaped focal spot is critical. The consequence of this event is a decrease in the irradiation uniformity on target leading to decreased target performance. | | |
| **Risk Event Likelihood:**<br><br>X high ☐ moderate ☐ low | | |
| **Risk Event Mitigation Measure:**<br><br>This risk can best be mitigated by using high-resolution wave-front measurements from a representative NIF UV beam during the phase plate design. New measurements will be required if existing wave-front information does not reflect the current state of the cumulative beam-line wave-front error. Wave-front measurements, coupled with a relevant statistical model of the NIF UV beam, will be used to complete accurate simulations of the focal spots on target using a distributed phase plate. Modification of the phase plate designs will be made to accommodate the anticipated variance in the irradiance due to the expected laser beam wave-front error. | | |

| **Risk Event ID:**<br>2 | **Risk Event Owner:**<br>T. Kessler | **Risk Event Status:** |
|---|---|---|

**Risk Event Description:**

**Polarization smoothing of the individual NIF laser beams does not meet the requirements of the point design.** DPR's are required for NIF PD experiments (see Section 3a) to achieve a modest amount of instantaneous focal-spot smoothing. The form of DPR involving bi-refringent wedges is used routinely on the OMEGA laser is precluded on the NIF since LLNL experimentally demonstrated that a full-aperture bi-refringent wedge produces excessive SRS scattering loss of UV energy. An alternative form of DPR is required as a part of the PD beam smoothing package. Meeting all NIF requirements with new DPR technology presents significant risk. The consequence of this event is a decrease in the irradiation uniformity on target leading to decreased target performance.

**Risk Event Likelihood:**

X high ☐ moderate ☐ low

**Risk Event Mitigation Measure:**

Alternative DPR (checkerboard) schemes are being developed at LLE. A 2x2 checkerboard of segmented KD*P wave-plates will be designed and tested on the NIF PDS to determine the energy loss due to SRS at half-aperture. Two alternative DPR materials have been demonstrated at small aperture and are being scaled in aperture to the NIF beam size. Small quartz optical rotators and small wave-plates made with glancing angle deposition (GLAD) coatings have both been successfully prototyped and tested. Aperture scaling of these DPR technologies is ongoing.

| **Risk Event ID:**<br>3 | **Risk Event Owner:**<br>T. Kessler | **Risk Event Status:** |
|---|---|---|
| **Risk Event Description:**<br><br>**The PDS is unavailable to test dedicated PD DPR's and DPP's.** The PDS is required first to optimize the early PD experiments that are designed to use the existing NIF indirect-drive optics (e.g., modest defocus of the phase plates is required to irradiate a 2-mm-diameter target; see Appendix E for a description of the PD experimental plan on the NIF). The PDS is a critical diagnostic for PD experiments conducted between 2014 and 2017. The longer term consequence of implementing uncharacterized optics on the NIF is a significant reduction in the allowed energy in the NIF beam lines and/or a reduction of energy reaching the target due to limitations imposed by the facility to protect the laser from potential beam modulation and/or scattering loss from the DPR. | | |
| **Risk Event Likelihood:**<br><br>X high ☐ moderate ☐ low | | |
| **Risk Event Mitigation Measure:**<br><br>This risk is mitigated by returning the NIF PDS to operational status, including the modifications necessary to deploy/test the existing IDI phase plates, the PD phase plates, and the dedicated DPR's within the FOA. | | |

<table>
<tr><td>Risk Event ID:<br>4</td><td>Risk Event Owner:<br>J. Zuegel</td><td>Risk Event Status:</td></tr>
<tr><td colspan="3">Risk Event Description:<br><br>The required angular divergence and bandwidth of MultiFM 1D SSD cannot be cleanly propagated through the NIF. MultiFM 1D SSD significantly increases the spectral bandwidth and angular divergence of laser pulses amplified in the NIF beam lines relative to the 1D SSD system applied for current indirect-drive experiments. This increases the probability of FM-to-AM conversion that could risk laser system damage and/or distort on-target irradiation compromising polar-drive target performance. If sufficient FM-to-AM conversion mitigation cannot be achieved using techniques outlined below, bandwidth and/or dispersion parameters in the point design will be re-optimized with some associated reduction in gain margin (by accepting either increased imprint or reduced drive energy).</td></tr>
<tr><td colspan="3">Risk Event Likelihood:<br><br>☐ high X moderate ☐ low</td></tr>
<tr><td colspan="3">Risk Event Mitigation Measure:<br><br>With FM-to-AM conversion being the primary issue associated with the propagation of bandwidth through the laser, sources of excessive conversion must be identified and mitigated. For example, pinhole clipping produces significant AM (the pinholes in the PAM are the most susceptible). Enlarging the limiting pinholes can reduce and/or eliminate the conversion mechanism. Similarly, dispersion and amplitude compensation schemes proven on both NIF and OMEGA EP can further reduce the risk that AM will limit the ultimate bandwidth.</td></tr>
</table>

| **Risk Event ID:**<br>5 | **Risk Event Owner:**<br>J. Zuegel | **Risk Event Status:** |
|---|---|---|
| **Risk Event Description:**<br><br>**The PDS is unavailable to test and validate MultiFM 1D SSD on the NIF.** MultiFM 1D SSD beam smoothing will be validated on OMEGA EP but the NIF beam-line architecture is slightly different with 192 beam lines that vary in exact details. Validating MultiFM smoothing on the NIF requires the PDS that has not been operated since 2007. Reactivating the PDS might not occur in time to support initial MultiFM experiments. | | |
| **Risk Event Likelihood:**<br><br>☐ high X moderate ☐ low | | |
| **Risk Event Mitigation Measure:**<br><br>Technical and scientific risks associated with reactivating the PDS should be low, since it has been successfully accomplished in the past. Cost and schedule risks are the primary concern. In addition, beam smoothing validations completed on OMEGA EP can be projected to NIF based on numerical simulations. | | |

<table>
<tr><td>Risk Event ID:<br>6</td><td>Risk Event Owner:<br>J. Zuegel</td><td>Risk Event Status:</td></tr>
<tr><td colspan="3">Risk Event Description:<br><br>The picket pulse widths cannot be generated or measured on the NIF. The PD ignition point-design pulse shape requires three fast rise time picket pulses preceding a main drive pulse. Polar-drive pulse-width and timing specifications may exceed the capabilities of the existing NIF pulse shaping and measurement systems.</td></tr>
<tr><td colspan="3">Risk Event Likelihood:<br><br>X high ☐ moderate ☐ low</td></tr>
<tr><td colspan="3">Risk Event Mitigation Measure:<br><br>New pulse shaping generation and measurement technology used to demonstrate MultiFM 1D SSD beam smoothing on OMEGA EP will be adapted and expanded to shape pulses for all 48 PAM inputs.</td></tr>
</table>

<table>
<tr><td>Risk Event ID:<br>7</td><td>Risk Event Owner:<br>J. Zuegel</td><td>Risk Event Status:</td></tr>
<tr><td colspan="3">Risk Event Description:<br><br>The NIF 3-TW power limit is exceeded due to limitations in the UV temporal diagnostics. The NIF UV temporal diagnostics may be unable to accurately diagnose peak UV output power due to amplitude modulation associated with the high MultiFM 1D SSD modulation frequencies. The concern here is only with the leading pickets (the main drive will not be smoothed using MultiFM), which will nominally have peak intensities 20% or less of the main drive.</td></tr>
<tr><td colspan="3">Risk Event Likelihood:<br><br>☐ high X moderate ☐ low</td></tr>
<tr><td colspan="3">Risk Event Mitigation Measure:<br><br>The NIF Operations team is already dealing with this issue. Simulations using the THGFT (or similar) code at LLNL are used to calculate the actual peak power and set observable energy levels accordingly.</td></tr>
</table>

| **Risk Event ID:**<br>8 | **Risk Event Owner:**<br>D. Froula | **Risk Event Status:** |
|---|---|---|
| **Risk Event Description:**<br><br>**The required implosion velocity and/or drive symmetry do not meet specifications due to drive losses caused by CBET.** | | |
| **Risk Event Likelihood:**<br><br>☐ high X moderate ☐ low | | |
| **Risk Event Mitigation Measure:**<br>(1) The PD phase plate design will be optimized to reduce CBET (ongoing experiments at OMEGA).<br>(2) Three-color tuning with moderate wavelength shifts between the PD cones will balance the net energy transfer among laser cones (has been shown computationally and will require experimental validation on the NIF; this is Campaign 2 in the PIC implementation plan (Appendix E)).<br>(3) LLE designers are considering are considering reduced intensity ignition designs that increase the diameter of the target and reduce the shell thickness to maintain the same implosion velocity, which would mitigate CBET.<br>(4) Higher Z ablator materials (including dopants) reduce the CBET volume and increase the electron temperature. Experiments to validate these ablator materials as suitable for ICF targets are part of the OMEGA experimental plan described in Appendix E. | | |

<table>
<tr><td>Risk Event ID:<br>9</td><td>Risk Event Owner:<br>D. Froula</td><td>Risk Event Status:</td></tr>
<tr><td colspan="3">Risk Event Description:<br><br>Failure to properly model laser absorption and loss mechanisms. Current absorption models and potential inaccuracies in calculating azimuthal gradients in the hydrodynamic codes will result in incorrect calculations of the under-dense plasma conditions leading to incorrect predictions for laser coupling to hydrodynamic motion (e.g., inverse Bremsstrahlung, CBET, TPD, SBS, SRS…) This is challenging when extending the hydrodynamic modeling from shorter plasma scale-lengths on OMEGA to the longer scale lengths on the NIF (and further complicated by the inherent asymmetry of PD illumination). In addition, LLE scientists are realizing that complex absorption mechanisms are energetically important and have begun to develop models to be included in the design codes. For example, large amplitude electron plasma waves (e.g. enhanced by TPD or SRS) have the potential to deposit significant energy into the under-dense plasma potentially decreasing hydro coupling and affecting the drive symmetry.</td></tr>
<tr><td colspan="3">Risk Event Likelihood:<br><br>☐ high X moderate ☐ low</td></tr>
<tr><td colspan="3">Risk Event Mitigation Measure:<br>(1) Scattered light measurements on the NIF will benchmark the hydrodynamic models in PD ignition-scale-length plasmas. These measurements are part of the goals of the early PD campaigns described in Appendix E.<br>(2) Thomson scattering experiments on Omega will validate the hydrodynamic models of the under-dense plasma regime. OMEGA EP provides a platform to drive large-scale-length temperature gradients similar to those expected in PD ignition experiments on the NIF.<br>(3) LLE designers are considering reduced intensity ignition designs that increase the diameter of the target and reduce the shell thickness to maintain the same implosion velocity. Such designs would mitigate laser plasma instabilities (i.e., reduce the large-amplitude electron–plasma waves and mitigate reduced hydrodynamic efficiency).</td></tr>
</table>

| **Risk Event ID:**<br>10 | **Risk Event Owner:**<br>D. Froula | **Risk Event Status:** |
|---|---|---|

**Risk Event Description:**

**The required implosion velocity and/or drive symmetry do not meet specifications due to drive losses caused by laser backscatter.** SBS and SRS reduce laser coupling to the target. Although the under-dense plasma scale-lengths are large, single-beam instabilities will likely remain below threshold during peak power as a result of the low single-beam intensities required for PD. A particular concern for backscatter is during the foot of the main drive pulse when the plasma temperature is relatively low.

**Risk Event Likelihood:**

☐ high X moderate ☐ low

**Risk Event Mitigation Measure:**

(1) Changing the ablator material to higher-Z materials (including dopants) reduces the under-dense plasma scale length and increases the electron temperature and reducing backscatter. Experiments are planned to study this mitigation strategy on OMEGA (see Appendix E).
(2) LLE designers are considering reducing the intensity in the foot of the drive pulse to allow the electron temperature to increase faster than the intensity. Possible experiments will be performed on OMEGA in FY13.
(3) LLE designers are considering reduced intensity ignition designs that increase the diameter of the target and reduce the shell thickness to maintain the same implosion velocity. Such designs would mitigate single-beam backscatter in the main drive.

| **Risk Event ID:**<br>11 | **Risk Event Owner:**<br>V. Goncharov | **Risk Event Status:** |
|---|---|---|

**Risk Event Description:**

**Hot-electron preheat (increased adiabat) reduce the in fuel compression, peak areal density, and hot-spot temperature below the point design requirements.** PD ignition requires that the main fuel adiabat stays at a low value (below 4) during the shell compression. Suprathermal electrons with energies above 100 keV generated by the TPD instability can deposit energy inside the cold fuel and raise the in-flight adiabat.

**Risk Event Likelihood:**

X high ☐ moderate ☐ low

**Risk Event Mitigation Measure:**

(1) Drive intensity on the target will be optimized to reduce the TPD instability growth and the fraction of the laser energy coupled into hot-electrons. A significant effort to understand the TPD instability experimentally and theoretically is already underway on OMEGA and will continue in FY13 (see Appendix E for the experimental ignition plan on OMEGA).
(2) Beam pointing will be optimized to minimize multi-beam effects in TPD instability. A significant experimental (on OMEGA) and theoretical effort is already underway to understand the TPD source and hot-electron coupling fraction into the implosion core. These experiments will continue into FY13.
(3) Introducing higher-Z materials (including dopants) in the ablator increases the coronal temperature and collisional damping of plasma waves. Both effects reduce the TPD instability and the fraction of the laser energy coupled into hot-electrons. Experiments on OMEGA have recently begun to address high-Z ablator materials and dopants in CH.

<table>
<tr><td>Risk Event ID:<br>12</td><td>Risk Event Owner:<br>V. Goncharov</td><td>Risk Event Status:</td></tr>
<tr><td colspan="3">Risk Event Description:<br>Inaccurate shock timing increases the in-flight adiabat above the point design requirements. A higher shell adiabat will result in a reduction in fuel compression, peak areal density, and hot-spot temperature. Controlling adiabat of the main fuel requires accurate timing of all shocks and hydrodynamic waves launched by variations in the laser intensity. Inaccuracy in the modeling of laser coupling in PD illumination and heat conduction could result in shock mistiming and adiabat degradation in the main fuel.</td></tr>
<tr><td colspan="3">Risk Event Likelihood:<br><br>☐ high X moderate ☐ low</td></tr>
<tr><td colspan="3">Risk Event Mitigation Measure:<br>(1) Shock velocity validation will be carried out by measuring leading shock velocity simultaneously at the pole and equator using dual-axis VISAR. This has already been demonstrated on the NIF for indirectly-driven targets. Plans are underway to field a similar target for direct-drive dual-axis shock timing on OMEGA (see Appendix E). The dual-axis shock timing platform will be used at the NIF during campaigns 5 and 8.<br>(2) Scattered light measurements on the NIF will benchmark the predictive capability for the laser absorption. These measurements will be made during all of the initial PIC campaigns.<br>(3) Individual picket energies and timing will be adjusted in the multiple-picket design based on shock velocity measurements.</td></tr>
</table>

<table>
<tr><td>Risk Event ID:<br>13</td><td>Risk Event Owner:<br>P. McKenty</td><td>Risk Event Status:</td></tr>
<tr><td colspan="3">Risk Event Description:<br><br>The NIF fails to meet the laser specifications for energy, power balance, pulse shaping, beam-to-beam timing, and beam pointing. The PD point design specifications in Appendix D were set according to the advertised capabilities of the facility shortly after commissioning. Significant underperformance of the laser would jeopardize the primary goal of the PD ignition campaign.</td></tr>
<tr><td colspan="3">Risk Event Likelihood:<br><br>☐ high ☐ moderate X low</td></tr>
<tr><td colspan="3">Risk Event Mitigation Measure:<br><br>LLE will work with the facility to ensure the laser performs to specification. If necessary, reduced facility capabilities could be incorporated into the ignition design provided adequate margin remains. LLE is currently using the polar-drive “exploding pusher” diagnostic commissioning shots to understand the integrated laser performance and validate some of the laser requirements for the polar-drive ignition point design.</td></tr>
</table>

<table>
<tr><td>Risk Event ID:<br>14</td><td>Risk Event Owner:<br>P. McKenty</td><td>Risk Event Status:</td></tr>
<tr><td colspan="3">Risk Event Description:<br><br>The PD point design fails to achieve ignition due to inadequate computational design or unanticipated physics phenomenology.</td></tr>
<tr><td colspan="3">Risk Event Likelihood:<br><br>☐ high X moderate ☐ low</td></tr>
<tr><td colspan="3">Risk Event Mitigation Measure:<br><br>The PIC team has developed an ignition point design that balances known technical risks among laser performance, target technologies, and physics uncertainties. However, intrinsic physics modeling within the radiation–hydrodynamics simulations requires continual comparison with experimental data to ensure the fidelity of ignition target calculations. To this end, the OMEGA and NIF experimental plans has been developed together to examine outstanding design issues involving, but not limited to, radiation pre-heat, thermal transport in the polar-drive configuration, and laser–plasma instabilities, as well as material opacities and equation of state verification. Overall, integrated capsule performance is evaluated on OMEGA to validate design calculation capabilities and to identify new phenomena. The early campaigns on the NIF will validate aspects of the ignition point design at energies and plasma scale-lengths not available on OMEGA.</td></tr>
</table>

| **Risk Event ID:**<br>15 | **Risk Event Owner:**<br>D. Harding | **Risk Event Status:** |
|---|---|---|
| **Risk Event Description:**<br><br>**The NNSA target vendor cannot manufacture the PD target (capsule and fill tube) to the required specifications.** | | |
| **Risk Event Likelihood:**<br><br>☐ high ☐ moderate X low | | |
| **Risk Event Mitigation Measure:**<br>The technical specification of concern is the ability to produce an adequately smooth ablator surface (especially if the outer layers of the capsule are doped with high-Z material or the ablator itself is not CH based). This risk is small considering: (1) that the DOE target contractor already produces doped-CH-based indirect-drive ignition capsules to a specification that is acceptable for PD; (2) the fabrication processes used to make the PD capsule and fill tube are the same as the processes used to make the indirect-drive ignition target; and (3) the PD capsule is a thinner wall shell than the indirect-drive capsule, and as surface roughness scales with shell wall thickness, prospects for making a PD target to the specifications should be good.<br>The greater risk for the PD drive target is a low production yield of useful target assemblies owing to the fragile nature of the capsule/fill-tube structure. This risk is being managed by: (1) a development effort to improve the toughness of the fill-tube material; (2) testing the durability of target assemblies in existing cryogenic equipment; (3) plans to produce target assemblies in greater numbers than are needed for the experiments (to cover attrition); and (4) target-handling design features that will be incorporated into the PD-TIC. | | |

| **Risk Event ID:**<br>16 | **Risk Event Owner:**<br>D. Harding | **Risk Event Status:** |
|---|---|---|

**Risk Event Description:**

**The DT ice layer does not meet the required smoothness at the desired internal gas density.** The PD layered targets require subcooling (see Appendix D), which can lead to high spatial frequency modulations on the inner ice surface as the crystal adjusts to the lower temperature.

**Risk Event Likelihood:**

☐ high X moderate ☐ low

**Risk Event Mitigation Measure:**

Equipment is under construction at LLE and experiments are planned to measure simultaneously the density of the DT gas and the DT ice surface roughness in fill-tube targets at discrete temperatures. Optical shadowgraphy will be used to acquire images to determine the two-dimensional roughness of the ice layer at the limb, and the presence of fractures in the ice at the front and rear surfaces of the target. The DT gas density will be measured using an interferometer that will be added to the cryogenic environment that surrounds the target. The rapid data acquisition of these two techniques will determine how the ice quality changes when the capsule is rapidly sub-cooled to achieve the desired gas density. Earlier experiments that are the basis for the current indirect-drive ignition experiments suggest that there is a 30-second time lapse before a target that is rapidly cooled to achieve the desired gas density experiences fractures in the ice layer due to thermal contraction-induced stresses, though no direct measurement of the gas density was made.

Separately, the sensitivity of implosion performance to different gas density and ice roughness values is being addressed using the DRACO hydro code. This information, together with the experimentally determine time-dependent values of gas density and ice roughness, will define an optimal operational regime.

| **Risk Event ID:**<br>17 | **Risk Event Owner:**<br>D. Harding | **Risk Event Status:** |
|---|---|---|
| **Risk Event Description:**<br><br>**DT ice layer cannot be "shimmed" with adequate precision.** The PD point design (see Appendix D) requires a precise P2 mode in the DT ice layer to reduce the equatorial mass driven by the laser ablation. The inability to shim the ice layer (an un-shimmed layer) will reduce the margin and gain of the target. | | |
| **Risk Event Likelihood:**<br><br>☐ high X moderate ☐ low | | |
| **Risk Event Mitigation Measure:**<br><br>Existing cryogenic equipment will be modified to shape the thermal isotherms surrounding a PD DT target at LLE. The purpose is to imprint a P2 mode into the ice layer. Thermal models of the target inside the layering sphere suggest that this task is feasible. Experiments are planned to: (1) verify the calculation; (2) refine the shape of the layering sphere to achieve a pure P2 mode in the ice; and (3) determine the sensitivity of the ice power spectrum to the position of the target in the layering sphere. | | |

| **Risk Event ID:**<br>18 | **Risk Event Owner:**<br>M. Shoup | **Risk Event Status:** |
|---|---|---|
| **Risk Event Description:**<br><br>**The PTIC does not meet the requirements for mechanical (vibration) and thermal stability (exchange gas pressure).** There are four technical risks specific to the cryogenic equipment to be employed on the NIF: (1) that the target will not be sufficiently stable (vibrates), which will affect the ability to use x-ray phase contrast to image the ice layer and may affect the ability to shim the ice layer; (2) that the shroud retraction mechanism imparts an impulse that does not attenuate sufficiently quickly so that the target is misaligned at the time of the shot; (3) that the shroud is insufficiently leak-tight and is unable to attain the required helium-gas pressure (this affects layer quality); and (4) that the sequence of events starting 30 seconds prior to shooting the target—sub-cool the target ~2K, retract the shroud, allow the target vibration to attenuate, and achieve the desired gas density—may not be tractable with a “clam-shell”-like shroud retractor. | | |
| **Risk Event Likelihood:**<br><br>☐ high X moderate ☐ low | | |
| **Risk Event Mitigation Measure:**<br>The PD cryostat is planned to be a modular attachment to the existing NIF Cryogenic TARPOS. Concepts needed to deploy a PD cryogenic target at the NIF need to be developed and the necessary technologies will be tested in surrogate equipment. The thermal requirement for this equipment, and the validation of discrete design features, will be tested in the existing cryogenic equipment that will be used primarily to measure the ice roughness and internal gas density.<br><br>The technical risks described above will be mitigated by designing and testing critical sub-components during the conceptual and preliminary design phases of the PTIC project. Upon successful completion of all relevant critical sub-components, a complete engineering prototype of the PITIC will be built and tested. Failure to achieve a leak-tight shroud system that can be retracted from same side as the PITIC may lead to the consideration of an opposed port shroud retractor; but this is currently not being considered as an alternative. | | |

<table>
<tr><td>Risk Event ID:<br>19</td><td>Risk Event Owner:<br>M. Shoup</td><td>Risk Event Status:</td></tr>
<tr><td colspan="3">Risk Event Description:<br><br>The PTIC will not fit within the existing space envelope of NIF ITIC support equipment (TAS and LLCS). The space envelope available on the NIF is smaller than the OMEGA cryogenic layering sphere and shroud.</td></tr>
<tr><td colspan="3">Risk Event Likelihood:<br><br>☐ high X moderate ☐ low</td></tr>
<tr><td colspan="3">Risk Event Mitigation Measure:<br><br>The minimum working size of the layering sphere will be evaluated in the same experimental apparatus used to mitigate layering and shimming risks. The minimally sized layering sphere used to validate target performance will be used as a design requirement for the production PTIC. The subsequent PTIC design will use the minimally sized layering sphere and NIF TAS working space envelope to bound the size the of the PTIC layering sphere. Failure to stay within the working envelope of the TAS will result in a redesign of the TAS and possibly impact the LLCS.</td></tr>
</table>

<table>
<tr><td>Risk Event ID:<br>20</td><td>Risk Event Owner:<br>C. Sangster</td><td>Risk Event Status:</td></tr>
<tr><td colspan="3">Risk Event Description:<br><br>The number of PD shots scheduled on the NIF is inadequate to achieve ignition. The experimental plan in Appendix E is a mixture of shots on the NIF, OMEGA, and OMEGA EP. Apart from the early shot campaigns (before the availability of MultiFM 1D SSD smoothing and dedicated PD optics), the primary goal of the PD NIF experiments is to validate target performance against modeling. The early shot campaigns may provide insufficient data to refine the design models. The later shot campaigns may uncover new phenomena which require extensive development of physics models and that cannot be explored further on OMEGA or OMEGA EP.</td></tr>
<tr><td colspan="3">Risk Event Likelihood:<br><br>☐ high X moderate ☐ low</td></tr>
<tr><td colspan="3">Risk Event Mitigation Measure:<br><br>The PD experimental campaigns are designed to unfold over five years. Performance issues that arise during one campaign and that cannot be resolved before moving to the next will lead to a request for additional shot time. In some instances, it is expected that performance issues may be resolved by developing/executing new campaigns on OMEGA or OMEGA EP before the next scheduled campaign on the NIF. Necessary adjustments to the PD campaign on the NIF can be made quarterly by the facility scheduling committee at the NIF; adjustments to the PD experimental campaigns on OMEGA and OMEGA EP can be made at least quarterly.</td></tr>
</table>

# Appendix G: Estimated Cost Range and Schedule

**Table G1. Estimated costs for PD ignition experiments ($ in thousands).***

| MTE | Site | Year 1 | Year 2 | Year 3 | Year 4 | Year 5 | Total |
|---|---|---|---|---|---|---|---|
| 10.1 | LLE | | | | | | $ 0 |
| | LLNL | $ 2,164 | $ 1,394 | $ 1,123 | | | $ 4,681 |
| | 10.1 Total | $ 2,164 | $ 1,394 | $ 1,123 | | | $ 4,681 |
| 10.3 | LLE | $ 1,116 | $ 80 | | | | $ 1,196 |
| | LLNL | $ 3,260 | $ 6,340 | $ 6,090 | $ 5,540 | $ 250 | $ 21,480 |
| | 10.3 Total | $ 4,376 | $ 6,420 | $ 6,090 | $ 5,540 | $ 250 | $ 22,676 |
| | | | | | | | |
| | LLE Total | $ 1,116 | $ 80 | | | | $ 1,196 |
| | LLNL Total | $ 5,424 | $ 7,734 | $ 7,213 | $ 5,540 | $ 250 | $ 26,161 |
| | Grand Total | $ 6,540 | $ 7,814 | $ 7,213 | $ 5,540 | $ 250 | **$ 27,357** |

*Proposals from LLE 8/3/11.

# Appendix H: Development Plan for the Polar Drive Distributed Polarization Rotators

The focal spot smoothing, provided by DPR's, is critical for PD target performance on the NIF. DPR's are required for each of the 192 beams to achieve smoothing of the focal plane speckle at spatial frequencies of primary concern for the target point design. For more than a decade, DPR's have been used on the OMEGA laser system to achieve an instantaneous increase in irradiation uniformity. This implementation uses a wedged plate of KDP that splits each beam into two beams of orthogonal polarizations and slightly different propagation directions. The target sees two orthogonally polarized copies of the speckle pattern shifted by a separation distance and experiences smoothing for spatial scales below this distance. For the large beams of the NIF laser, the energy loss caused by SRS at 351 nm precludes the use of a bi-refringent wedge at full aperture. The gain–length product is excessive for full-aperture bi-refringent materials such as KDP and KD*P. The form of polarization smoothing adopted for indirect drive on the NIF, where the polarizations of two beams of each quad are rotated through 90°, provides smoothing only on very small spatial scales (corresponding to interfering elements in different beams). This provides no significant benefit for direct drive, as the smaller-scale speckle is rapidly smoothed by thermal conduction.

The baseline DPR scheme for NIF PD, shown in figure H1(a), uses a 2 x 2 checkerboard array of KD*P half-wave plates as polarization rotators. KD*P is preferred because it has a lower SRS gain than KDP. In this scheme, the beam is broken into two beams of orthogonal polarizations and different near-field distributions, producing two independent far-field speckle patterns. It is envisioned that the opposite diagonal positions would be left unfilled. Raman scattering is not expected to be a problem as the maximum gain–length product is reduced by a factor of 2. However, the PDS at the NIF would be valuable in measuring the irradiance modulation from the edges of the DPR's and to determine the level of SRS generated by a segmented DPR. Implementation of this scheme would involve apodization of the beam profile earlier in the laser chain (as is done to remove energy from damaged portions of individual beam lines) with some energy loss. This is necessary to remove the potential of near-field irradiance modulation resulting from diffraction at the inner edges of the polarization rotators. This 2 x 2 configuration has a potentially high feasibility for implementation. The NIF PDS will be required to measure SRS at the relevant pulse-shape, energy level, and beam smoothing.

Alternative schemes, operating within the UV portion of the NIF FOA's are being developed to enhance beam smoothing for PD. An alternative concept, shown in Figure H1(b), requires significant development. This DPR involves a 4 x 4 (or higher) array that produces alternating regions with right- and left-handed circular polarization using linear birefringence or with +45 and -45 linear polarization using circular birefringence. One option using linear birefringence involves individually coating each region using GLAD. A thickness of ~4 µm has been demonstrated, producing the desired quarter-wave retardance at 351 nm. Continued development of GLAD coatings will include scaling the coating area and determining the laser-damage threshold for NIF applications. Another option using circular birefringence involves synthetic quartz rotators. An important advantage of these concepts relative to the KD*P half-wave plates is that apodization of the beam profile is not required.

- Clear aperture of UV optic > 40 cm
- Laser damage threshold at 351 nm, 5 ns > 12 J/cm$^2$
- Transmission at 351 nm (Fresnel or shadowing) > 96%
- Near-field (UV FOA) Irradiance modulation (P-A) < 15%
- Wave-front quality at 351 nm < l/2
- Input polarization H or V
- Output energy imbalance of orthogonal polarizations < 20%
- Polarization overlap < 20%
- Polarization sub-aperture size > 20 mm
- Pulse-width broadening (15 mm at n= 1.5) < 25 ps

The baseline DPR requires three areas of development to ensure good performance on the NIF laser: 1) designing low-distortion mounting; 2) finishing the plate perimeter to minimize loss and irradiance modulation; and 3) performing prototype testing on a NIF beam to demonstrate acceptable level of SRS loss.

- Select 2 x 2 KD*P array as baseline DPR for NIF PD (completed).
- Develop mounting scheme for 2 x 2 array with two quarter-aperture plates of KD*P held diagonally, including modeling of optical distortion due to gravitational force (in process).
- Assemble and test a full-aperture 2 x 2 array on the NIF PDS to determine the energy loss due to SRS in KD*P at a reduced (gIL) product (3QFY13).
- Modify the edges and corners of the KD*P plates to further minimize (gIL) product (4QFY13).

The development plan for alternative NIF DPR's is ongoing and contains the following goals:

- Identify material options for N x N arrays to produce orthogonal sets of either circularly or linearly polarized laser light **(completed)**.
- Demonstrate optical rotators using both left-handed and right-handed synthetic quartz to obtain +45 and -45 rotation **(completed)**.
- Carry out test depositions of silica by GLAD to create a bi-refringent coating suitable for fabrication of a quarter-waveplate to produce circularly polarized light from a linearly polarized laser **(completed)**.
- Fabricate a 100-mm-diameter component with four coated regions similar to that envisioned for the final device, with each circular coated region having its GLAD orientation 90º to that of the adjoining regions. Coated regions will alternate between right- and left-hand circular polarizers, for an incident linearly-polarized beam **(completed)**.
- Fabricate a 100-mm-square component with four quartz optical rotators encapsulated within UV compatible resin **(in process)**.
- Deposit an electron-beam evaporated antireflection coating for use under and between the GLAD regions, to minimize both overall reflectance and spatial modulation of reflected light resulting from the varying GLAD thickness at the edges of the patterned regions. A suitable antireflection coating design has been developed and testing of the design is in process. Laser damage testing of the antireflection coating

and the GLAD/antireflection coating combination will be carried out on the UV damage testing facility at LLE **(in process)**.

- Deposit four square regions of GLAD coating on a 100-mm substrate patterned similar to that of the final device, placing the coated regions as close to one another as possible. Diffraction and scatter effects from the coating patterns will be evaluated. Evaluate the coated/patterned substrate with large-area testing using a CW UV lasers. Small area damage testing will be carried out at LLE **(FY12)**.
- Develop and fabricate a sub-scale motorized substrate stage suitable for GLAD fabrication of multiple patterned regions, in order to fabricate a larger (~6 inch) patterned component in a single vacuum cycle. Develop a coating process for multiple GLAD-coated regions on a single substrate in a single vacuum cycle. Evaluate the coated/patterned substrate with large-area testing using CW and pulsed UV lasers. Large area damage testing will be carried out at LLE (OMEGA EP) and LLNL (NIF PDS) **(FY13).**
- Develop and fabricate a full-scale motorized substrate stage suitable for GLAD fabrication of multiple patterned regions, in order to fabricate a full aperture patterned component in a single vacuum cycle **(completion TBD)**.
- Complete construction of full-scale GLAD coater. Demonstrate full aperture DPR using GLAD coatings. Testing will include offline CW testing of physical optics including speckle smoothing, and propagation induced irradiance modulation. Full performance testing will be carried out on a beam line of NIF or the NIF PDS to ensure FOA component safety **(completion TBD)**.

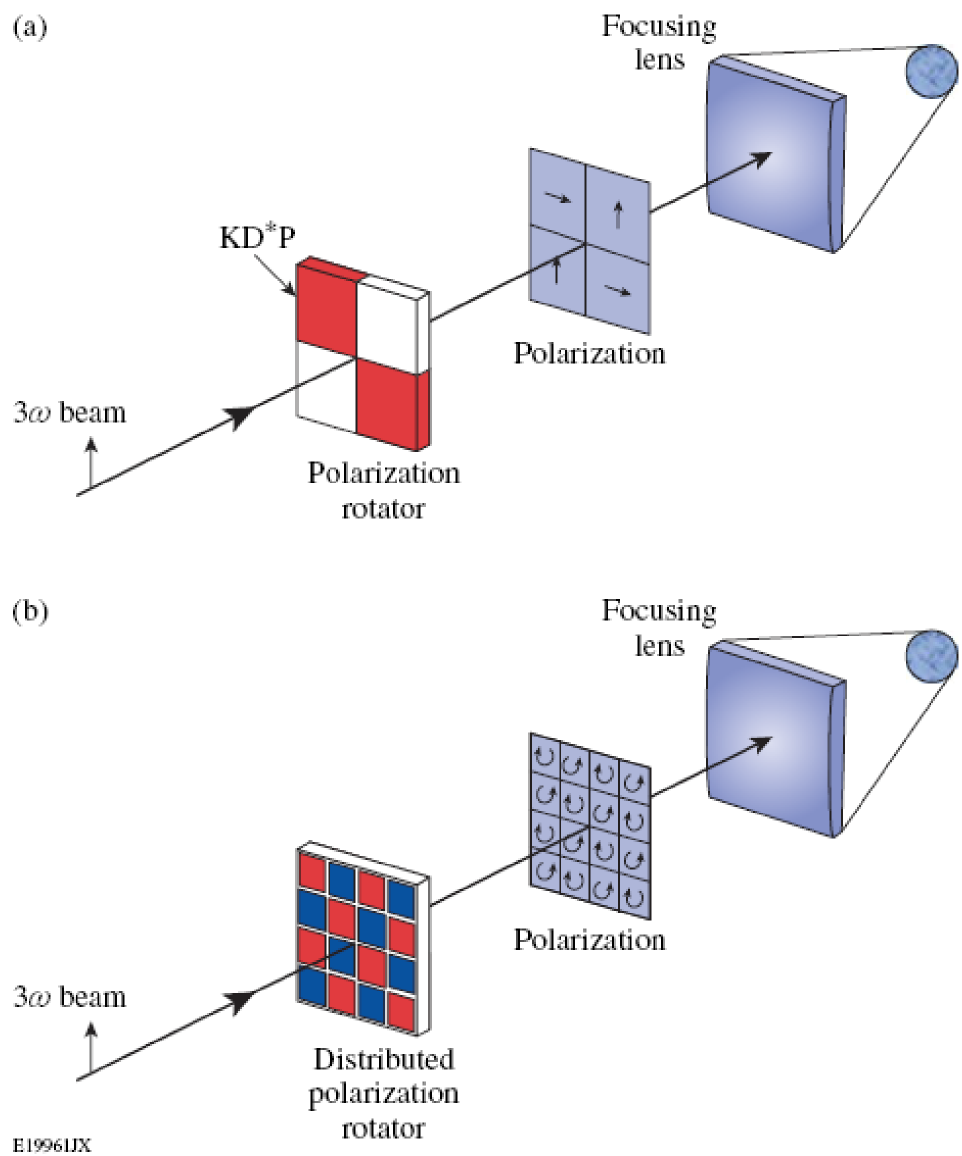


**Figure H1: Two concepts for polarization rotators for PD ignition target designs: (a) two KD*P half-wave plates form the baseline design, and (b) a 4 × 4 array (or higher) of polarization components deposited on a single substrate that produce approximately equal amounts of right-handed and left-handed circularly polarized light.**

# Appendix I: Development plan for MultiFM 1D SSD on the NIF

The NIF MultiFM 1D SSD system conceptual design is based on technology proven by a prototype system on OMEGA EP. Additional development will be required to extend the system to NIF to provide the required seed sources for 48 independent PAMs. A time-multiplexed system, shown schematically in Figure I1, will minimize the cost and space envelope for implementing MultiFM 1D SSD and triple-picket pulse shaping with DBWR in the NIF MOR.

## I1 SEED SOURCE DEVELOPMENT

The output from a continuous-wave, single-frequency laser oscillator is amplified and chopped into long pulses (up to 1 μsec) by an acousto-optic modulator (AOM). This chopped pulse is split into two parallel channels that apply MultiFM and standard SBSS/SSD phase modulation that will be subsequently amplitude modulated to produce picket and main pulse shapes, respectively. The "main pulse" channel will be capable of delivering pulse shapes required for indirect-drive operation. Fiber amplification will be included in the system (not shown for clarity) to recover component insertion losses and to provide the required 750-pJ seed pulses to the PAMs.

Fail-safe (F/S) monitoring systems will ensure that sufficient FM bandwidth is present on each chopped pulse to suppress SBS in the NIF final optics. If sufficient phase modulation is detected in both channels, fail-safe optical gates permit the chopped pulses to proceed to a pulse shaping stage. The F/S gates in each leg will include low-bandwidth pulse shaping to pre-compensate slow temporal distortion in the fiber amplification chain that the long chopped pulses will experience.

After the fail-safe systems, a 1 × 8 fiber splitter directs the chopped pulses to time-multiplexed amplitude modulator chassis (TAMC) systems that will supply pulse shapes to all 48 NIF PAMs. Figure I1 illustrates a configuration that feeds six separate time-multiplexed systems, plus two diagnostic channels. Since different wavelengths are required to mitigate cross beam transfer for indirect-drive ignition, multiple laser oscillators can be wavelength multiplexed before the AOM and de-multiplexed after the fail-safe gates into these six separate branches. Alternately, separate seed sources can be implemented for each time-multiplexed system. Only minor development and repackaging efforts will be required to realize the seed sources described, as outlined in Table I1.

## I2 TIME-MULTIPLEXED PULSE SHAPING DEVELOPMENT

The AOM-chopped pulses are distributed to TAMC systems that produce two parallel trains of eight picket and main pulse shapes, as shown schematically in Figure I2. Two dual-amplitude modulators (DAMs) are driven by the output from a long-record AWG (LAWG). Ultra-wideband radio-frequency (RF) amplifiers boost the LAWG output signals to drive the DAMs at their operating voltages. One modulator of each DAM produces trains of both pickets and main pulses using the high-bandwidth LAWG analog output. The second set of "gating" modulators suppresses the unwanted portion in each channel (main or picket pulse) using binary signals generated by marker channels from the LAWG with the same temporal resolution as the analog outputs.

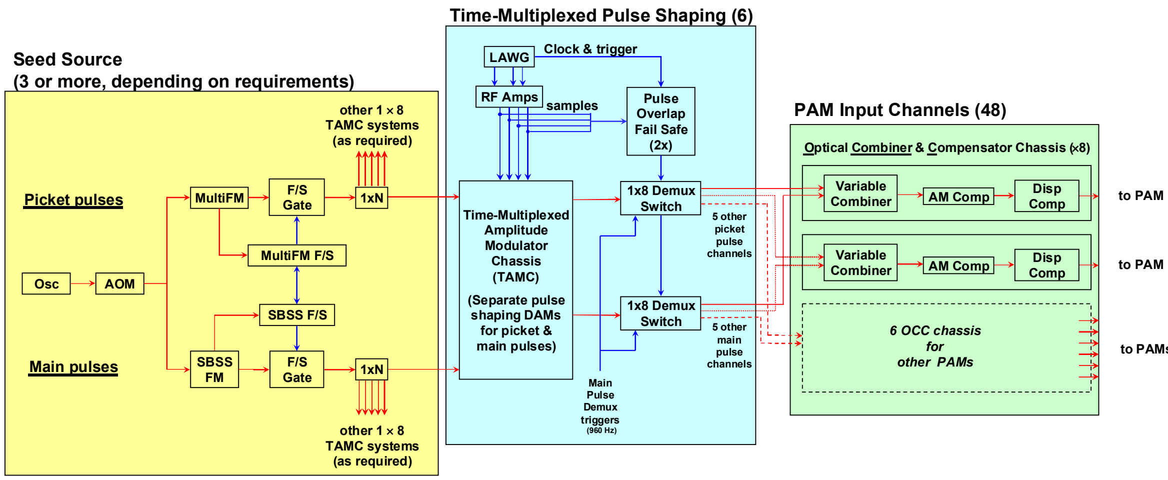


**Figure I1: Block diagram for NIF MultiFM seed source that will be developed for NIF. Picket and main pulses with MultiFM and SBSS bandwidth, respectively, will be temporally shaped in a modular, time-multiplexed system that provides <100-ps temporal resolution while also minimizing cost and space requirements.**

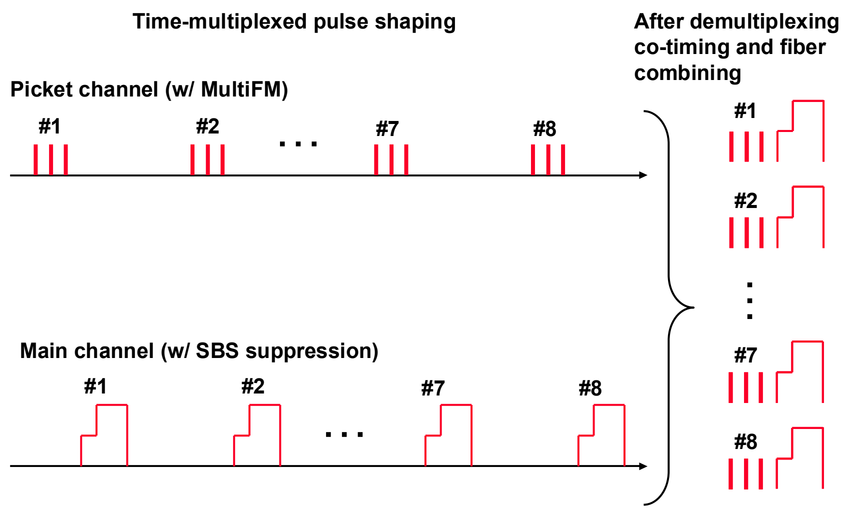


**Figure I2: Parallel trains of picket and main pulses are produced using a time-multiplexed pulse shaping driven by a single LAWG. Each train of pulses is de-multiplexed into individual picket and main pulses that are fiber combined and co-timed to produce the polar-drive ignition pulse shapes that are used to seed the NIF PAM.**

Two electro-optical 1 × 8 de-multiplexing (demux) switches direct individual pairs pulses to their respective PAM input channels. Static fiber delay lines (not shown) deliver the pulses at nominally the same times. Fine timing of the combined pulses will be accomplished by adjusting the timing of waveforms loaded into the LAWG.

A pulse overlap fail-safe system monitors the electrical output signals from the LAWG and compares them with expected patterns to prevent separately generated picket and main pulses from overlapping, which is a potentially dangerous condition. This is analogous to finding bit errors in a data stream once the analog pulse train is first converted to a binary pattern. Two redundant systems will provide independent checks and both will be required to enable the $1 \times 8$ (demux) switches. New hardware and control software development will be required to key elements of the time-multiplexed pulse shaping system, as outlined in Table I1. An FY13–14 development project at LLE will complete a detailed design and engineering proof-of-principle demonstration that will be integrated into the NIF ICCS by an FY14–15 engineering project at LLNL. Procurement and installation/commissioning will be accomplished in FY16.

## I3 PAM INPUT CHANNELS DEVELOPMENT

Picket and main pulses are combined in the Optical Combiner and Compensator Chassis to produce an input for each PAM. Variable fiber combining and/or amplifier gain in the picket- and main-pulse channels sets the relative amplitudes of the two pulses to achieve the best dynamic range possible. This avoids the need for extra AWG dynamic range to accurately shape the pickets that are much smaller than the main pulse at the input of the PAM due to gain saturation in the NIF amplification chain. Pulse shape measurements of each PAM input channel (not shown) are made using the existing NIF system.

Gain tilt (AM) and dispersion compensation are applied to each pulse before they are delivered to the PAMs. Compensation for each unique fiber path length will be tuned to minimize FM-to-AM conversion since the high modulation frequencies and large bandwidth required for MultiFM 1D SSD are sensitive to these effects. The baseline OCC chassis design uses a fiber-connectorized, free-space design developed for the OMEGA EP demonstration.

Only minor development and repackaging efforts will be required to realize the PAM input channels described, as outlined in Table I1.

## I4 PAM FIELD CHANGE KIT DEVELOPMENT

An additional SSD grating is required in the PAM to disperse the MultiFM bandwidth. A translation stage at relay plane #4 in the MPA positions the retro-reflection mirror, the standard 1D SSD grating or the MultiFM 1D SSD grating for operation.

Only minor development and repackaging efforts will be required to realize the PAM field change kits required to install the gratings, as outlined in Table I1.

**Table I1. NIF MOR system developments to implement MultiFM 1D SSD on NIF.**

| Subsystem | Technology | Development Status |
|---|---|---|
| Seed source | 1. Cw sources, AOM chopper, fiber amplification (also used in other subsystems) | No development required—already proven on NIF and OMEGA EP; possibly repackage for NIF. |
| | 2. MultiFM phase modulation | No development required—already proven on OMEGA EP; possibly repackage for NIF. |
| | 3. MultiFM failsafe system | No development required—already proven on OMEGA EP; possibly repackage for NIF. |
| | 4. Low-bandwidth pulse shaping to compensate fiber gain saturation | Minor development required—simple extension of standard pulse-shaping technology. |
| Time-multiplexed pulse shaping | 5. Long-record arbitrary waveform generator | LLE development project—hardware and control software for existing LAWG technology demonstrated in OMEGA EP; should port to next-generation LAWGs being developed by Tektronix + Agilent; demonstrate during FY13–14 project. |
| | 6. Pulse Overlap Fail-Safe System | LLE development project—detailed design and engineering proof-of-principle demonstration during FY13–14 project. |
| | 7. Time-multiplexed amplitude modulator chassis | Minor development required—package two dual-amplitude modulators with high-bandwidth RF amplifiers and DC biasing. |
| | 8. Pulse shape de-multiplexing | LLE development project—detailed design and engineering proof-of-principle demonstration during FY13–14 project. |
| | 9. Integrated Computer Control System development | LLNL development project—complete engineering design for new MOR systems during FY14–15 project. |
| PAM input channels | 10. Optical Combiner + Compensator Chassis | Minor development required—repackage integrated AM + dispersion compensator system proven on OMEGA EP. |
| | 11. Pulse shape measurement system | No development required—reuse NIF design for new system |
| | 12. Optical fiber timing delays | No development required—reuse NIF design for new system |
| | 13. PAM injection fiber management | No development required—reuse NIF design for new system |

| Subsystem | Technology | Development Status |
|---|---|---|
| PAM grating | 14. Add MultiFM 1D SSD grating to MPA | Minor development required—redesign translation stage in MPA. |

# Appendix J: Acronym Definitions

| | |
|---|---|
| 1D | One-Dimensional |
| 2D | Two-Dimensional |
| AM | Amplitude Modulation |
| AR | Anti-Reflection |
| AWG | Arbitrary Waveform Generator |
| BL4 | OMEGA EP beam line #4 |
| CBET | Cross-Beam Energy Transfer |
| CIF | Capability and Infrastructure Framework |
| CMF | Component Manufacturing Framework |
| CPP | Continuous Phase Plate |
| DAM | Dual-Amplitude Modulator |
| DBWR | Dynamic Bandwidth Reduction |
| DIME | Defect-Induced Mix Experiment |
| DOE | Department of Energy |
| DPM-FAC | Dual PM Fiber Amplifier Chassis |
| DPR | Distributed Polarization Rotator |
| DT | Deuterium Tritium |
| ETP | Equivalent Target Plane |
| FABS | Full Aperture Backscatter |
| FEP | Front-end Processor |
| FM | Frequency Modulation |
| FOA | Final Optics Assembly |
| FODI | Final Optics Damage Inspection |
| FSC | Fail-safe Chassis |
| FSOC | Fail-safe Optical Chassis |
| FSOG | Fail-safe Optical Gate |
| FY | Fiscal Year |
| GA | General Atomics |
| GLAD | Glancing Angle Deposition |
| GRH | Gamma Reaction History Diagnostic |
| GXD | Gated X-ray Detector |
| HED | High Energy Density |
| HEDSS | High Energy Density Stockpile Stewardship |
| HXRD | Hard X-Ray Detector |
| ICCS | Integrated Computer Control System |
| ICF | Inertial Confinement Fusion |
| ICS | Industrial Control System |
| IDI | Indirect-Drive Ignition |
| IFAR | In-Flight Aspect Ratio |
| IPT | Integrated Product Team |
| IQ | Installation Qualified |
| ISM | Integrated Safety Management |
| ITA | Integrated Target Assembly |

| | |
|---|---|
| ITIC | Ignition Target Insertion Cryostat |
| ITPS | Integrated Target Positioning System |
| KDP | Potassium Dihydrogen Phosphate |
| KD*P | Potassium Dihydrogen (deuterated) Phosphate |
| LANL | Los Alamos National Laboratory |
| LAWG | Long-Record Arbitrary Waveform Generator |
| LLCS | Load, Layer, and Characterization Station |
| LLE | Laboratory for Laser Energetics |
| LLNL | Lawrence Livermore National Laboratory |
| MIT | Massachusetts Institute of Technology |
| MJ | Megajoule ($10^6$ joules) |
| MOR | Master Oscillator Room |
| MOU | Memorandum of Understanding |
| MPA | Multi-Pass Amplifier |
| MRS | Magnetic Recoil Spectrometry |
| MultiFM | Multiple Frequency Modulation |
| NAD | Neutron Activation Diagnostic |
| NEPA | National Environmental Policy Act |
| NIC | National Ignition Campaign |
| NIF | National Ignition Facility |
| NIS | Neutron Imaging System |
| NNSA | National Nuclear Security Administration |
| NRL | Naval Research Laboratory |
| nTOF | neutron Time of Flight |
| OFSS | Overlap Fail-safe System |
| OMF | Optics Mitigation Factory |
| OPSR | Opposed Port Shroud Retractor |
| OQ | Operational Qualification |
| OSCC | Optical Splicer and Compensator Chassis |
| PAM | Preamplifier Module |
| PCF | Predictive Capability Framework |
| PCFR | Primary Criteria and Functional Requirements |
| PD | Polar Drive |
| PDC | Pulse De-multiplexing Chassis |
| PDS | Precision Diagnostic Station |
| PEP | Project Execution Plan |
| PIC | Polar Drive Ignition Campaign |
| PIL | Process Integration Laboratory |
| PMC | Phase Modulation Chassis |
| PQ | Performance Qualification |
| RAM | Reliability, Availability, and Maintainability |
| RF | Radio Frequency |
| RMP | Risk Management Plan |
| RT | Rayleigh–Taylor |
| SBS | Stimulated Brillouin Scattering |
| SBSS | Stimulated Brillouin Scattering Suppression |
| SDR | System Design Requirement |

| | |
|---|---|
| SPBTD | South Pole Bang Time Detector |
| SR | System Requirement |
| SRS | Stimulated Raman Scattering |
| SSD | Smoothing by Spectral Dispersion |
| SSMP | Stockpile Stewardship and Management Plan |
| SSP | Stockpile Stewardship Program |
| TAMC | Time-Multiplexed Amplitude Modulator |
| TARPOS | Target Positioner |
| TAS | Target Alignment System |
| TPD | Two-Plasmon Decay |
| TRD | Technical Requirements Document |
| TW | Terawatt |
| U/R | University of Rochester |
| UV | Ultraviolet |
| VISAR | Velocity Interferometry System for any Reflector |
| WBS | Work Breakdown Structure |
| YOC | Yield-Over-Clean |